An introduction to Radio Loud AGN

Paola Grandi & Eleonora Torresi
INAF-IASF Bologna

Laboratorio X
24.11.2015

INAF - IASF BOLOGNA
ISTITUTO DI ASTROFISICA SPAZIALE
E FISICA COSMICA - BOLOGNA

Outline

- RADIO-LOUD AGN IN GENERAL
  1) AGN classification
  2) Different SED in AGN
  3) The FRI/FRII dichotomy

- RADIATIVE PROCESSES
  1) Thermal emission
     - Accretion
  2) Non-thermal emission
     - Jets, Hot spots, Lobes

Almost every galaxy hosts a black hole

but...

Almost every galaxy hosts a black hole but...

1% active

99% silent

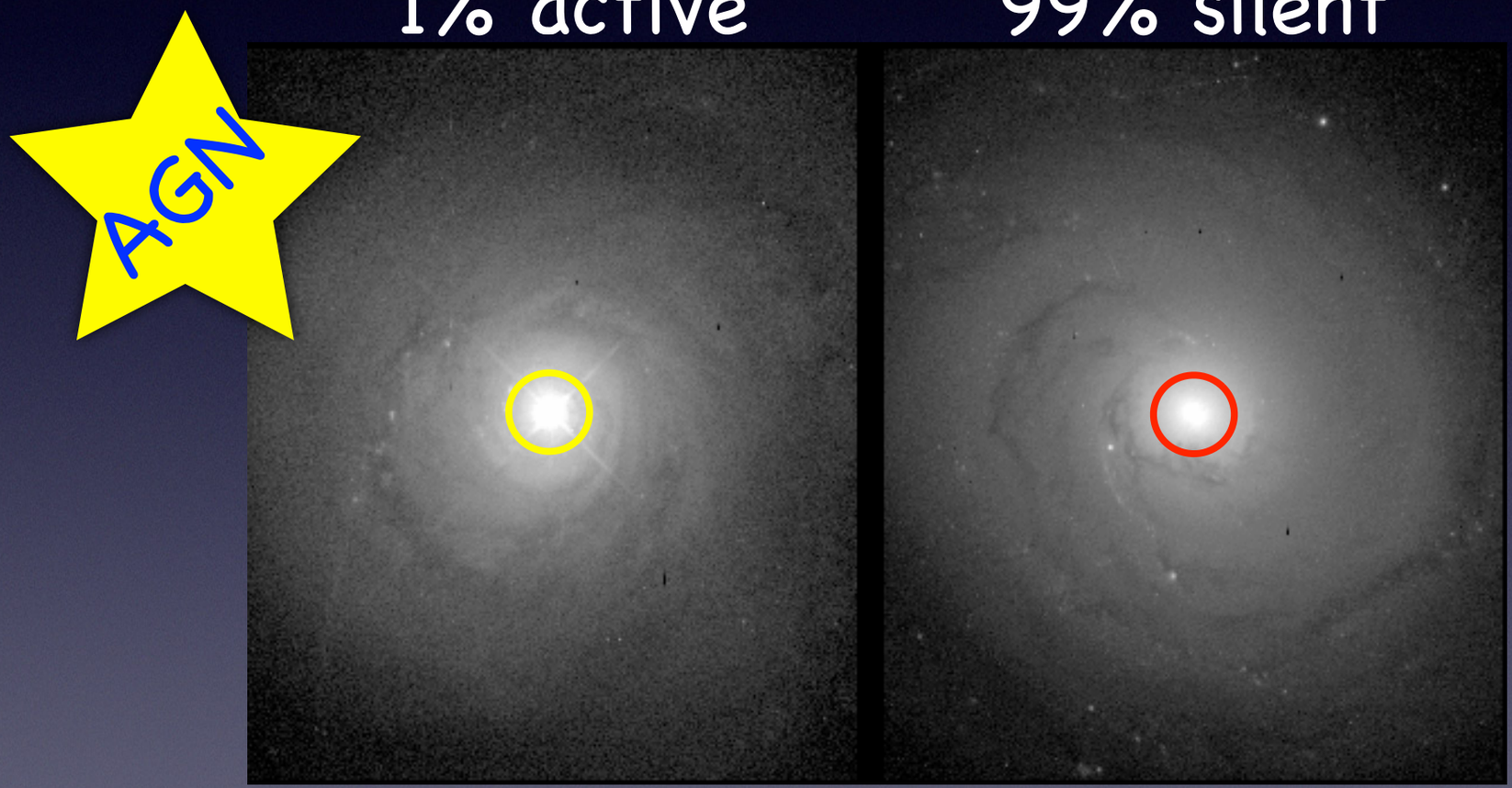

Almost every galaxy hosts a black hole but...

1% active

99% silent

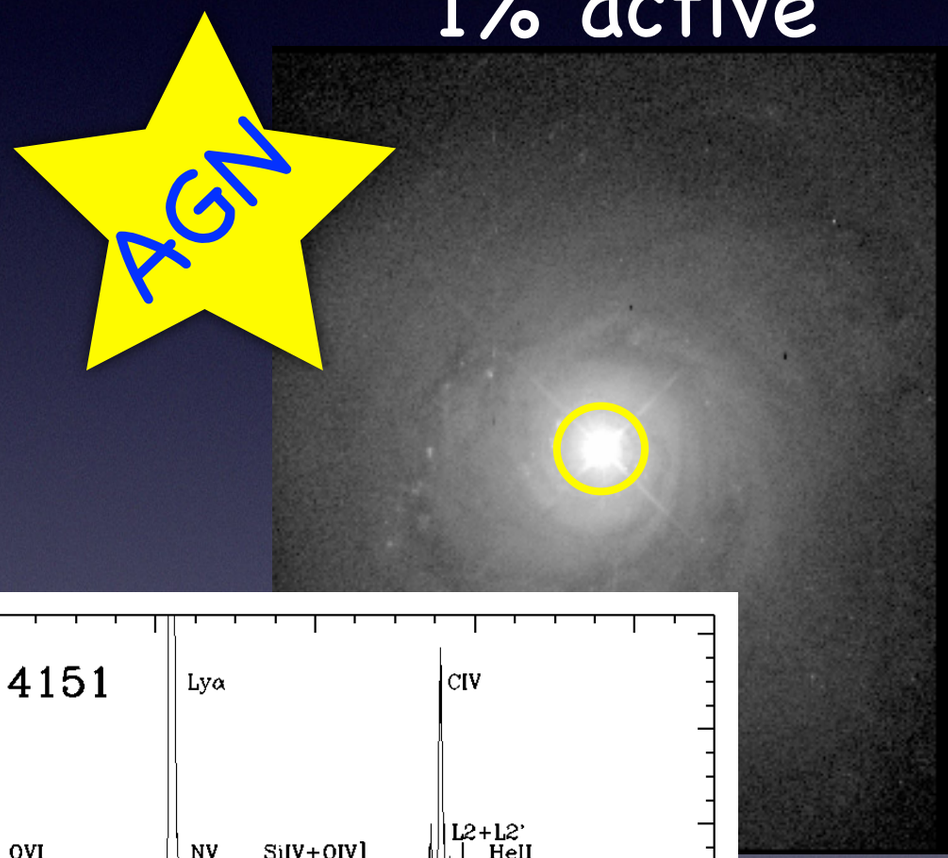

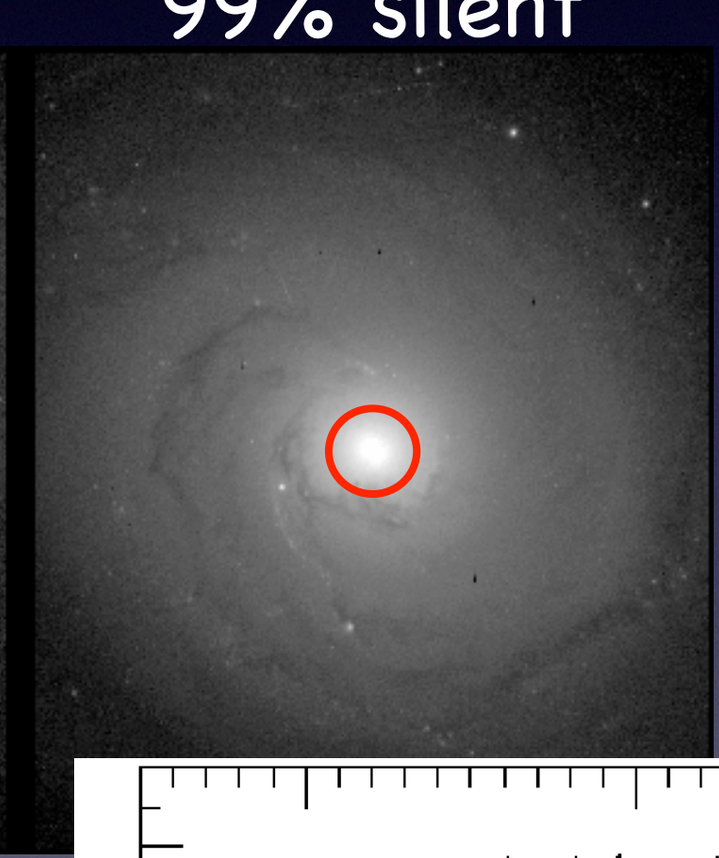

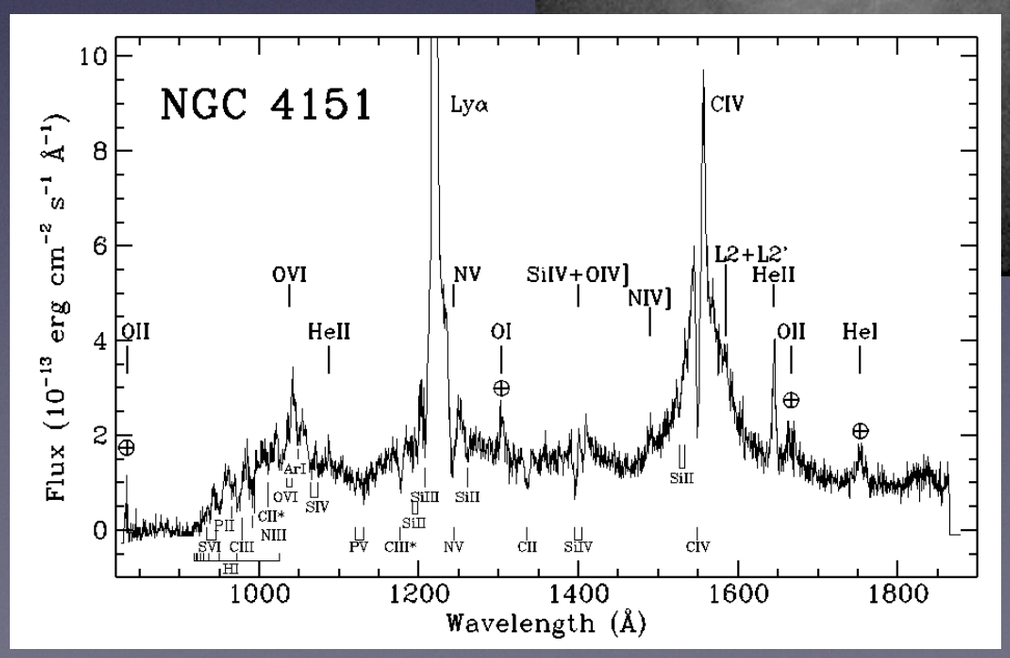

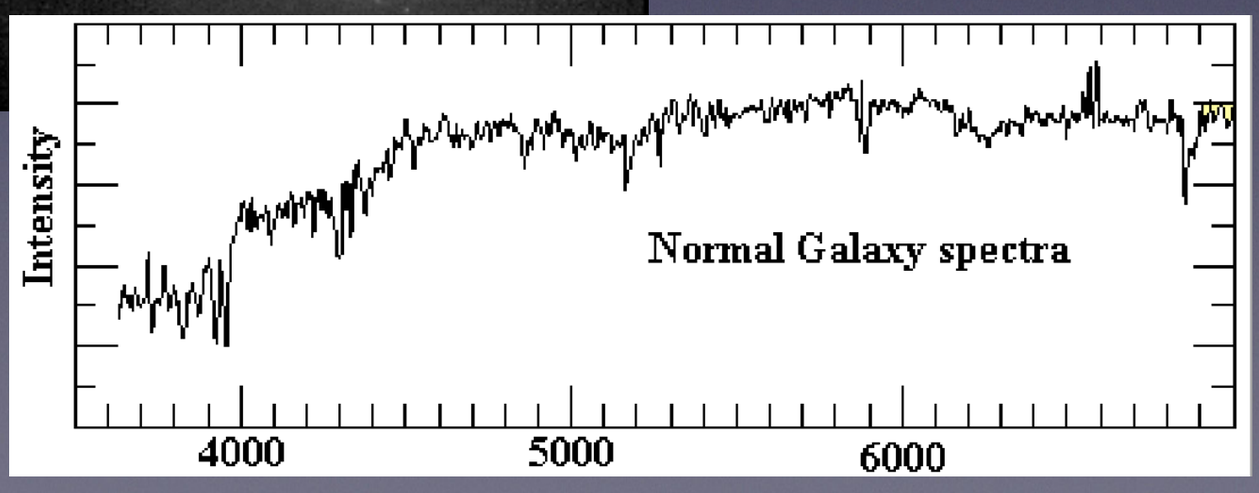

The engine occupies a tiny region in the center of the galaxy

30 kpc

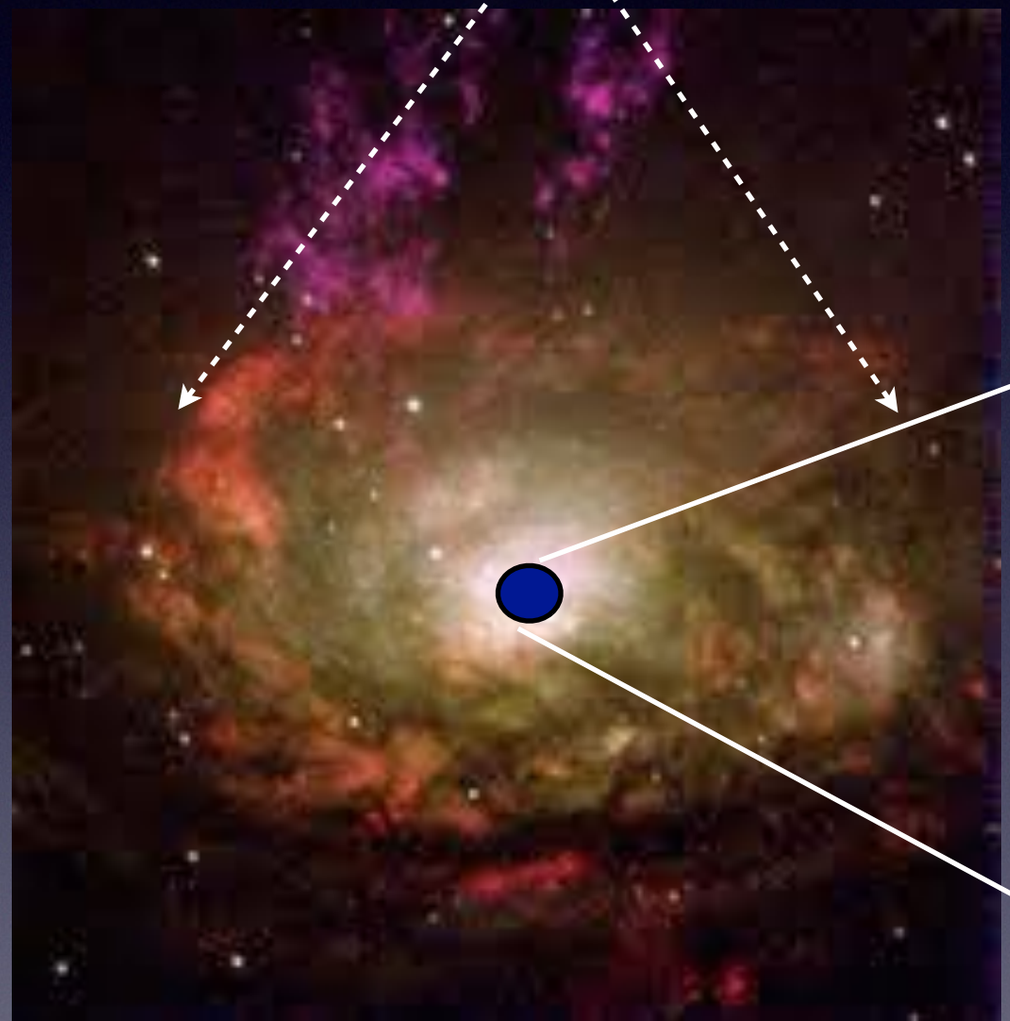

2-3 pc

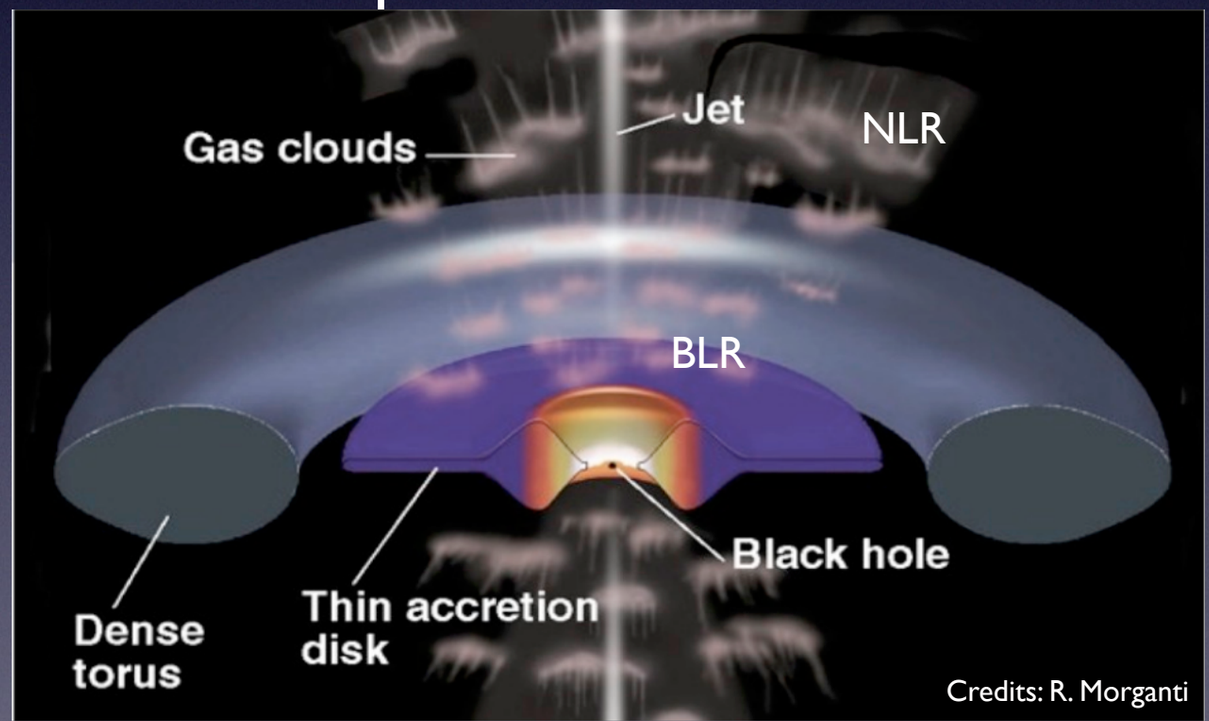

The extraordinary amount of energy is produced through accretion of gas close to a SMBH

About 15-20% of AGNs is Radio-Loud (RL) (Urry & Padovani 95)

An AGN is RL when

$$R = \frac{F_{5GHz}}{F_B} \geq 10$$

Kellermann et al. 1989

R= radio loudness parameter

$$\log R_X = \frac{\nu L_\nu(5\mathrm{GHz})}{L_X} <= -4.5$$

Terashima & Wilson 2003

RL AGNs lie in ellipticals

RQ AGNs lie in spirals and ellipticals

Local Space Densities of Some Objects

Object		*Gpc^{-3}*
Spiral Galaxies	$M_v < -20$	5×10^6
	$M_v < -22$	3×10^5
	$M_v < -23$	3×10^3
Elliptical Galaxies (incl. S0)	$M_v < -20$	1×10^6
	$M_v < -22$	1×10^5
	$M_v < -23$	10^4
Rich Clusters of Galaxies		3×10^3
Radio Galaxies	$P_{1.4\ GHz} > 10^{23.5}$ W Hz^{-1}	3×10^3
	$P_{1.4\ GHz} > 10^{25}$ W Hz^{-1}	10
Radio Quasars	$P_{1.4\ GHz} > 10^{25}$ W Hz^{-1}	3
Radio Quiet Quasars	$M_v < -23$	100
	$M_v < -25$	1
Sy 1	$M_v < -20$	4×10^4
Sy 2	$M_v < -20$	1×10^5
BL Lac	$P_{1.4\ GHz} > 10^{23.5}$ W Hz^{-1}	80
Strong IRAS Galaxies	$L_{IR} > 10^{12}\ L_\odot$	300

from Blandford, Netzer and Woltjer, "Active Galactic Nuclei", *Lecture Notes 1990*

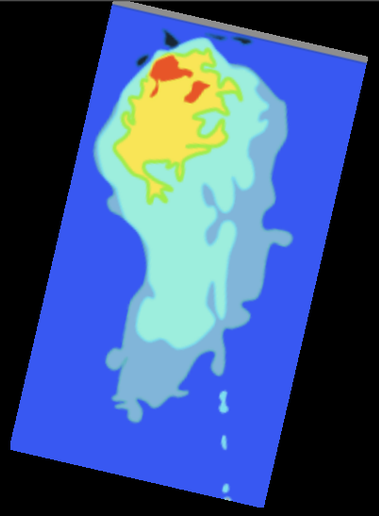

Radio Lobe

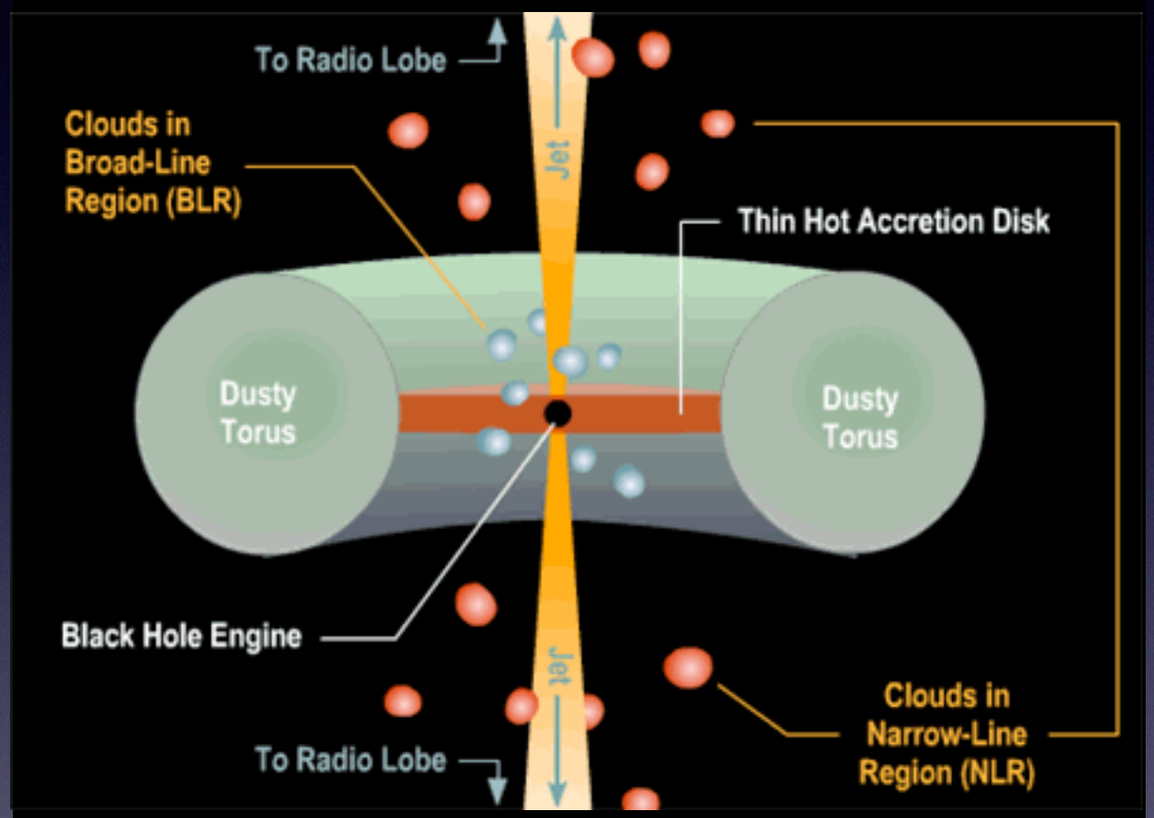

Some numbers for a typical AGN

BH Mass $\sim 10^8 M\odot$

Luminosity $\sim 10^{44}\ erg\ s^{-1}$

BH radius $\sim 3 \times 10^{13}\ cm$

BLR radius $\sim 2 - 20 \times 10^{16}\ cm$

NLR radius $\sim 10^{18} - 10^{20}\ cm$

In RL AGNs

Jet can be observed at $\sim 10^{17}\ cm$

Jets end at Kpc distances forming radio lobes

Fornax A

Radio lobes

Elliptical galaxy

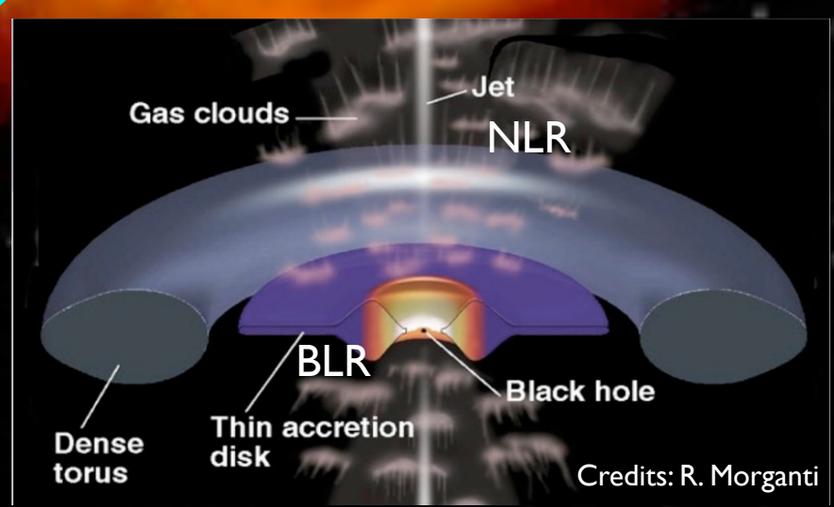

2-3 pc

Central engine

VLA/HST

Black hole-galaxy feedback

Supermassive black holes have a profound effect on the formation and evolution of galaxies (Silk & Rees 1998, Fabian 1999, and many others) by regulating the amount of gas available for the star formation

-> strong link between BH formation and properties of the stellar bulge (correlations between host galaxy properties and masses of SMBHs)

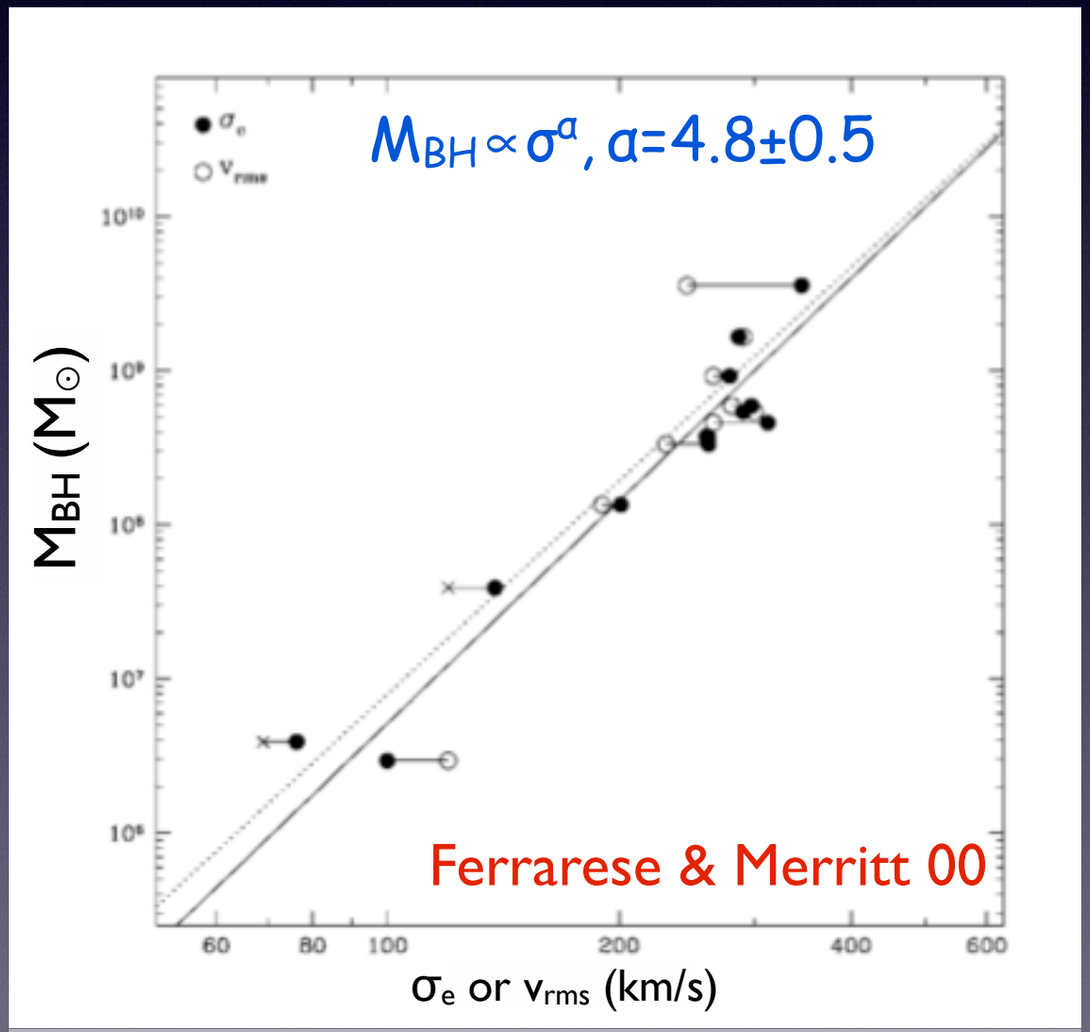

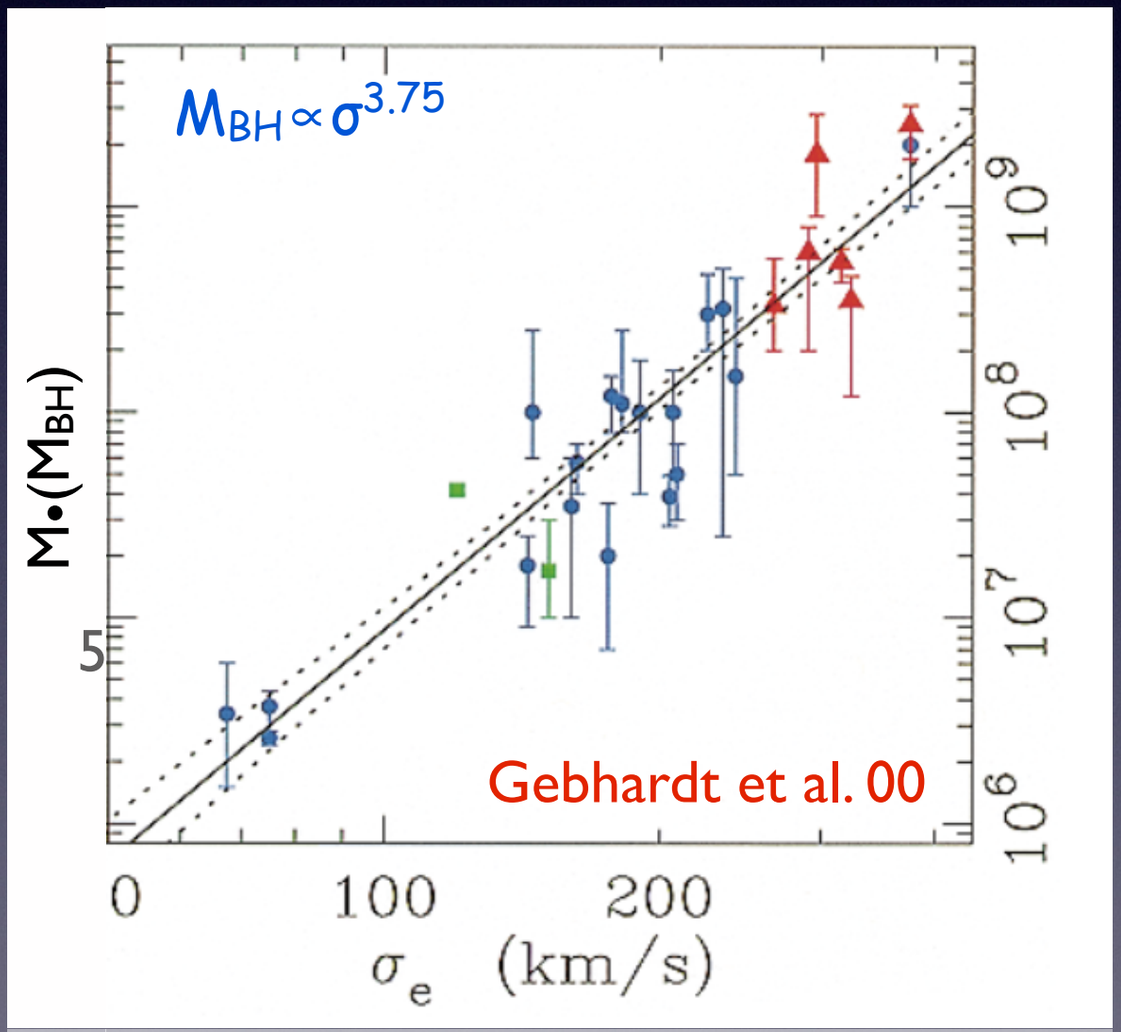

There are two types of feedback

RADIATIVE FEEDBACK radiative heating (primarily X-rays) nearby the SMBH (Ciotti & Ostriker 2007) that reduces cooling flows at the 10^2–10^3 pc scale.

MECHANICAL FEEDBACK feedback due to mechanical and thermal deposition of energy from jets and winds emitted by the accretion disk around the central BH (Ciotti, Ostriker & Proga 2009). The inner parts (10^1–10^2 pc) of elliptical galaxies are heated and the inflow to the central BH is reduced.

BOTH TYPES OF FEEDBACK (acting on different radial scales) ARE REQUIRED

(Ciotti, Ostriker & Proga 2009; 2010)

radiative feedback is required to balance and consume the cooling flow gas ;
mechanical feedback is required to limit the growth of the SMBH.

1. AGN classification

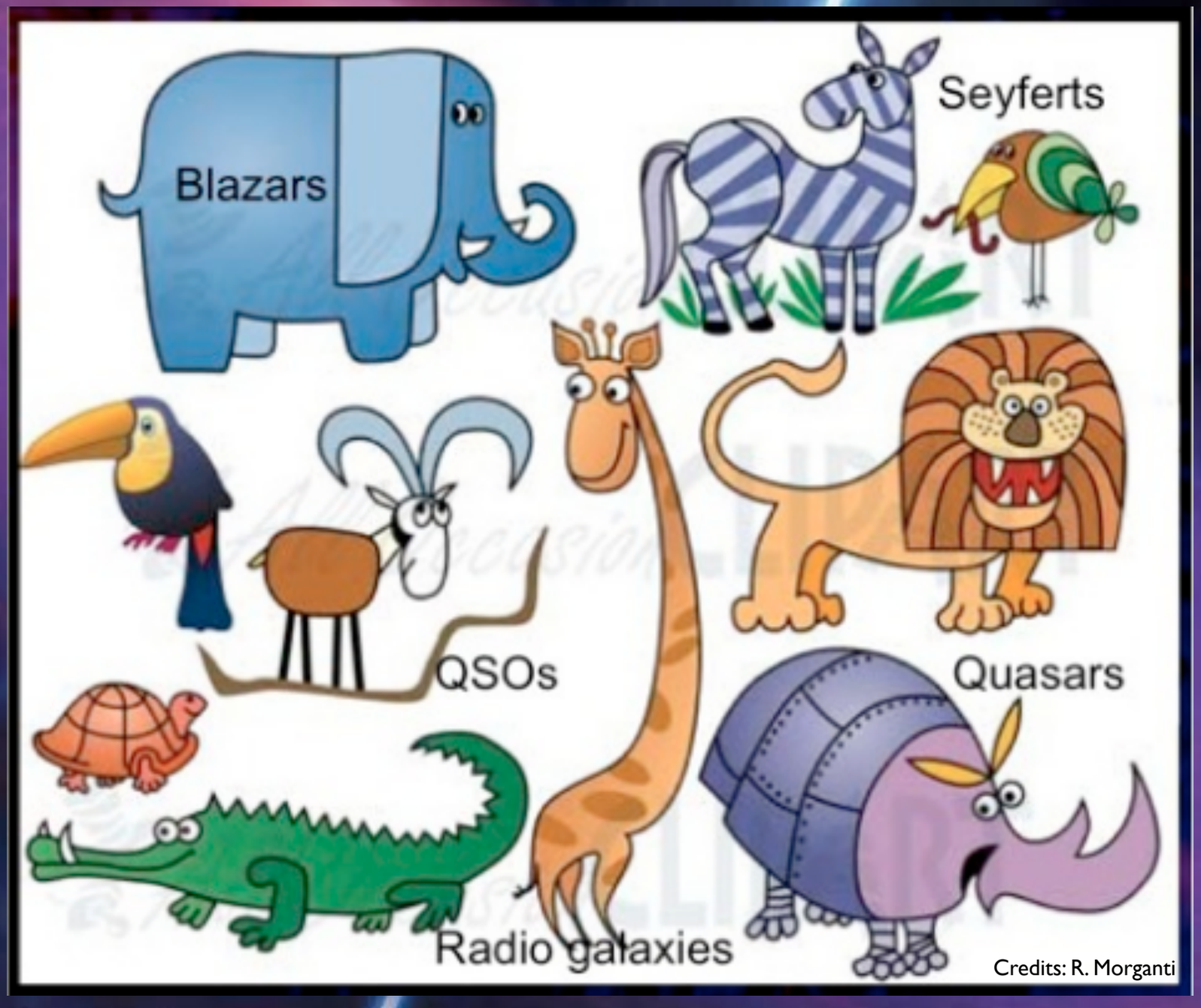

AGN classification

Optical classification

Type I	**bright continuum and BROAD emission lines from hot high velocity gas (FWHM~10^{3-4} km s^{-1})**
Type II	**weak continuum and only NARROW emission lines (FWHM~10^{2} km s^{-1})**

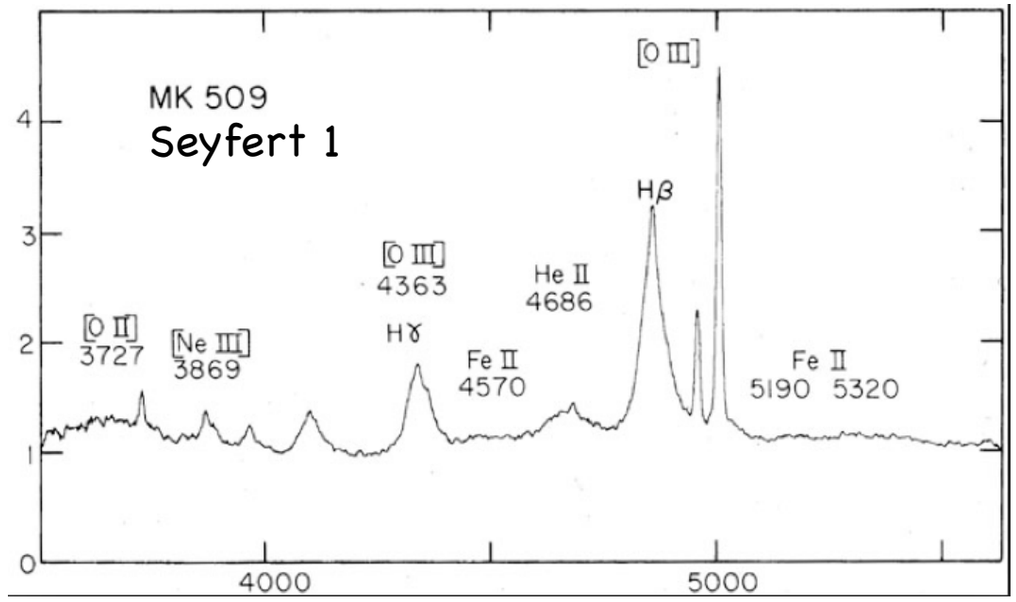

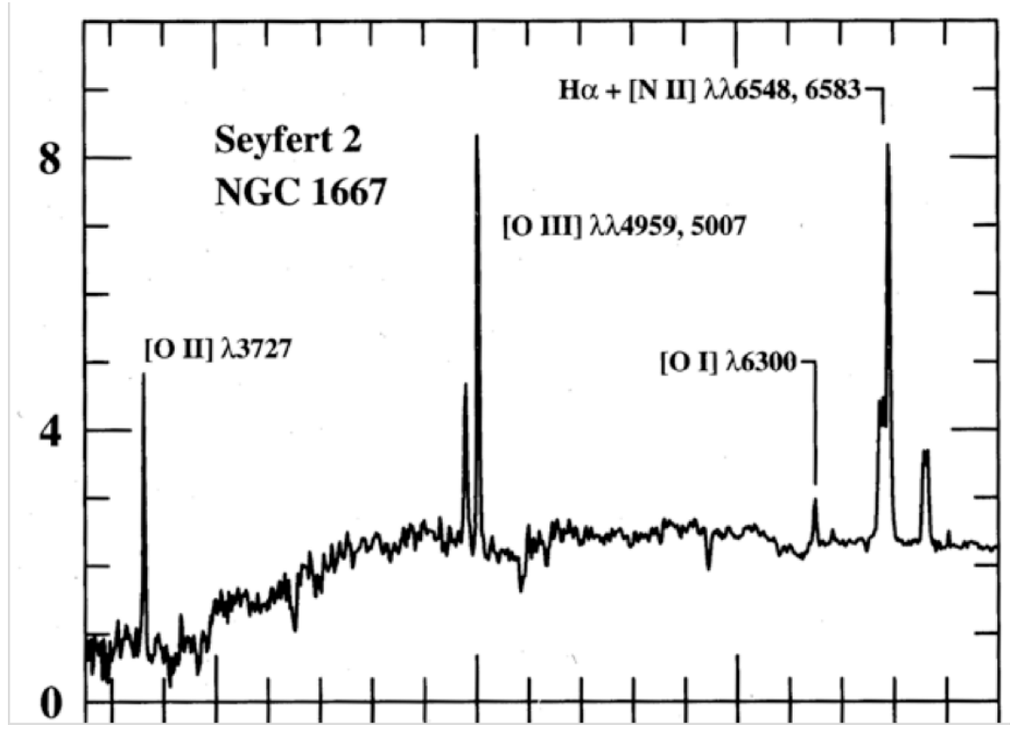

RL AGN classification

Optical classification		Radio classification
Type I/BLRGs Broad Line Radio Galaxies Flat Spectrum Radio Quasars/ Steep Spectrum Radio Quasars	bright continuum and BROAD emission lines from hot high velocity gas (FWHM~10^{3-4} km s^{-1})	**FRII**
Type II/NLRGs **HEG** Narrow Line Radio Galaxies/ High Excitation Galaxies	weak continuum and only NARROW emission lines (FWHM~10^{2} km s^{-1})	**FRII**
Type II/NLRGs **LEG** Narrow Line Radio Galaxies/ Low Excitation Galaxies	narrow emission lines: $EW_{[OIII]}$>10 Å and/or O[II]/O[III]>1	**FRII** **FRI**
Type 0	Almost featureless in the optical band and extremely variable	**BL Lac**

FRI - $P_{178MHz} < 10^{25}$ W Hz^{-1} sr^{-1}

FRII - $P_{178MHz} > 10^{25}$ W Hz^{-1} sr^{-1}

(Fanaroff & Riley 1974)

Observed radio morphologies: The Fanaroff-Riley classification

FRI/jet dominated

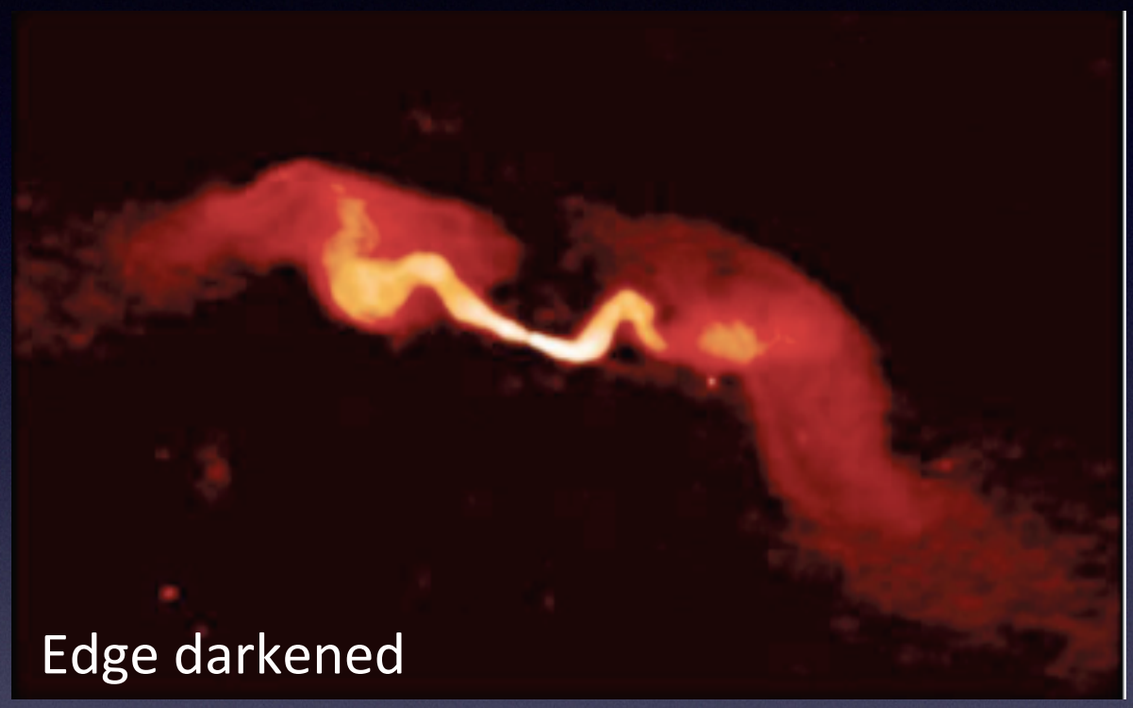

In FRI the jets are thought to decelerate and become sub-relativistic on scales of hundred of pc to kpc.

The nuclei of FRI are not generally absorbed and probably powered by inefficient accretion flows.

The jets in FRII are at least moderately relativistic and supersonic from the core to the hot spots.
Most FRII are thought to have an efficient engine and a dusty torus.

FRII/lobe dominated

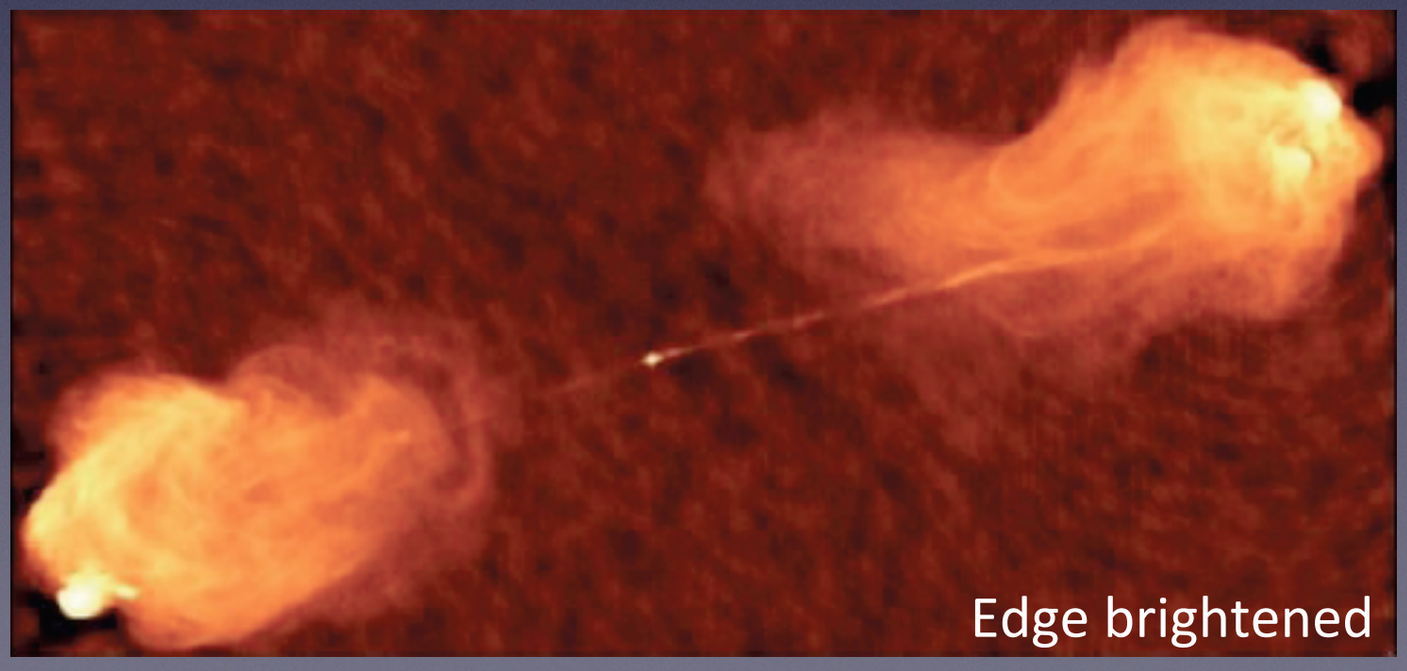

Whether a radio-loud AGN is a blazar or a radio galaxy depends on the alignment of the relativistic jet with the line-of-sight

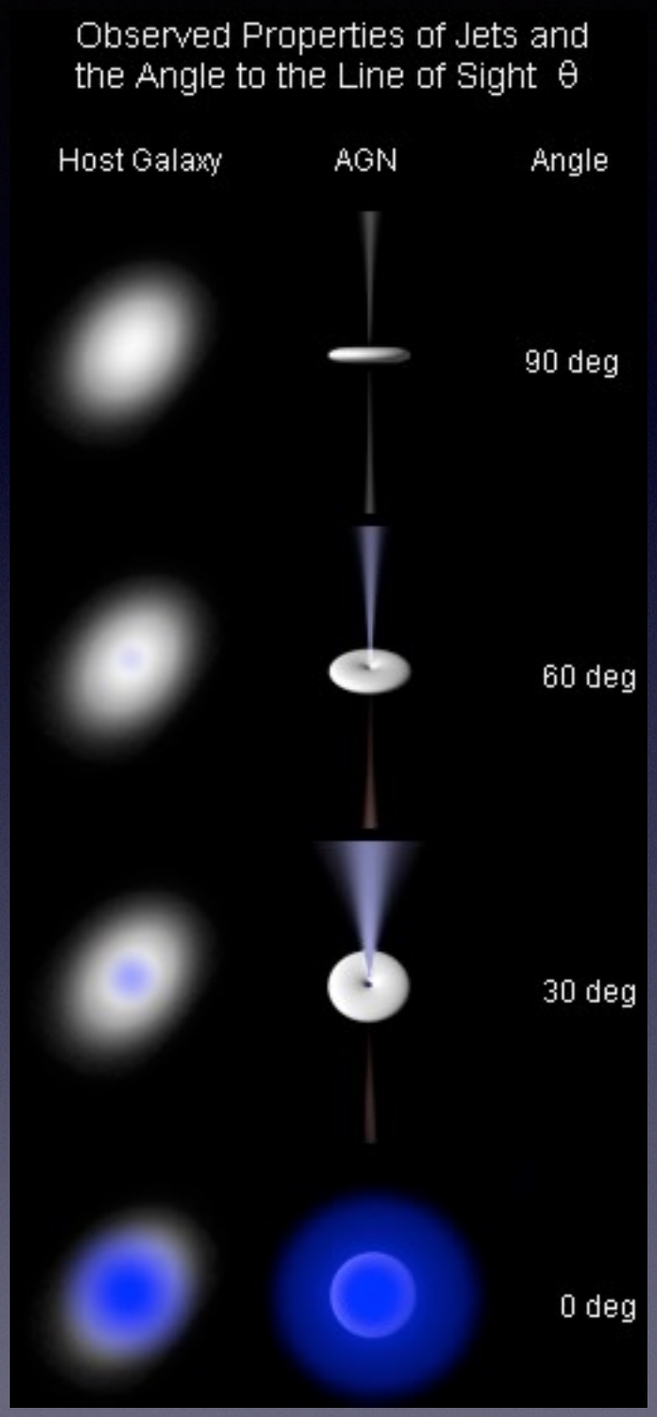

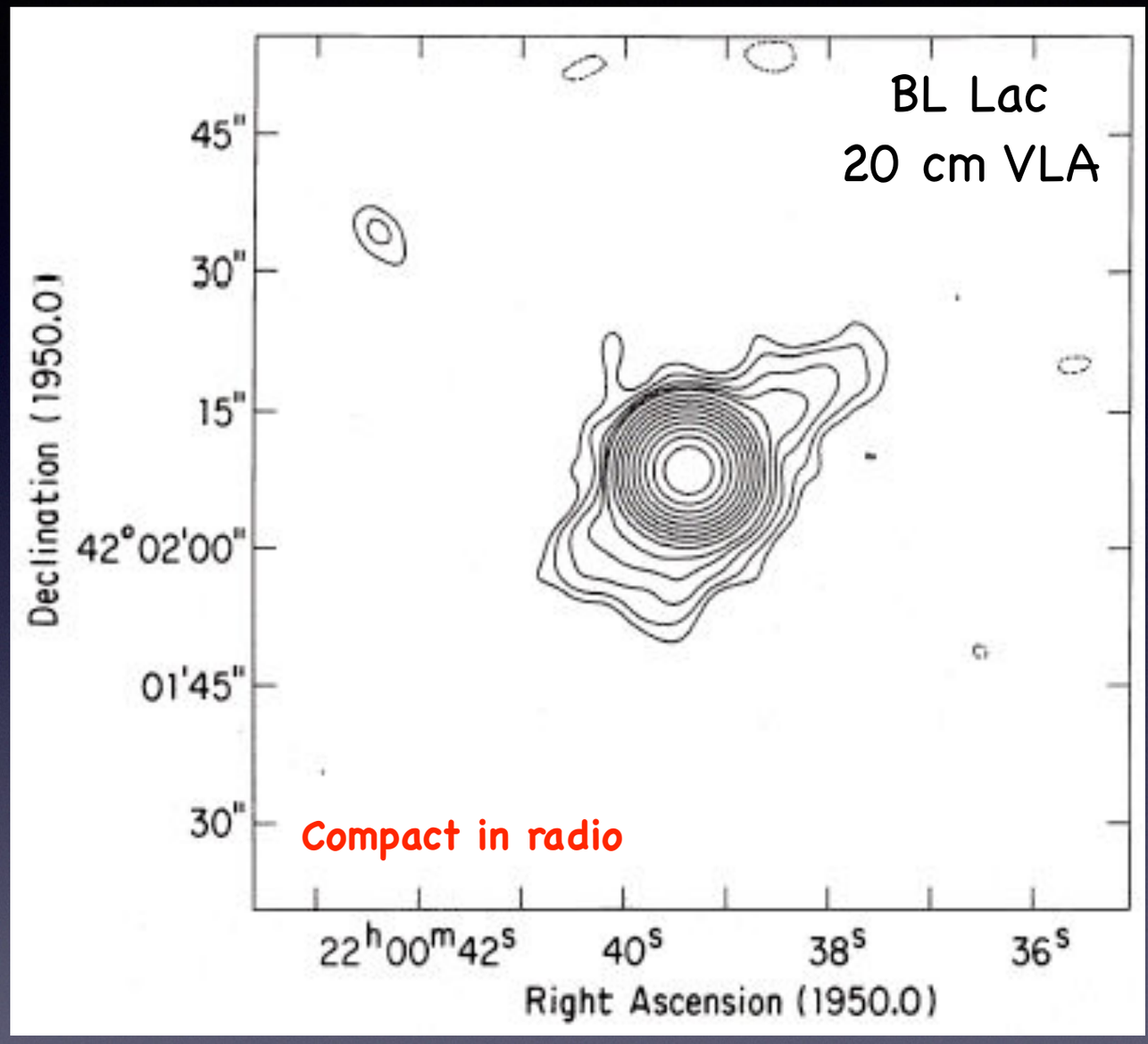

(Antonucci 1986)

FRIs are considered the
PARENT POPULATION of BL LACs

(Urry & Padovani 1995)

FRIIs are considered the PARENT POPULATION of Flat Spectrum Radio Quasars (Urry & Padovani 1995)

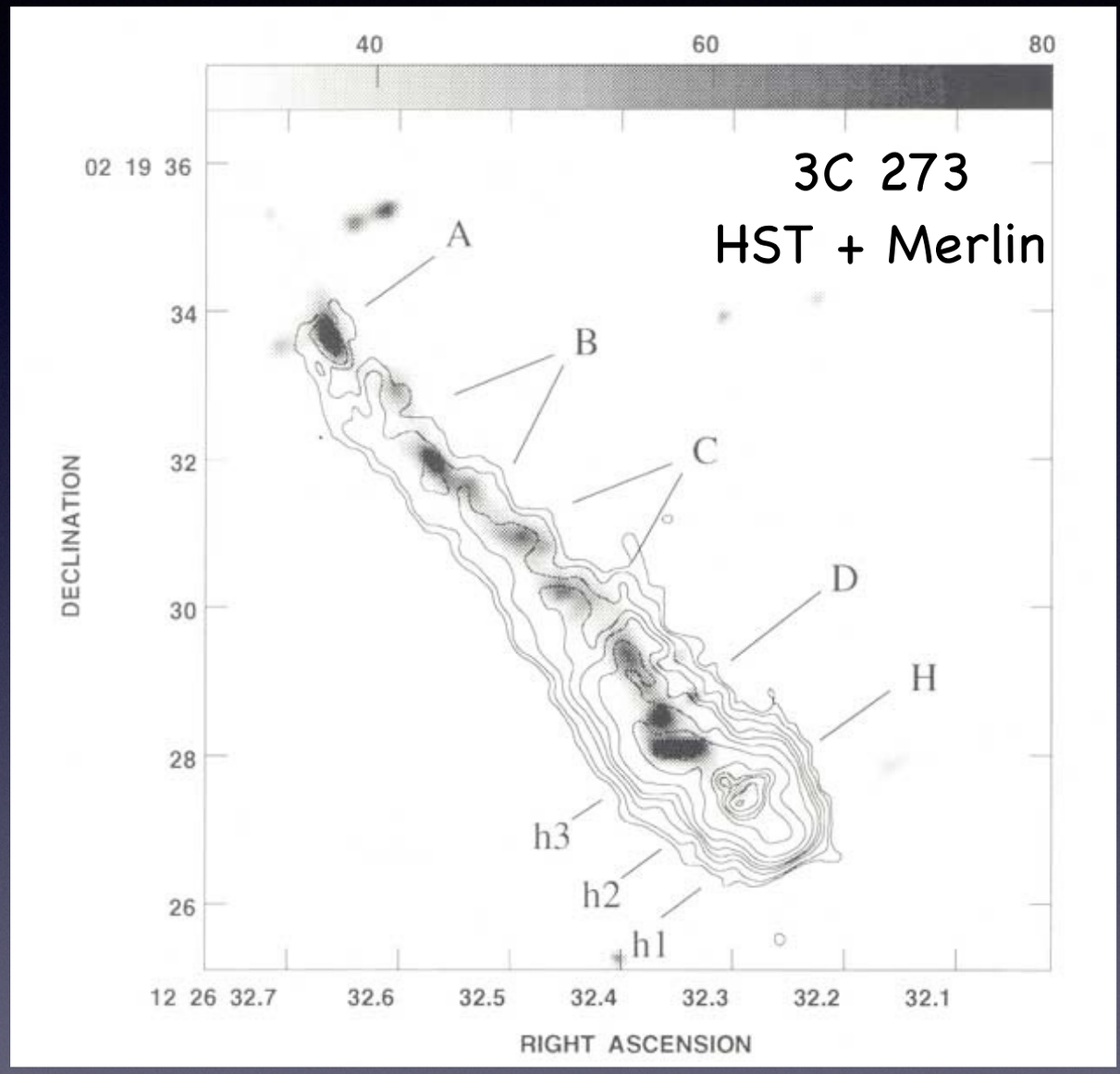

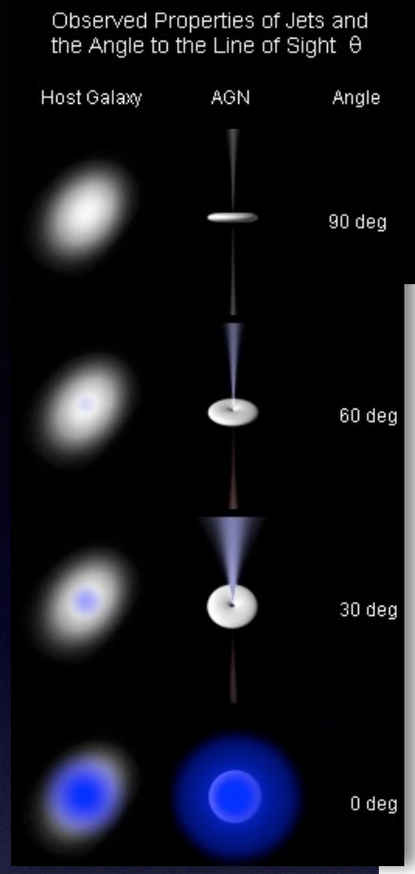
Observed Properties of Jets and
the Angle to the Line of Sight θ
Host Galaxy
AGN
Angle
90 deg
60 deg
30 deg
0 deg

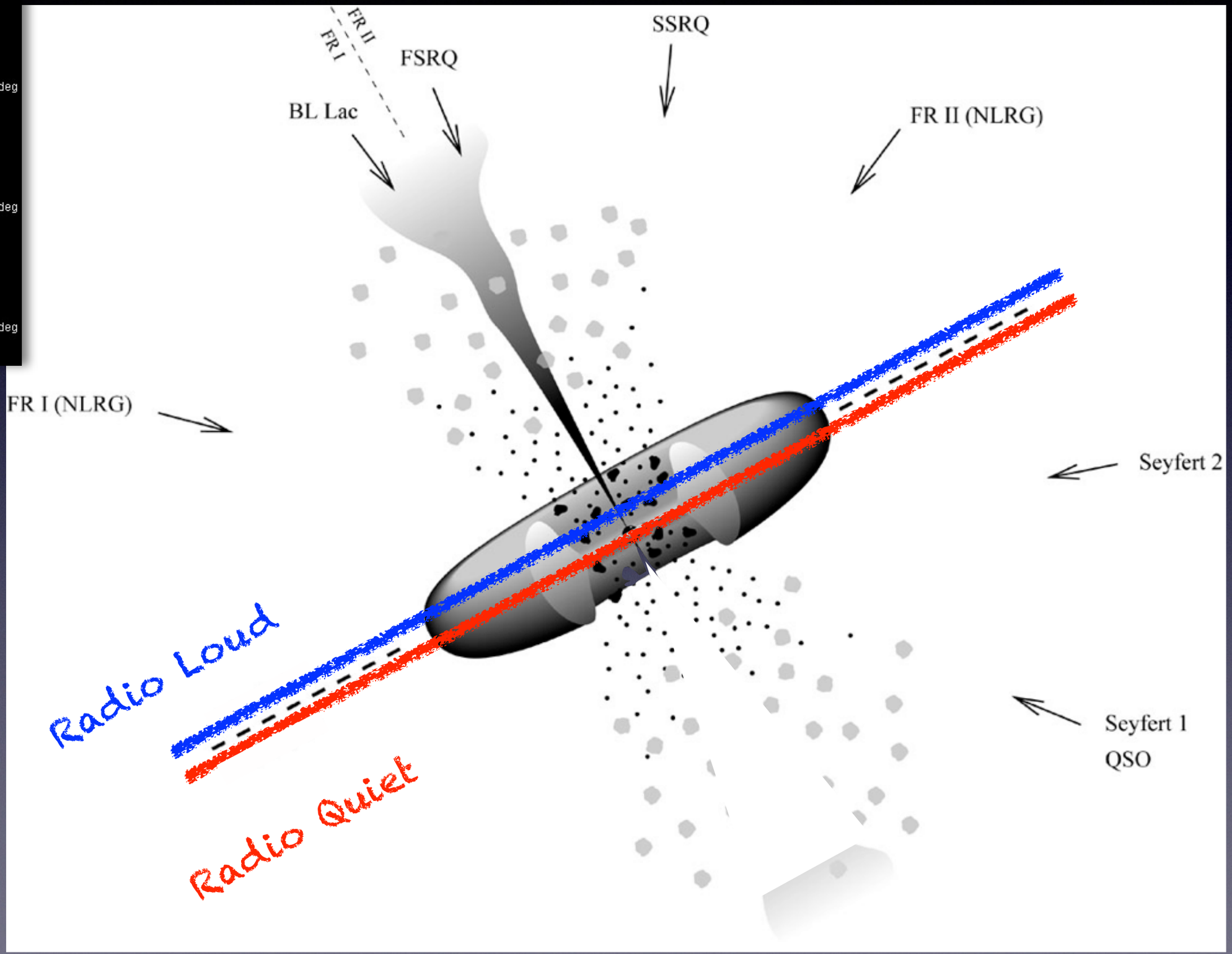
FR II
FR I
FSRQ
SSRQ
BL Lac
FR II (NLRG)
FR I (NLRG)
Seyfert 2
Radio Loud
Radio Quiet
Seyfert 1
QSO

2. Spectral Energy Distribution of AGN

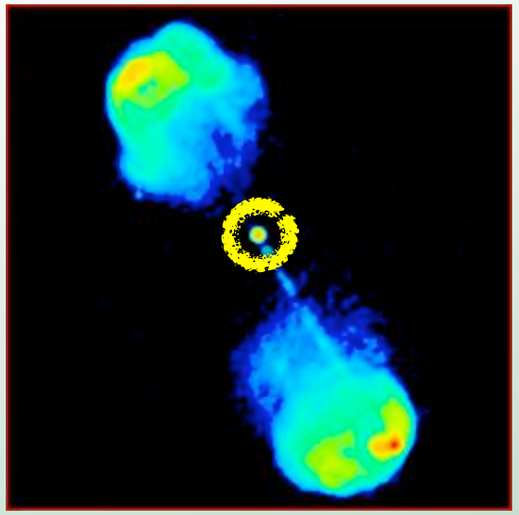

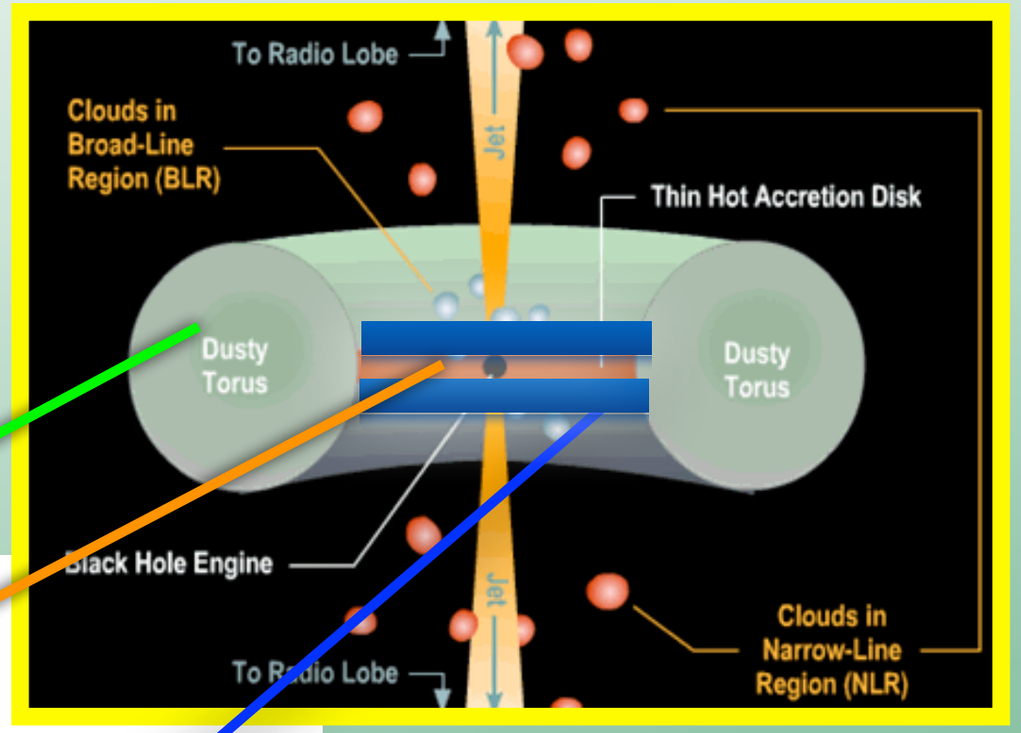

Spectral Energy Distribution (SED)

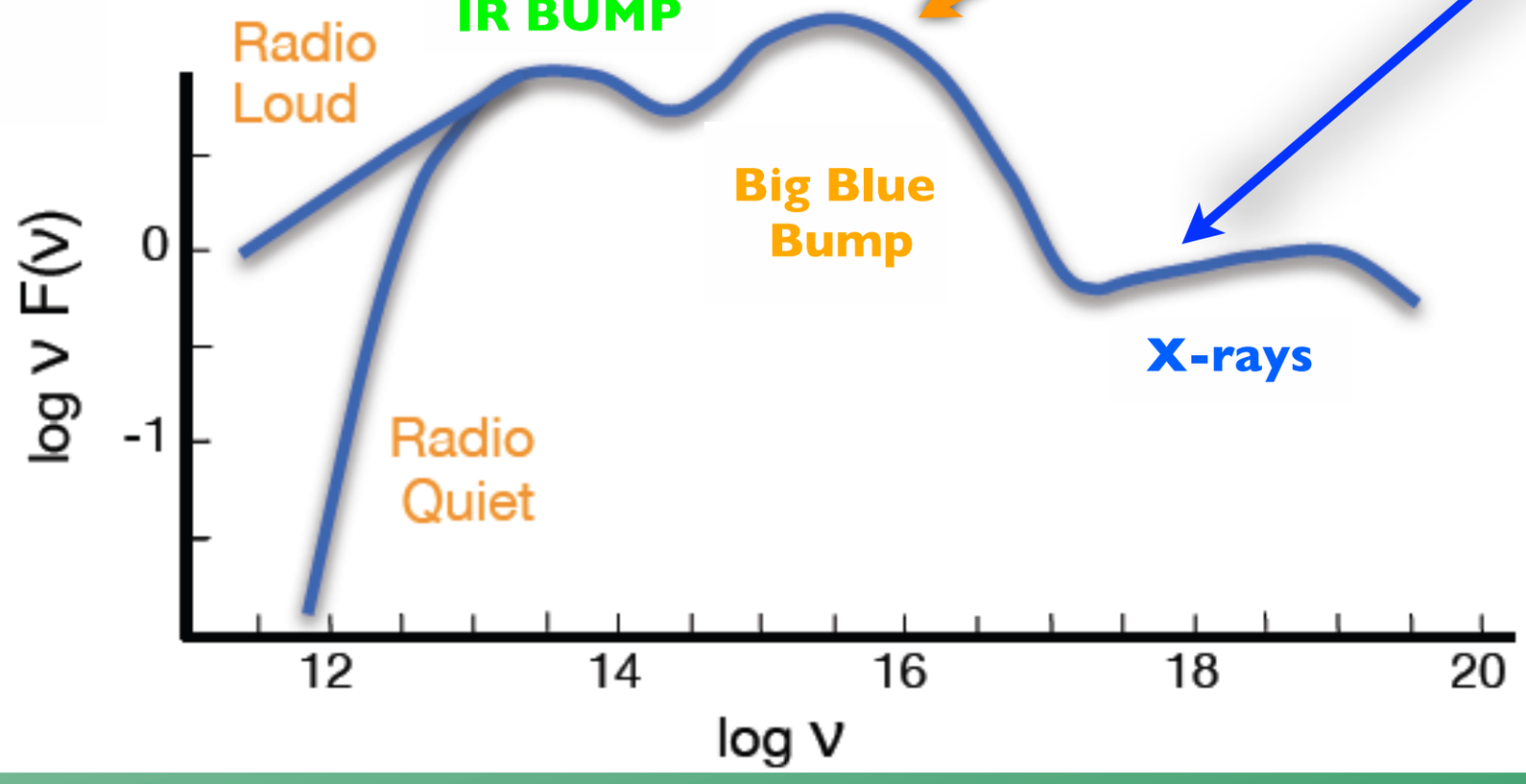

Radio Galaxies: kpc components

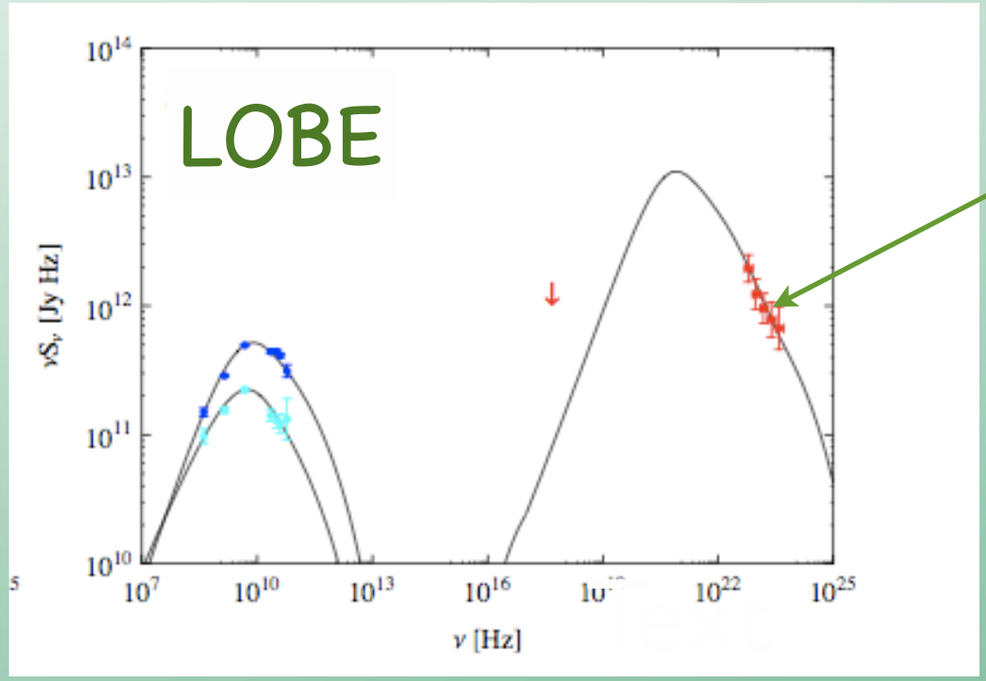

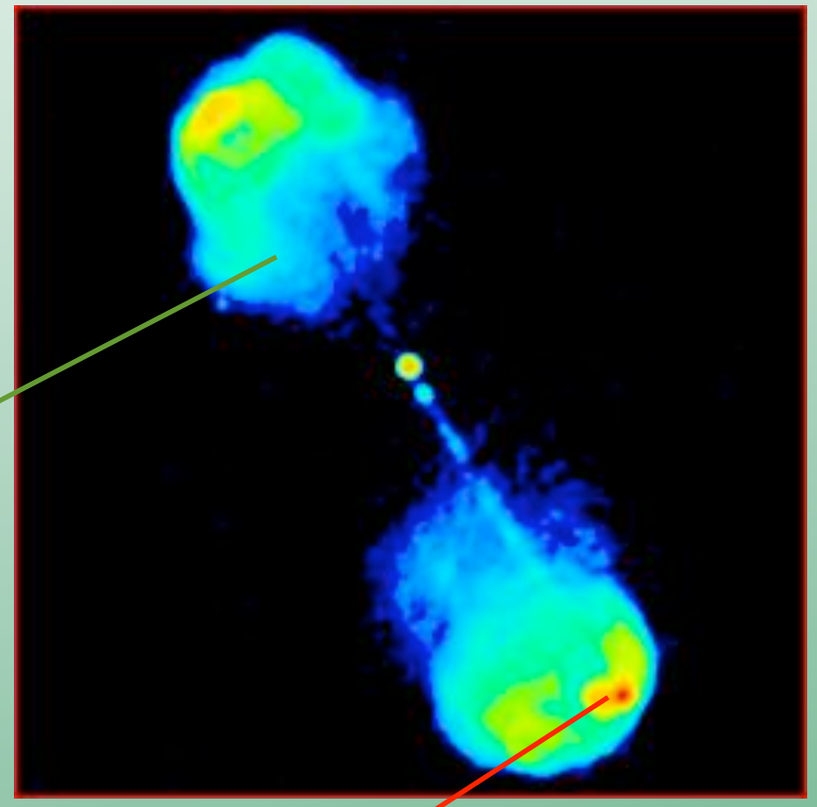

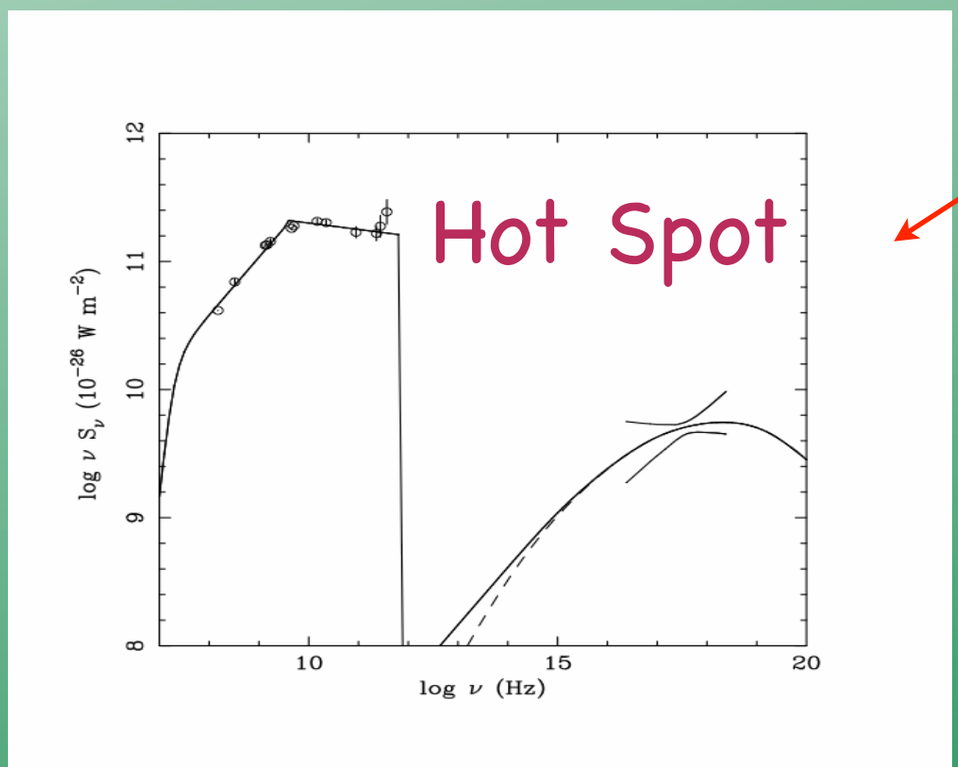

Synchrotron

Inverse Compton

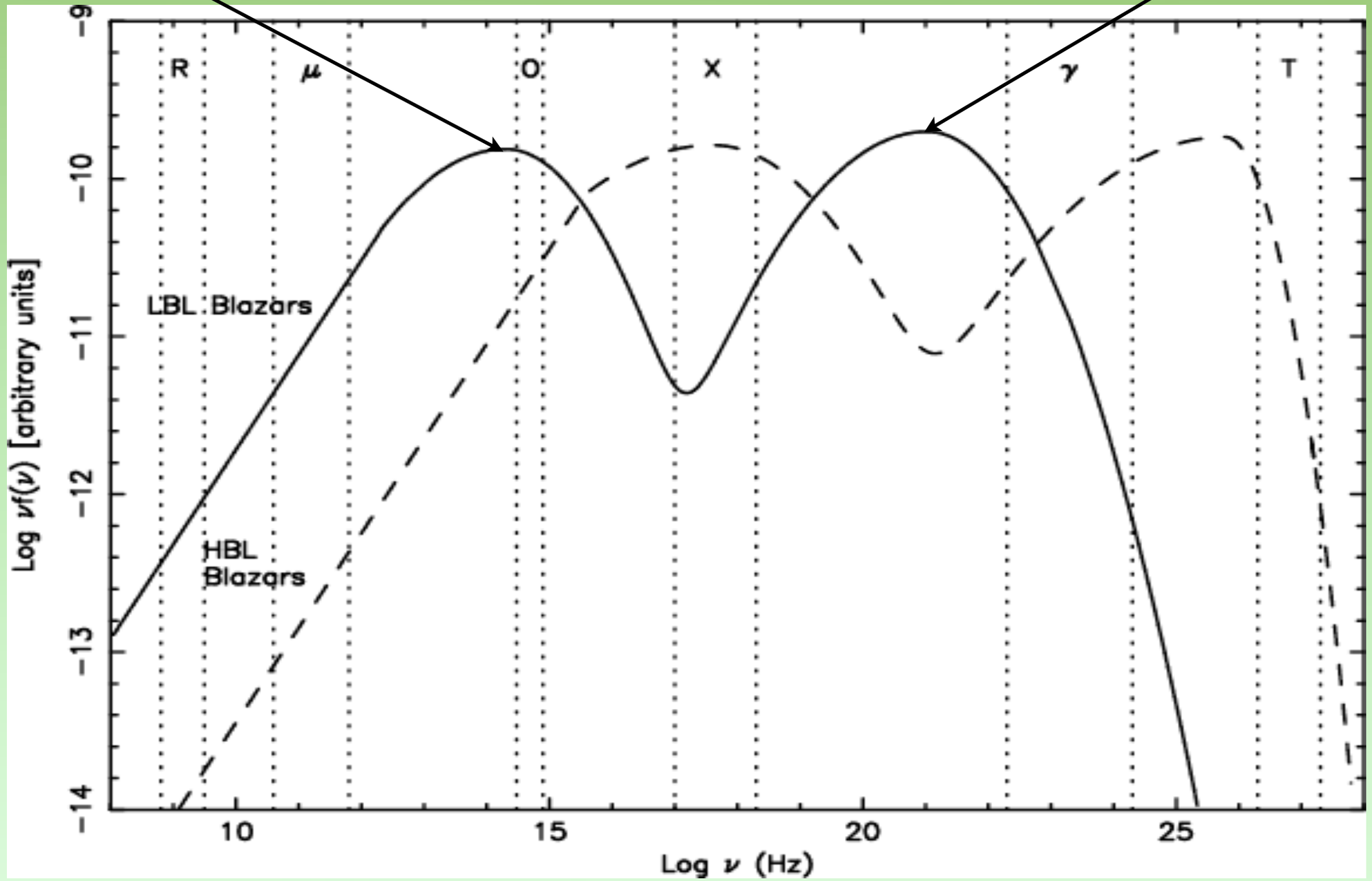

LBL= low-frequency peaked blazars

HBL= high-frequency peaked blazars

BLAZARS: double peaked SEDs

Synchrotron

Inverse Compton

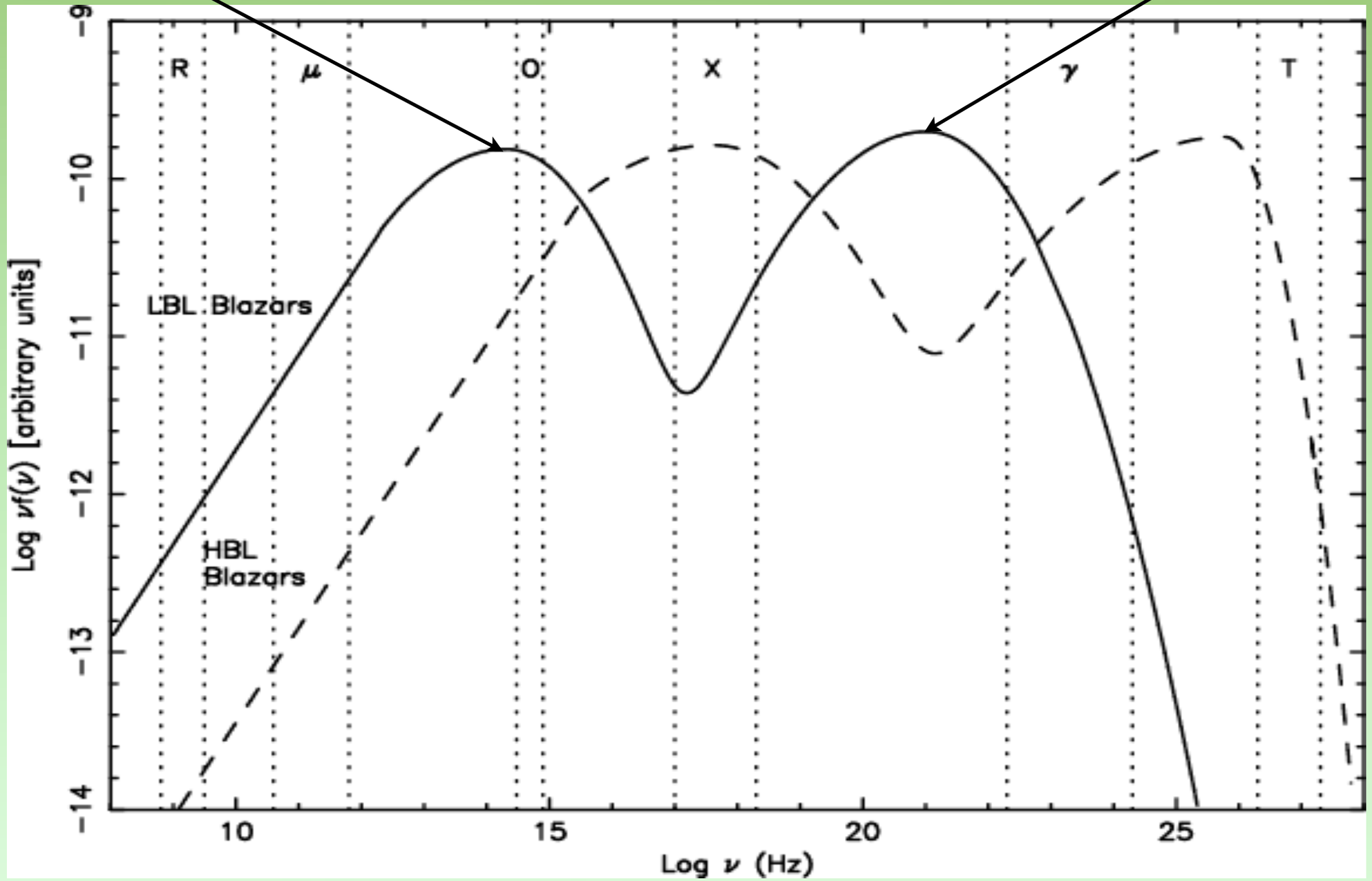

LBL= low-frequency peaked blazars

HBL= high-frequency peaked blazars

BLAZARS: double peaked SEDs

Synchrotron

Inverse Compton

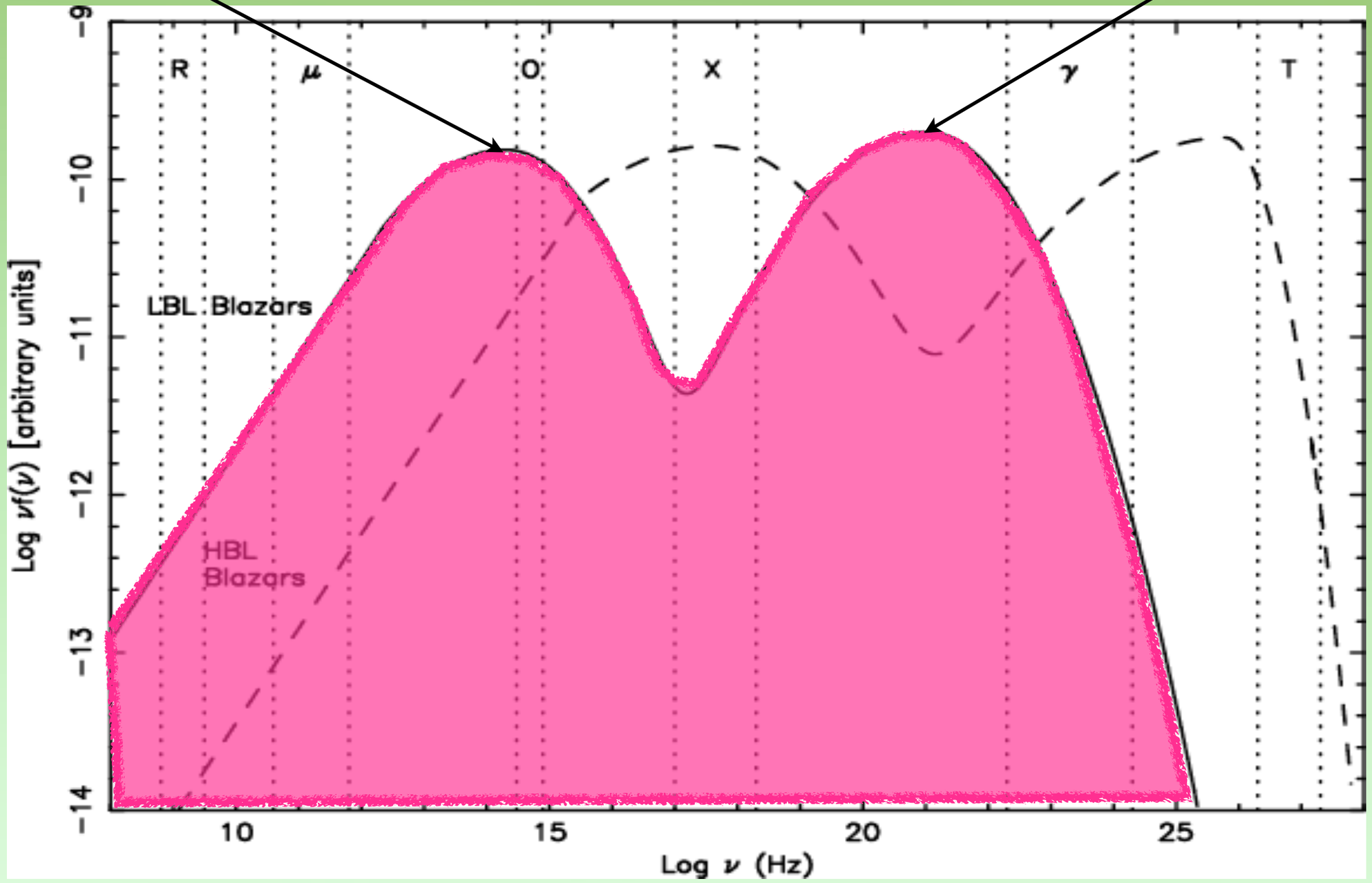

LBL= low-frequency peaked blazars

HBL= high-frequency peaked blazars

BLAZARS: double peaked SEDs

Synchrotron

Inverse Compton

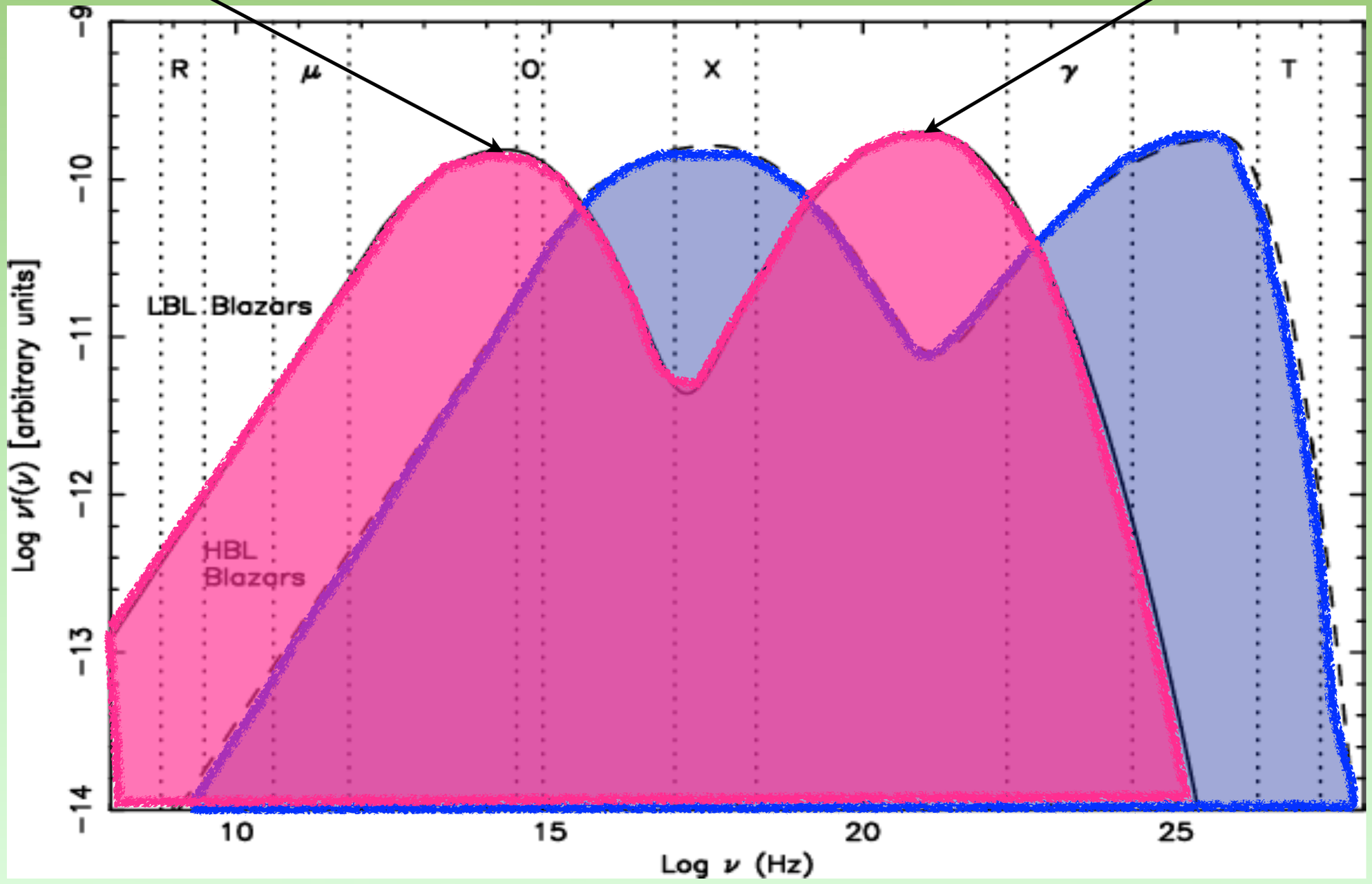

LBL= low-frequency peaked blazars

HBL= high-frequency peaked blazars

The jet emission from blazars is strongly Doppler boosted with respect to radio galaxies

The key parameter is the Doppler Factor $\delta(\beta, \theta)$

$$\delta = [\gamma(1 - \beta cos\theta)]^{-1}$$

$=\sqrt{(1-\beta^2)}$
Lorentz factor

=v/c
bulk velocity

angle between the jet axis and the line of sight

The Doppler factor relates intrinsic and observed flux for a moving source at relativistic speed v=β c.

For an **intrinsic** power law spectrum: $F'(\nu') = K (\nu')^{-\alpha}$
the **observed** flux density is

$$F_\nu(\nu) = \delta^{3+\alpha} F'_{\nu'}(\nu)$$

$$\Delta t = \Delta t' / \delta$$

The jet emission from blazars is strongly Doppler boosted with respect to radio galaxies

The key parameter is the Doppler Factor $\delta(\beta, \theta)$

$$\delta = [\gamma(1 - \beta cos\theta)]^{-1}$$

$=\sqrt{(1-\beta^2)}$ Lorentz factor

=v/c bulk velocity

angle between the jet axis and the line of sight

The Doppler factor relates intrinsic and observed flux for a moving source at relativistic speed v=β c.

For an **intrinsic** power law spectrum: $F'(\nu') = K (\nu')^{-\alpha}$ the **observed** flux density is

$$F_\nu(\nu) = \delta^{3+\alpha} F'_{\nu'}(\nu)$$

$$\Delta t = \Delta t' / \delta$$

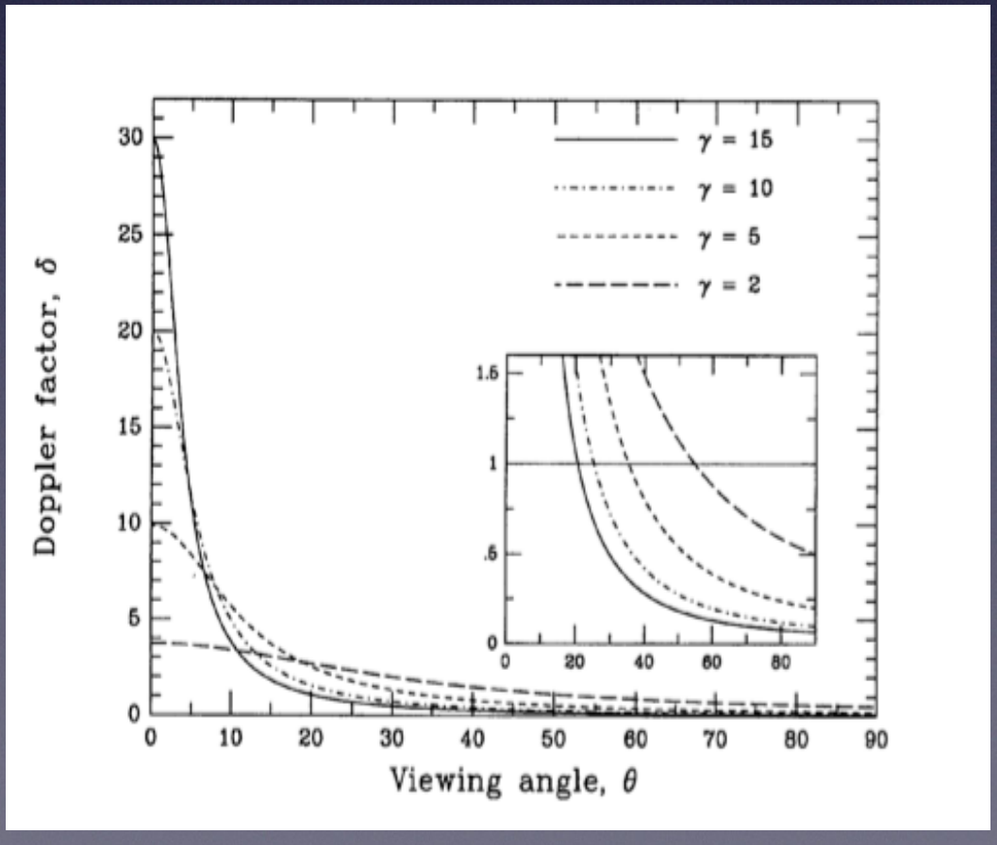

3. The FRI/FRII dichotomy

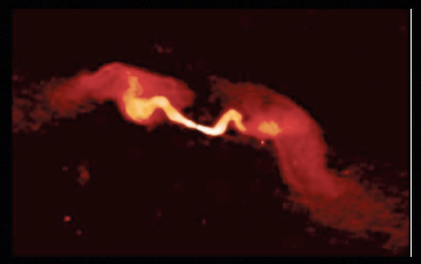

It is still unclear what causes the FRI/FRII dichotomy

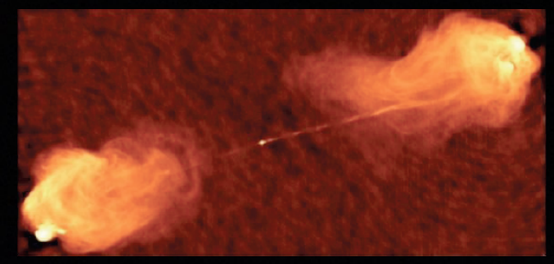

1) Ledlow & Owen (1994) found a correlation between the radio power at the FRI/FRII transition and the host galaxy magnitude

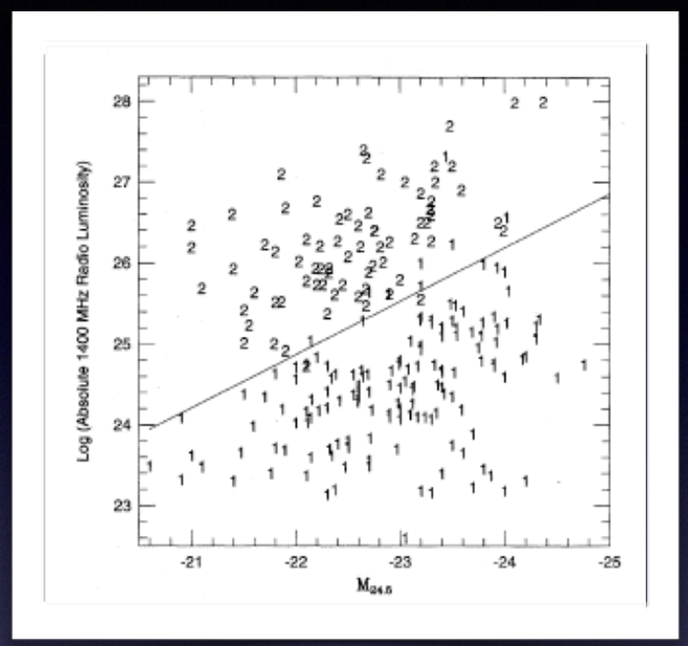

2) Bicknell 1995 points to different ways in which the jet interacts with the ambient medium: the FRI jets start highly relativistic and decelerate between the sub-pc and kpc scales

3) Baum et al. (1995) and Reynolds et al. (1996) suggest different nuclear intrinsic properties of the accretion and jet formation and the jet content

4) Ghisellini & Celotti (2001) indicate that the **accretion process** itself might play a key role in the deceleration and dichotomic behavior by affecting the pc-kpc scale environment

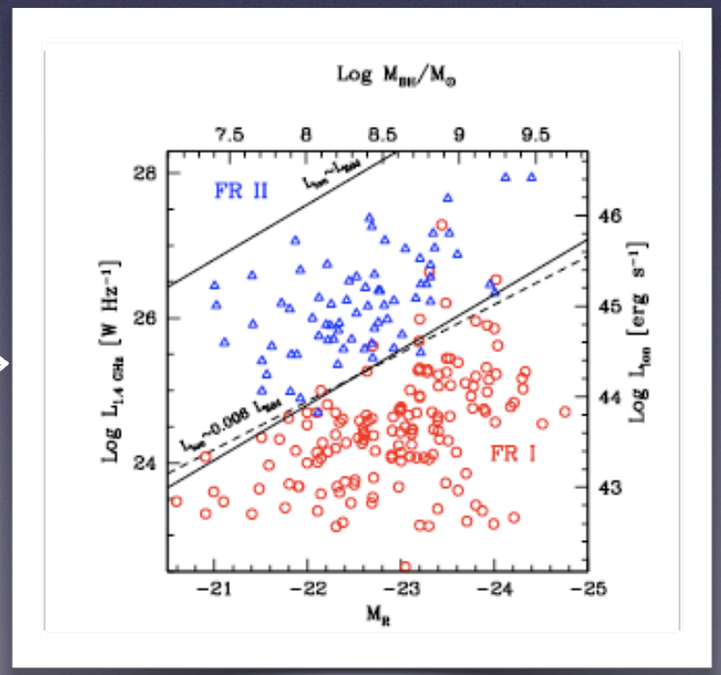

Optical observations seem to indicate that FRIs and FRIIs have different accretion regimes

The optical flux of FRIs shows a strong correlation with the radio core one over four decades, arguing for a non-thermal synchrotron origin of the nuclear emission (Chiaberge et al. 2002)

There is no nuclear absorption in FRI HST images. The weakness of the optical lines is not due to obscuration (Chiaberge et al. 2002)

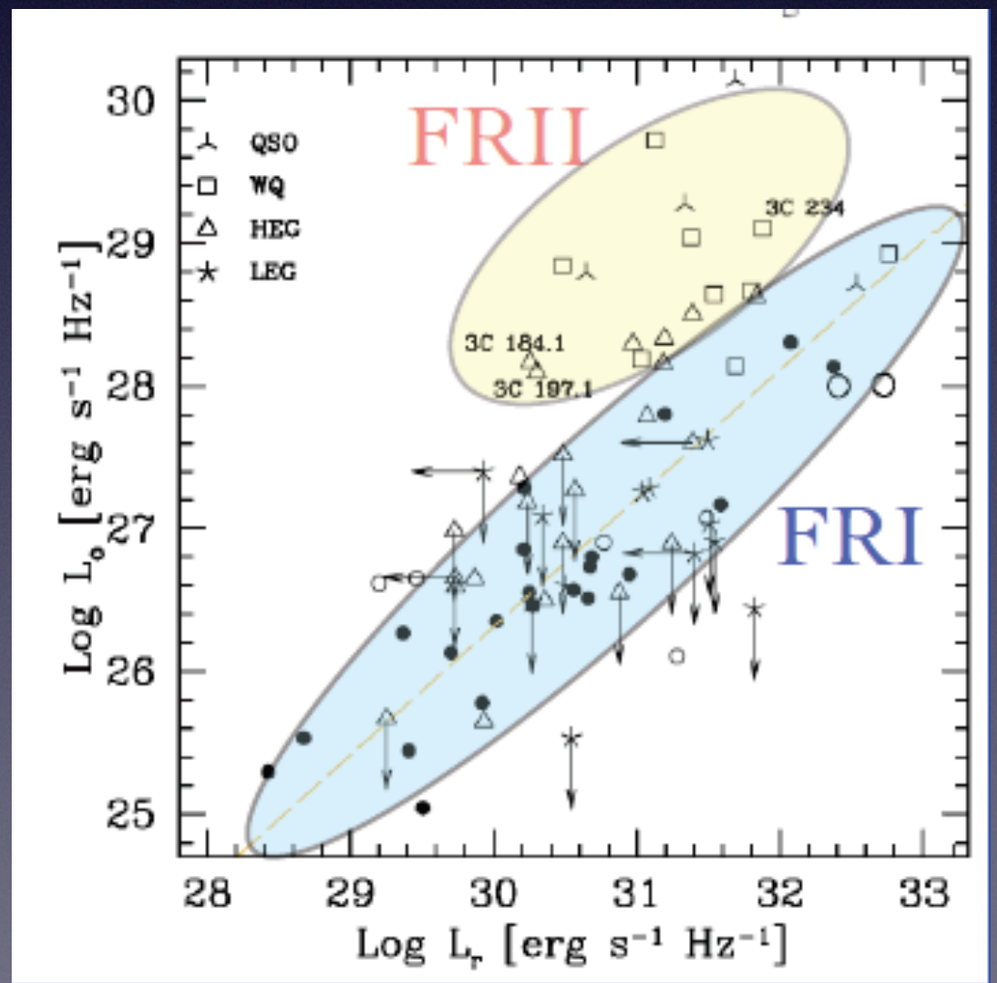

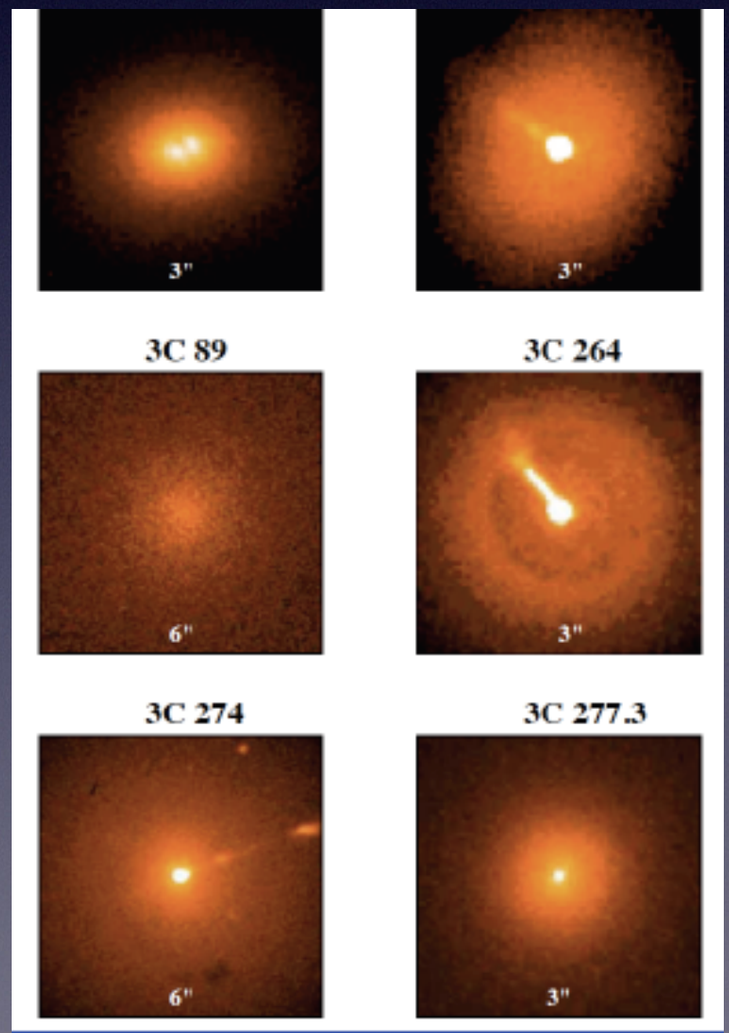

This scenario is also supported by IR observations...

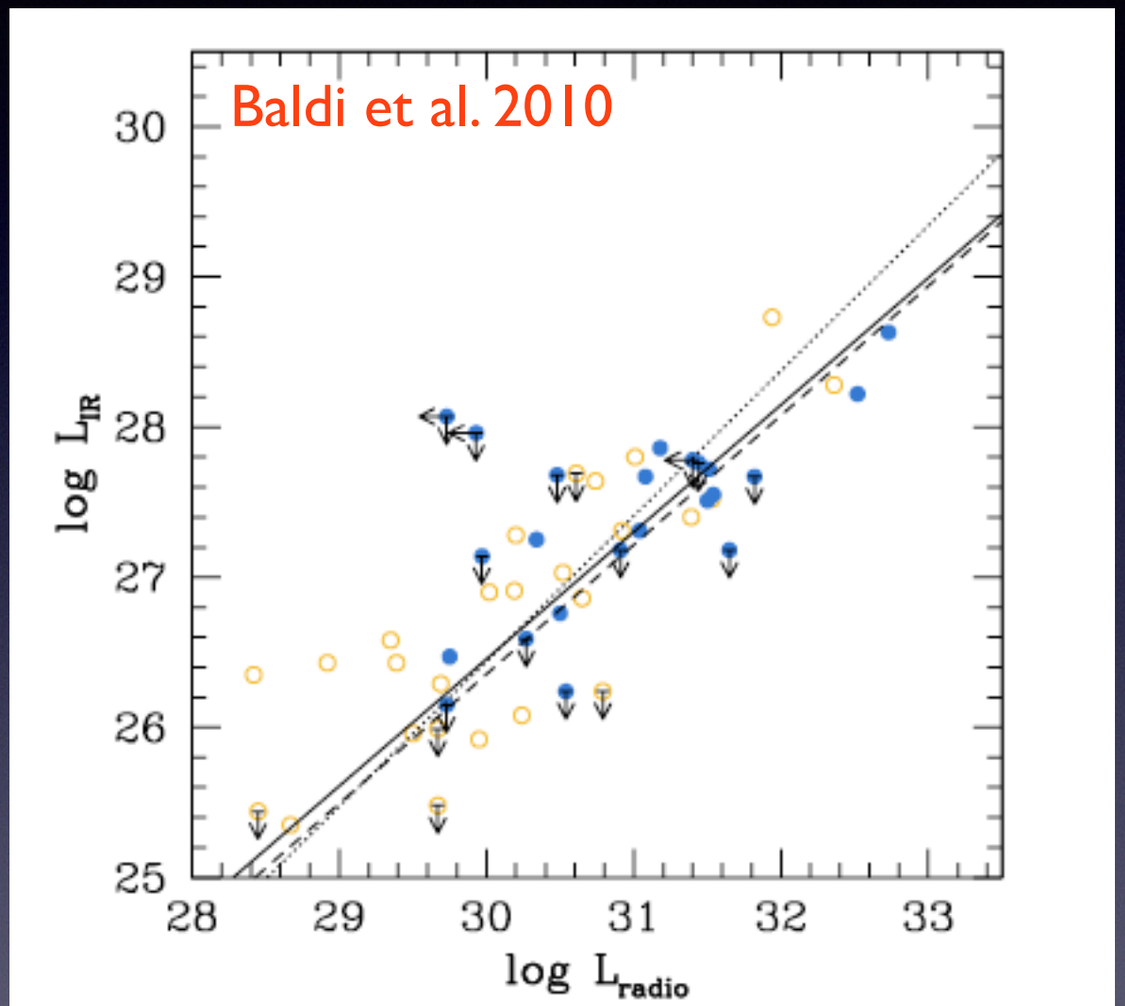

The NIR nuclear emission of FRIs has a non-thermal origin

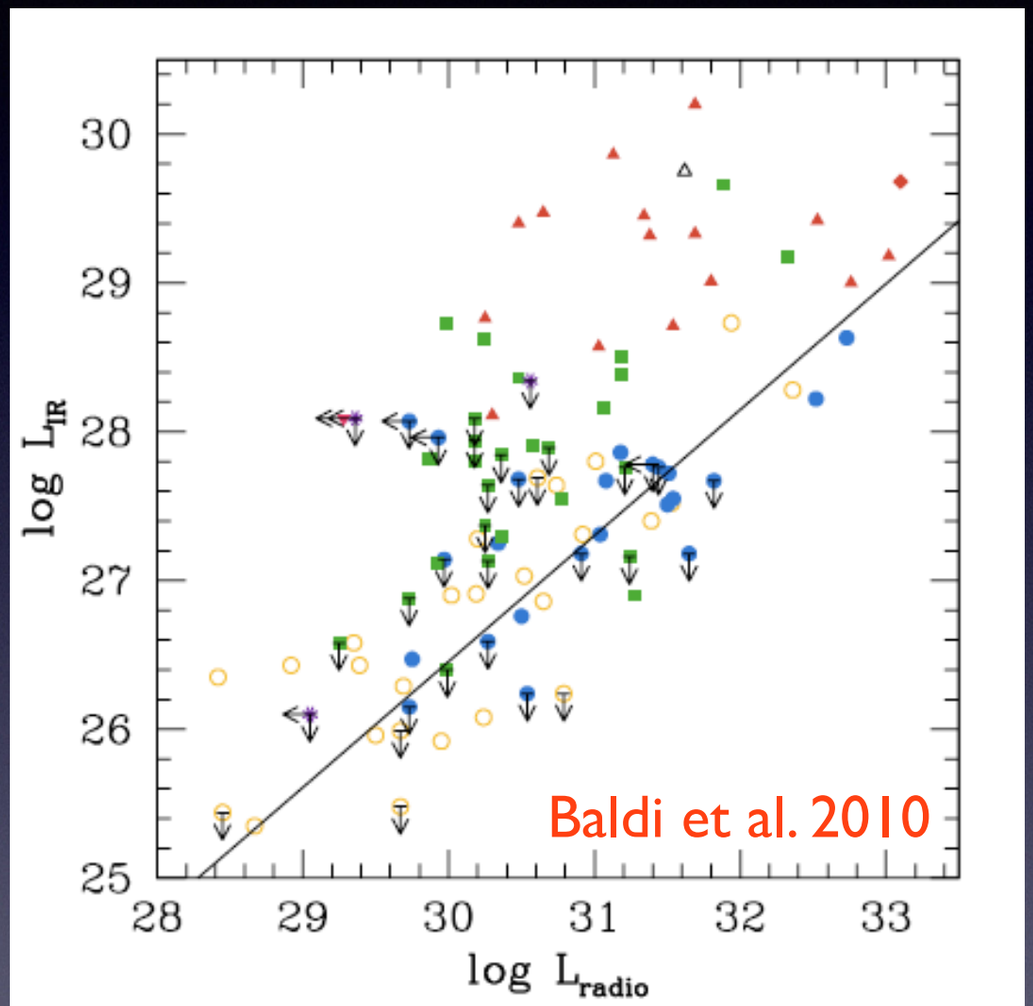

FRIIs show an unresolved NIR nucleus and a large NIR excess --> hot circumnuclear dust (dusty torus)

…and X-ray observations

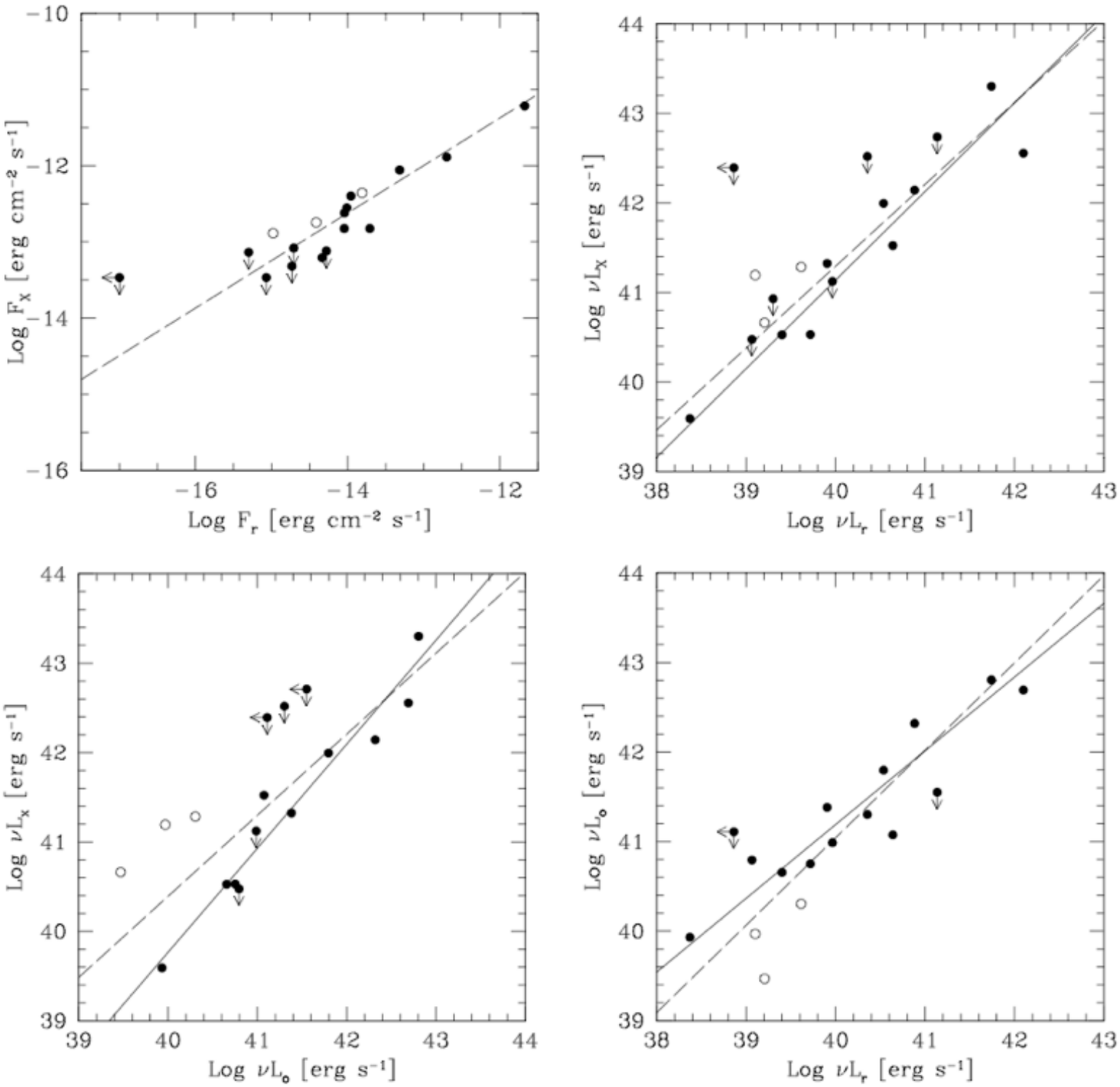

Fig. 2. Comparison of (*top left*) radio (5 GHz) and X-ray (0.5–5 keV) nuclear fluxes, (*top right*) radio and X-ray luminosities, (*bottom left*) optical (5500 Å) and X-ray luminosities, (*bottom right*) optical and radio luminosities. The empty circles represent the objects for which we have detected an intrinsic absorption $>10^{22}$ cm^{-2}. The solid line reproduces the best linear fit after having excluded the 3 X-ray absorbed nuclei, while the dashed line is the fit on the whole sample.

Balmaverde, Capetti & Grandi 2006

The accretion rate distribution is bimodal:
Low accretion rate => FRI
High accretion rate => FRII +Quasar

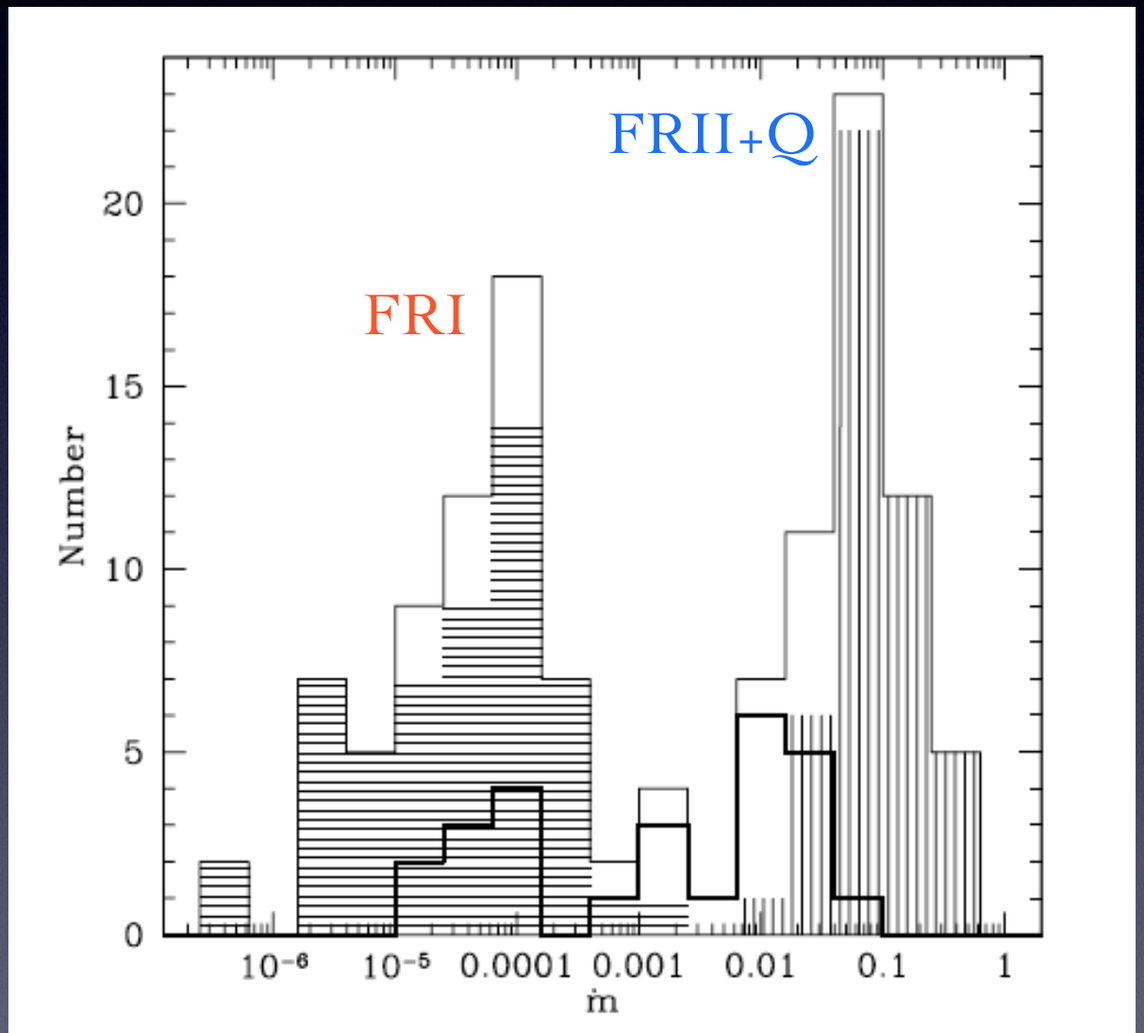

Marchesini et al. 2004

$$\dot{m} = \frac{L_{Bol}}{\eta L_{Edd}}$$ accretion rate in Eddington units

5. Radiative processes

Thermal emission

Accretion flow

Thermal Comptonization

Reprocessed features

Non-thermal emission

Synchrotron

Inverse Compton

Photon-electron interactions:

Thompson scattering: free electron and low energy photons $h\nu << m_e c^2 \sim 0.5 \text{ MeV}$

$$h\nu_f = h\nu_i$$

Compton scattering : $h\nu \lesssim m_e c^2$

$$h\nu_f = \frac{h\nu_i}{1+h\nu_i(1-cos\theta)/mc^2}$$

Inverse Compton: when the electron has significant kinetic energy $E = m_e c^2(\gamma - 1)$ as compared to the energy of the photon, then energy can be transferred from the electron to the photon, resulting in the scattered photon having a higher frequency.

$$h\nu_f \sim \gamma^2 h\nu_i$$

Open issues

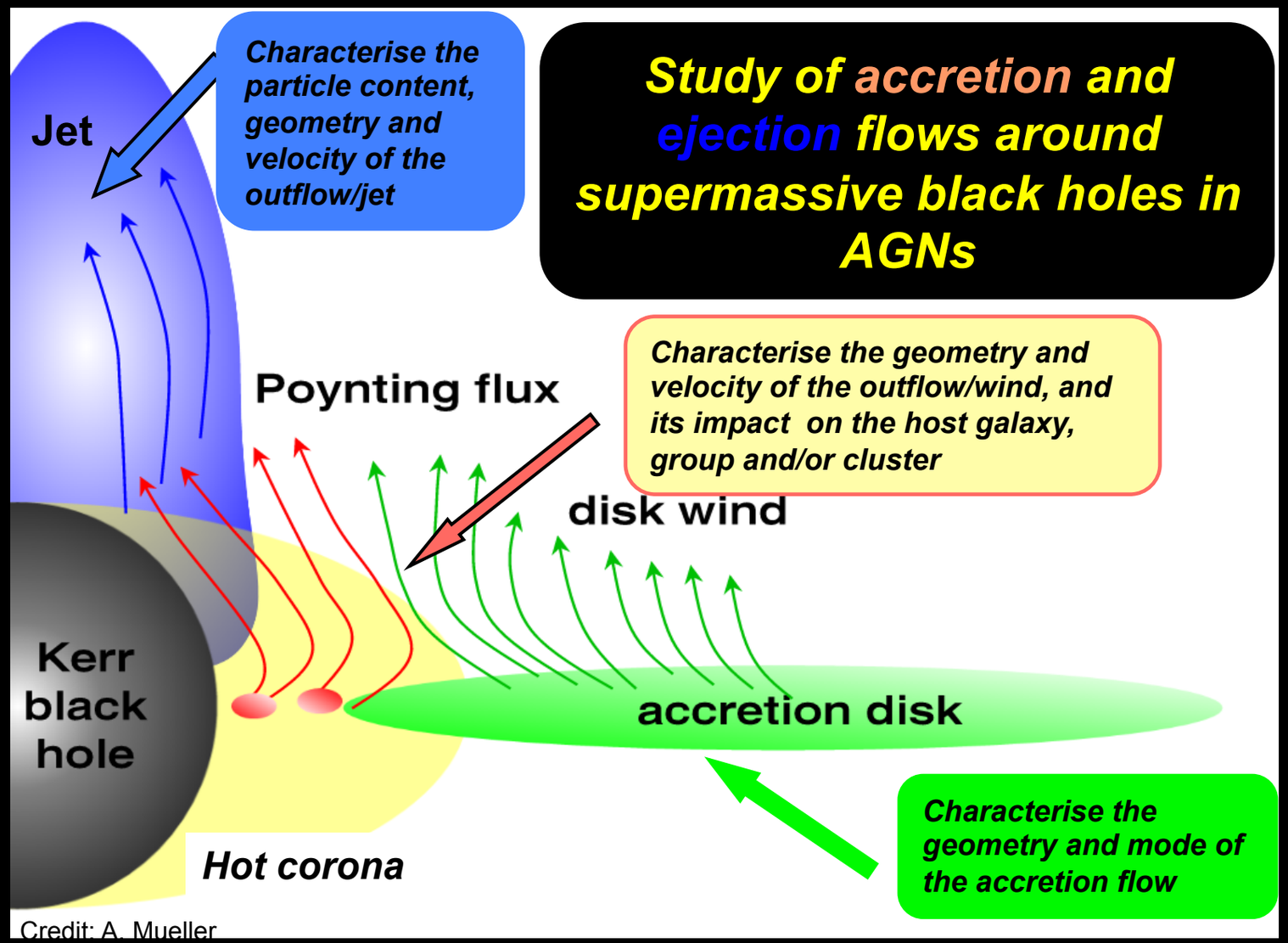

Ieri : SSD disk, warm absorber, winds

Oggi: ADAF, jets

Accretion

THERMAL PROCESS

Accretion processes around black holes involve rotating gas flow. Therefore the accretion flow structure is determined by solving simultaneously four conservation equations:

1. conservation of vertical momentum
2. conservation of mass
3. conservation of energy
4. conservation of angular momentum

Four solutions are currently known.
The most famous solutions are:

i) Shakura & Sunyaev thin optically thick disk model (SSD: standard model)
ii) Optically thick Advection-Dominated Accretion Flow (ADAF)

SSD (Shakura-Sunyaev disk)

Disks usually rotate such that each fluid element is moving almost in a circular orbit. As the angular velocity is a function of radius, there is a shearing flow. This means that coupling between adjacent radii exerts a force. Given that the outer parts rotate more slowly, inner try to speed up outer, giving it a higher velocity. This increases the angular momentum of the outer, decreases the angular momentum of the inner, so net result is that angular momentum is transferred outwards and mass flows inwards.

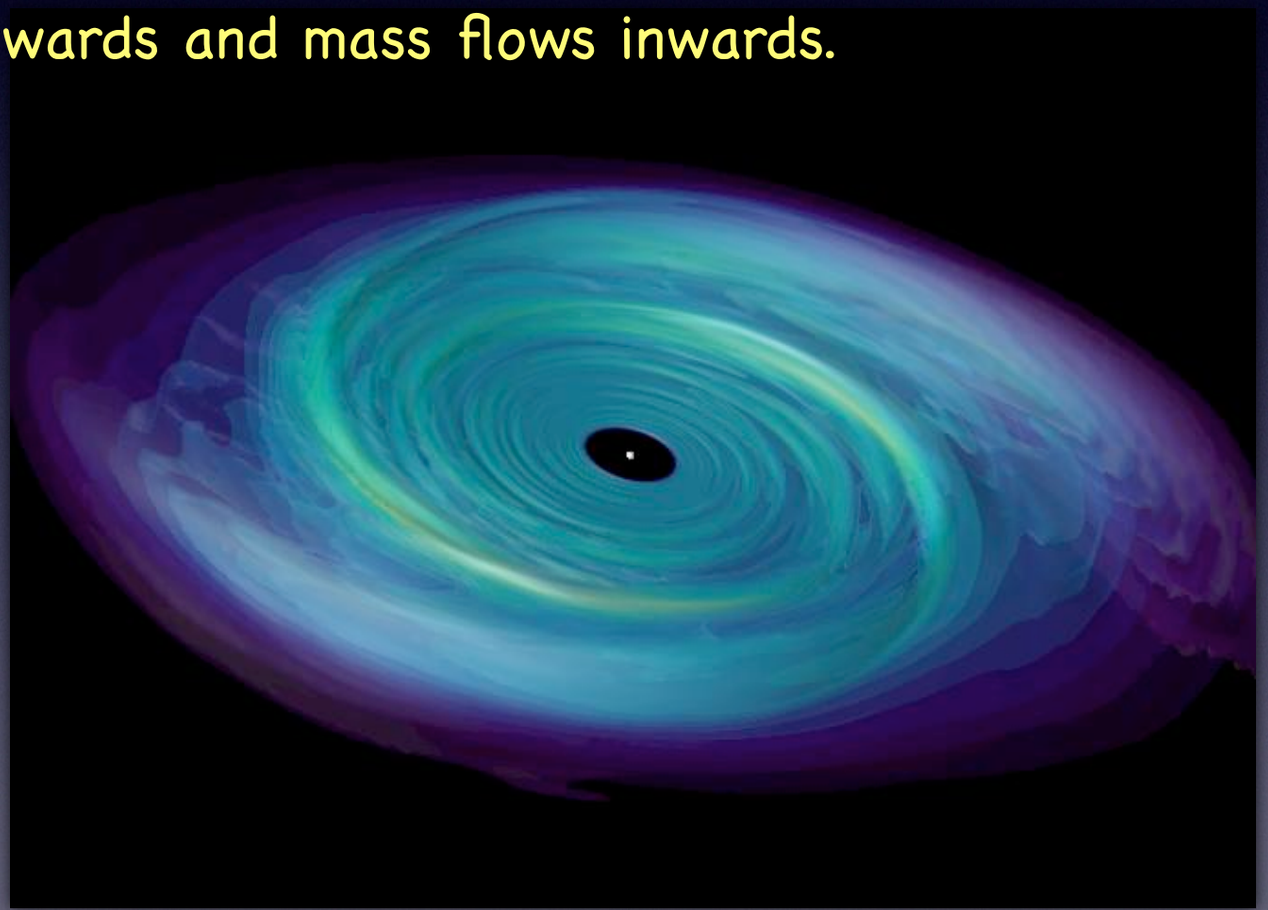

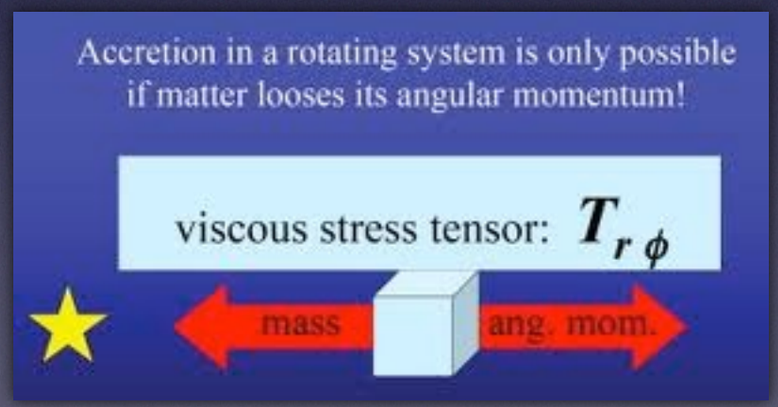

Viscosity transports angular momentum outward, allowing the accretion gas to spiral in toward the BH. Viscosity acts as a source of heat that is radiated away.

Ann. Rev. Astron. Astrophys. 1981. 19:137–62

ACCRETION DISCS IN ASTROPHYSICS

J. E. Pringle
Institute of Astronomy, University of Cambridge, Madingley Road, Cambridge, CB3 0HA, England

1. INTRODUCTION

If we put a particle in a circular orbit around a central gravitating body, it will stay in that orbit. If we then extract energy and angular momentum from the particle we may allow it to spiral slowly inwards. The amount of energy that can be extracted by such a process is equal to the binding energy of the innermost accessible orbit. For orbits around sufficiently compact objects a reasonable fraction of the particle's rest mass energy can be extracted. For example, of order 10 percent of the rest mass can be obtained from orbits around a neutron star and up to around 40 percent for orbits around a black hole. Thus, the accretion process can be an efficient converter of rest mass to radiation. The problem is to set up the process that can extract the energy and angular momentum.

If we consider a blob of gas in a circular orbit then we have more flexibility. In particular, if we can find a method of redistributing angular momentum among the gas particles in order to let some of them fall into the potential well, then we are in a position to extract the potential energy so released. The accretion disc provides just such a method. The efficiency with which energy is released and the ubiquity of angular momentum explains why accretion discs are popular in models for some of the most luminous objects—X-ray stars and quasars. However, accretion disc theory predates the discovery of both these, and it is to these initial developments that we now turn our attention.

Accretion is the physical process by which black hole aggregates matter from their surroundings. The gravitational energies that such matter must release for accretion to occur is a powerful source of luminosity L.

$$L_{rad} = \eta \dot{M} c^2$$

EFFICIENCY of the process

$\eta \propto M/R$ (COMPACTNESS OF THE SYSTEM)

ACCRETION RATE

$M_{\odot} yr^{-1}$

$$L = \eta \dot{M} c^2 \quad \text{with} \quad \eta \propto \frac{M}{r}$$

The potential energy of a mass m a distance r from the central mass M is

$$U = \frac{GMm}{r}$$

The rate at which the energy potential can be converted in radiation is given

$$L \sim \frac{dU}{dt} = \frac{GM}{r}\frac{dm}{dt} = \frac{GM\dot{M}}{r}$$

This efficency is maximized in the case of a black hole
the size of which can be defined as

$$R_s = \frac{2GM}{c^2}$$

that can be derived by the escape velocity of the light

$$V_{escape} = c = \left(\frac{2GM}{R}\right)^{1/2}$$

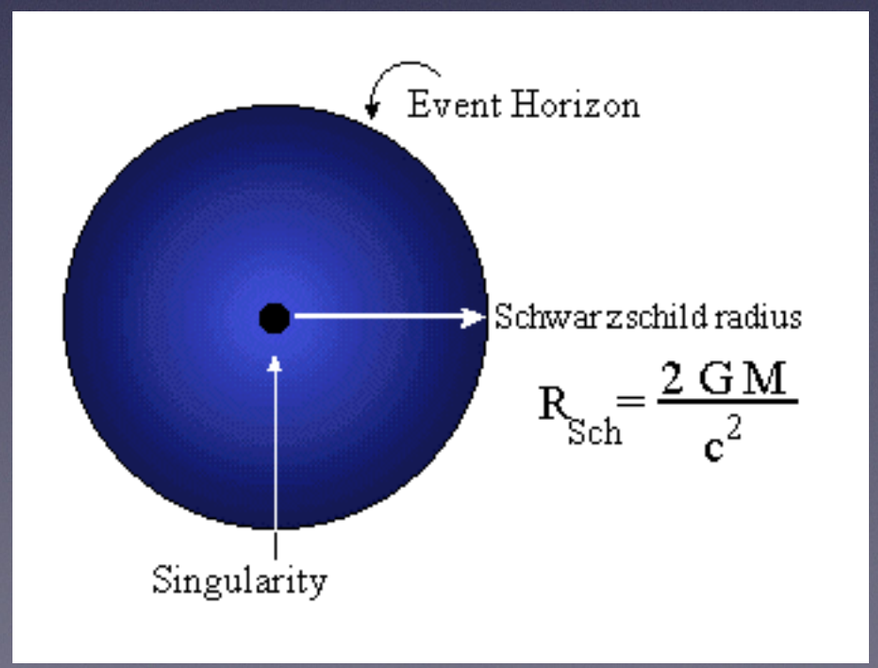

Eddington Luminosity L_E is the luminosity at which the outward force of the radiation pressure is balanced by the inward gravitational force

$$L_E = \frac{4\pi G m_p c}{\sigma_e} M \sim 1.3 \times 10^{38} \, (M/M_\odot) \, (erg \; s^{-1})$$

There is a natural limit, known as the Eddington limit to the luminosity that can be radiated by a compact object of mass M. When the luminosity exceeds the Eddington limit the gas will be blown away by the radiation.

$$\dot{M} = \frac{L}{\eta c^2} = 1.8 \times 10^{-3} (\frac{L_{44}}{\eta}) \qquad M_\odot \; yr^{-1}$$

accretion on to a black hole must power the most luminous phenomena in the universe

$$L_{acc} = \frac{GM}{R}\dot{M} = \eta c^2 \dot{M}$$

Quasars: $L \approx 10^{46} erg/s$ requires $\dot{M} = 1 M_{sun}/yr$

X—ray binaries: $L \approx 10^{39} erg/s$ $10^{-7} M_{sun}/yr$

Gamma—ray bursters: $L \approx 10^{52} erg/s$ $0.1 M_{sun}/\mathrm{sec}$

Shakura & Sunyaev thin optically thick disk model (standard model)

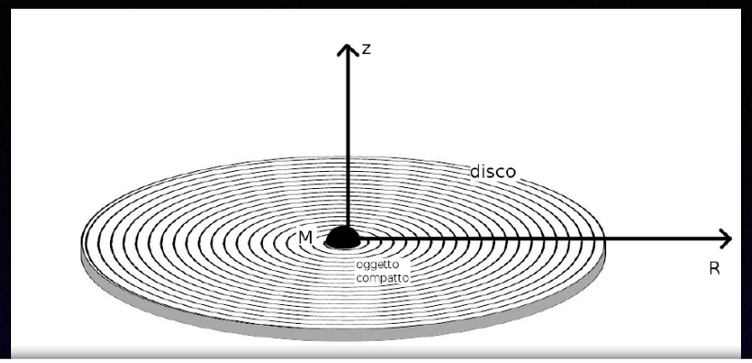

Thin H/R<< 1

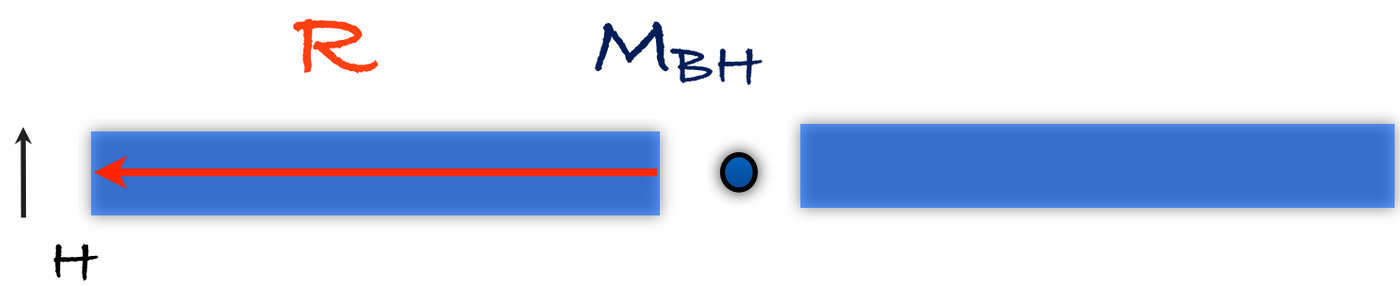

Thick, in the sense that each element of the disk radiates as a black body

If the disk is optically thick will radiate ad a blackbody.
Hence via Stephan' Law

$$L = \frac{GM\dot{M}}{2r} = 2\pi r^2 \sigma T^4$$

$$T = \left(\frac{GM\dot{M}}{4\pi\sigma r^3}\right)^{1/4}$$

$$T(r) = 6 \times 10^5 (\frac{\dot{M}}{\dot{M}_E})^{1/4} (\frac{M}{M_8})^{-1/4} (\frac{r}{R_S})^{-3/4} \text{ K}$$

Temperature increases inward ($r^{-3/4}$): accretion disk continuum spectrum superposition of many BB's with different temperatures

$$R_S = 2GM/c^2$$

Temperature increases with accretion rate

$$R_S = 2GM/c^2 \qquad \dot{M}_E = \frac{L_E}{\eta c^2}$$

UV-Optical Continuum

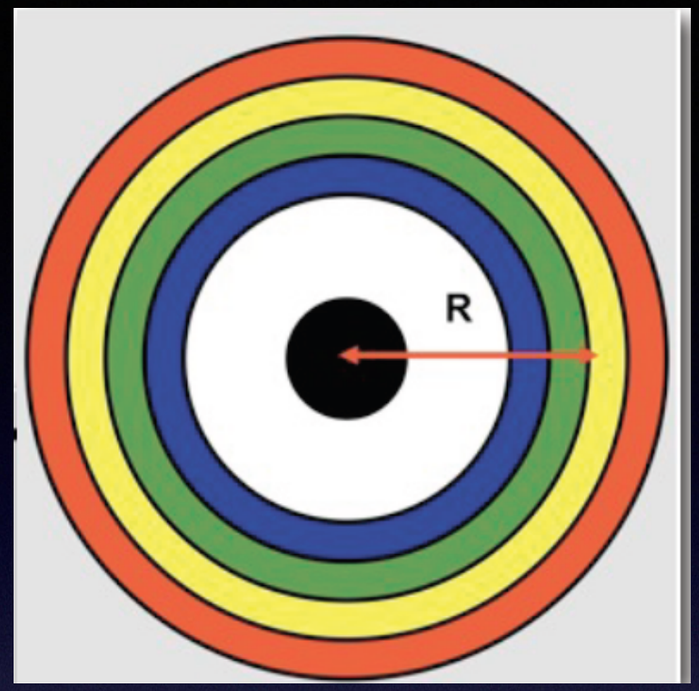

The superposition of these BB spectra will thus look like:

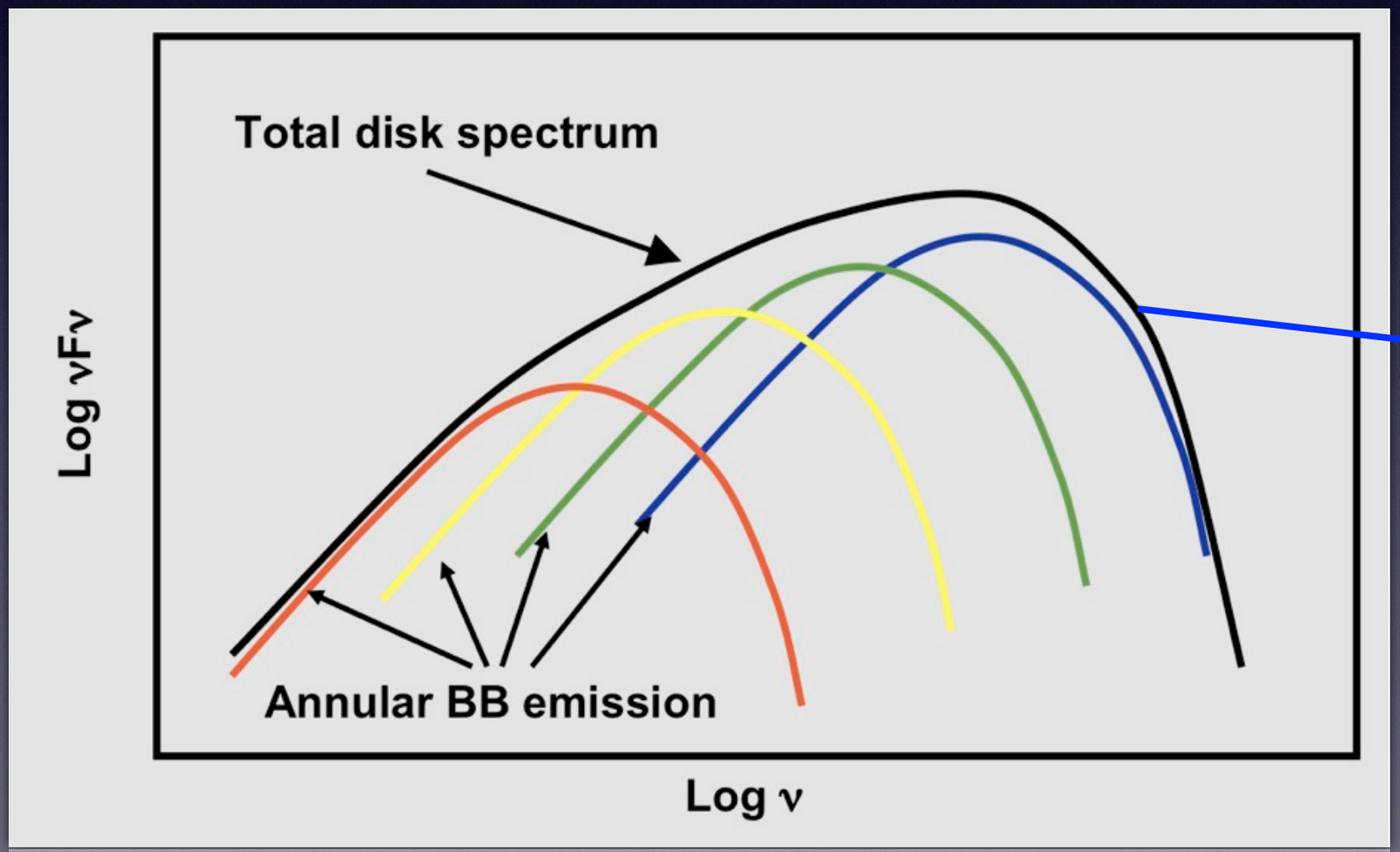

Corona

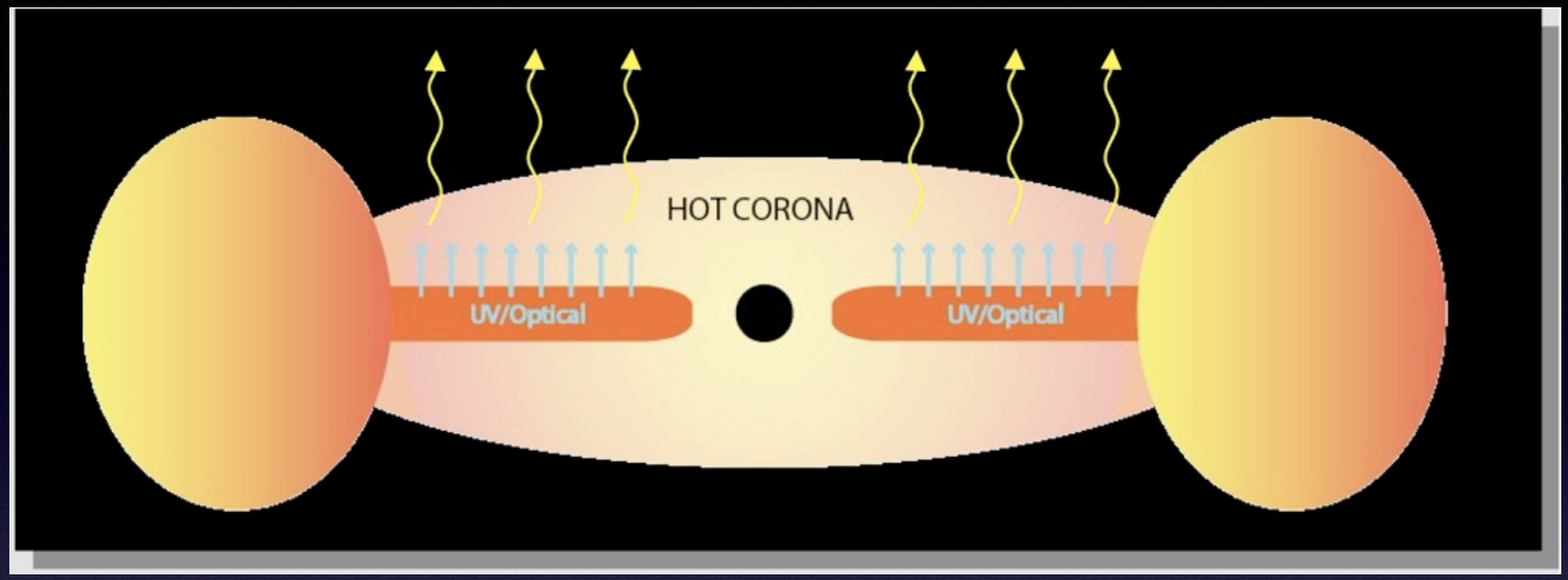

Thermal Comptonization

With this term we mean the process of multiple scattering of a photon due to a **thermal (Maxwellian)** distribution of electrons.

There is one fundamental parameter measuring the importance of the Inverse Compton process in general, and of multiple scatterings in particular: the Comptonization parameter, usually denoted with the letter **y**.

y = [average # of scatt.] x[average fractional energy gain for scatt.]

Thermal Comptonization

Comptonization on a thermal plasma of electrons characterized by a temp. T and optical depth τ

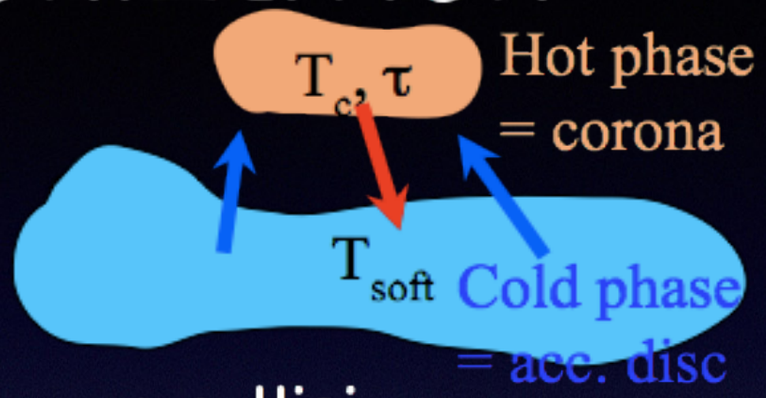

✓ mean relative energy gain per collision

$$\frac{\Delta E}{E} \simeq \left(\frac{4kT}{mc^2}\right) + 16\left(\frac{kT}{mc^2}\right)^2 \quad \text{for } E \ll kT$$

$$\leq \quad 0 \quad \text{for } E \gtrsim kT$$

✓ mean number of scatterings

$$N \simeq (\tau + \tau^2)$$

➡ Compton parameter $y = \frac{\Delta E}{E} N$

$$E_f = E_i\, e^y$$

Thermal Comptonization Spectrum: the continuum

$$F_E \propto E^{-\Gamma(kT,\tau)} \exp\left(-\frac{E}{E_c(kT,\tau)}\right)$$

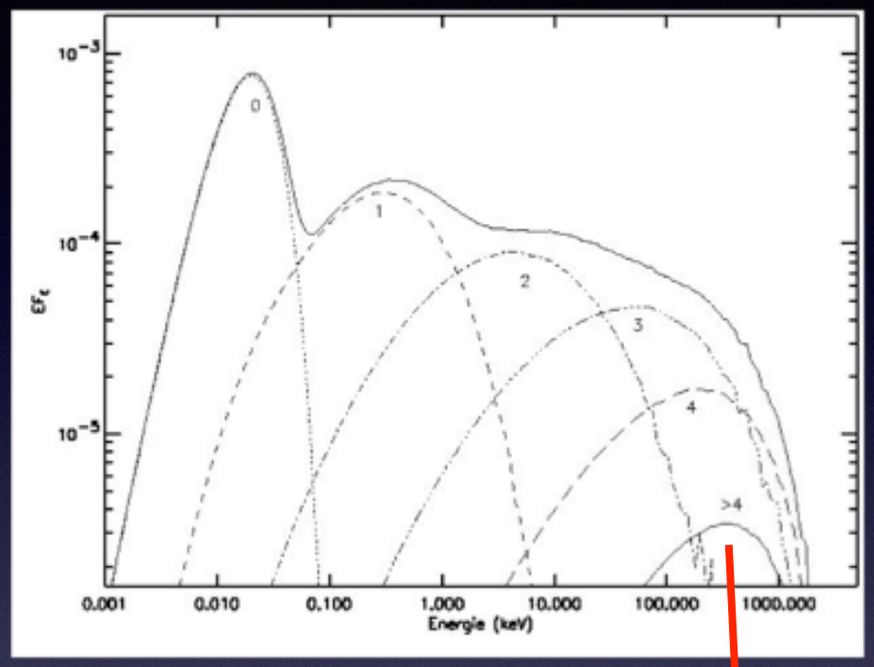

$\Gamma(\tau, kT)$

The exact relation between spectral index and optical depth depends on the geometry of the scattering region.

$E_c \simeq kT$

As photons approach the electron thermal energy, they no longer gain energy from scattering, and a sharp rollover is expected in the spectrum.

The observed high energy spectral cutoff yields information about the temperature of the underlying electron distribution.

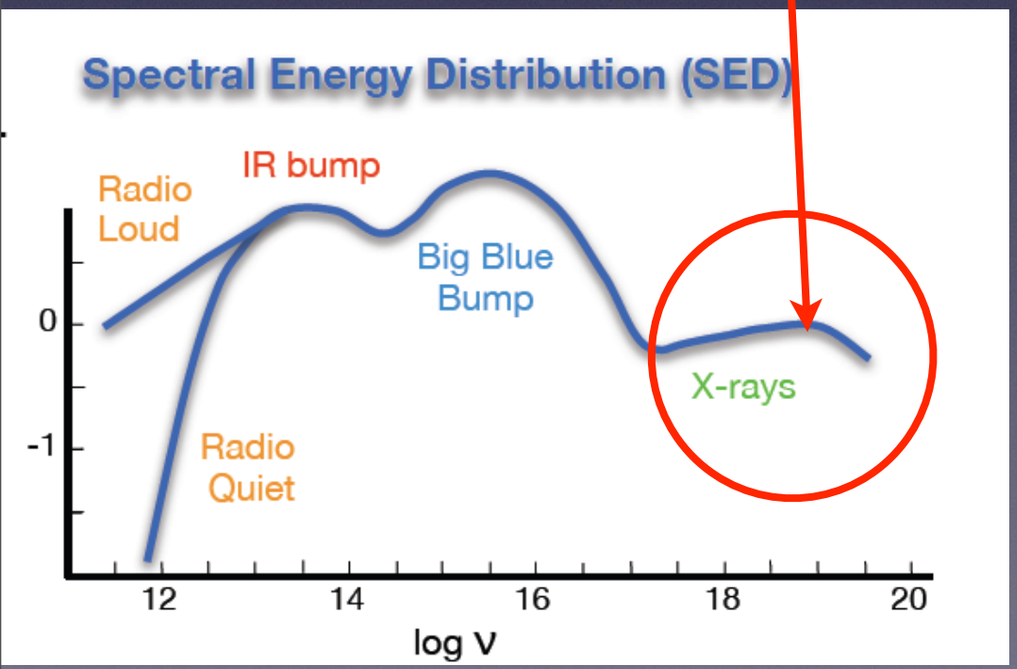

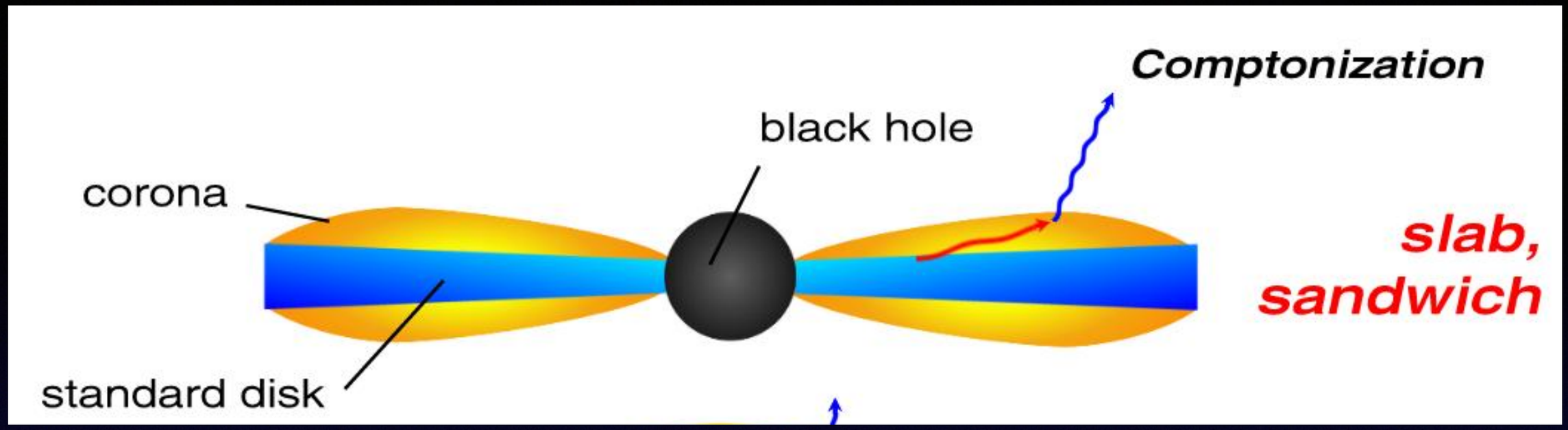

- Thermal Comptonization

- Hard X-ray reprocessing

Iron line

Compton hump

Only half of hard X-ray flux escapes from the source while the other half impinges on the cool disk. The latter is in part (15%-20%) reflected giving rise to the observed spectral hump in the 10-30 keV range. In small part it is reemitted as an Fe fluorescence line, but the largest part (80-90%) is absorbed,reprocessed and reemitted into black body photons which contribute to the soft photon input for Comptonization.

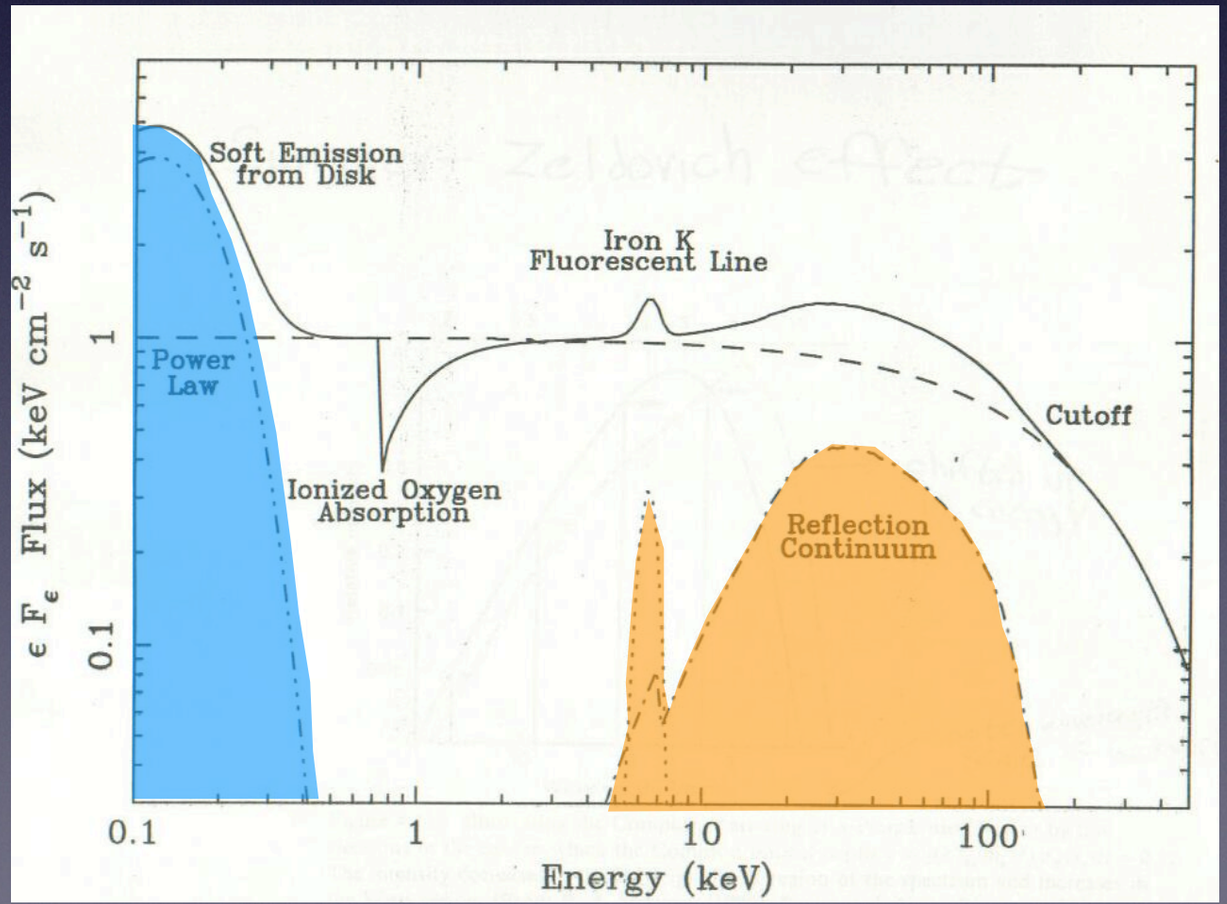

Reflection

At low energies <10 keV the high-Z ions absorb the X-rays. A major part of the opacity above 7 keV is due to Fe K-edge opacity.

At high energies the Compton shift of the incident photons becomes important.

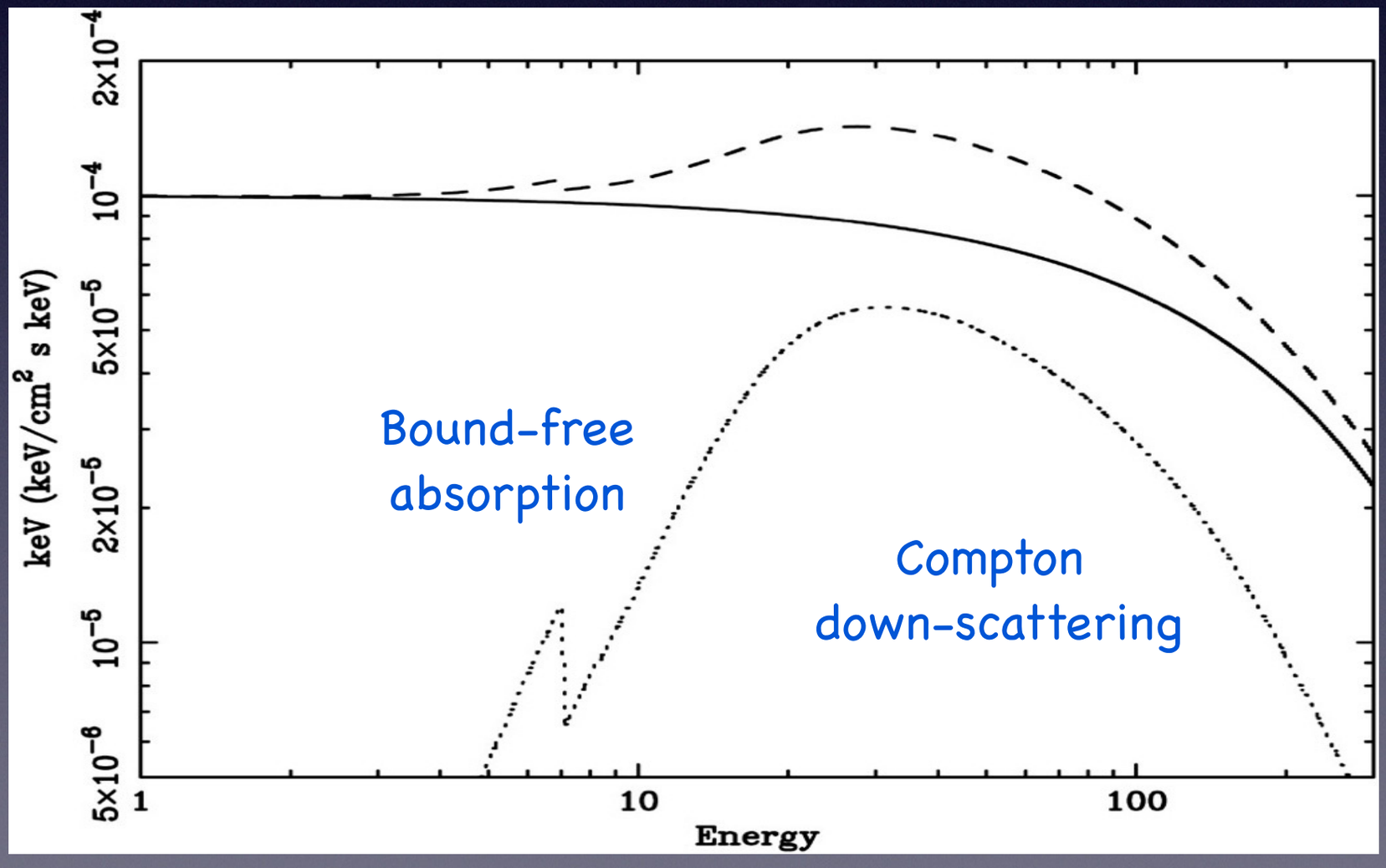

Photon-electron interaction

Direct Compton Scattering

In this process the photon is absorbed and immediately re-radiated by the electron into a different direction but it looses part of its initial energy. It can be thought as an heating mechanism.

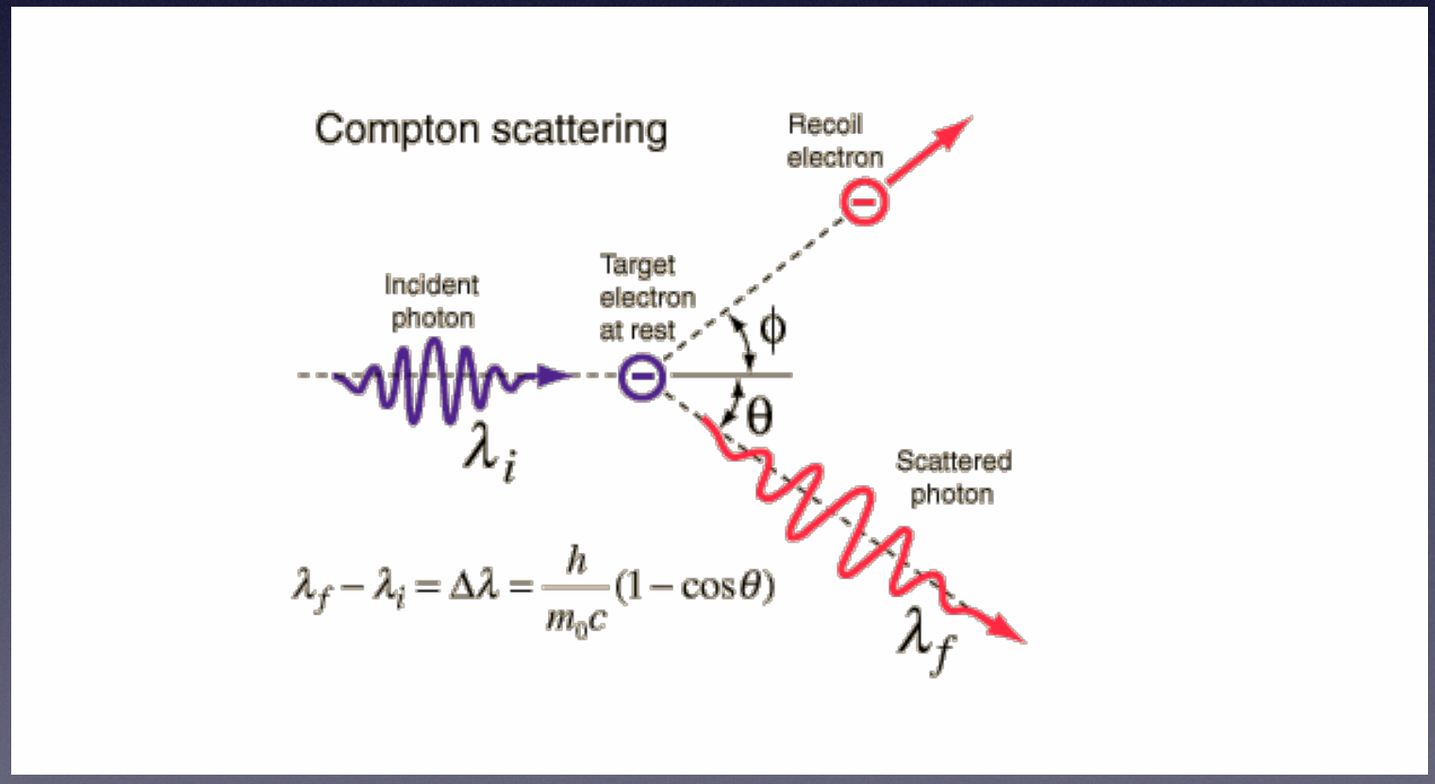

Iron Line

The fluorescent iron line is produced when one of the 2 K-shell (n=1) electrons of an iron atom (or ion) is ejected following photoelectric absorption of an X-ray. Following the photoelectric event, the resulting excited state can decay in one of two ways. An L-shell (n=2) electron can then drop into the K-shell releasing 6.4 keV of energy either as an emission line photon (34 % probability) or an Auger electron (66 % probability).

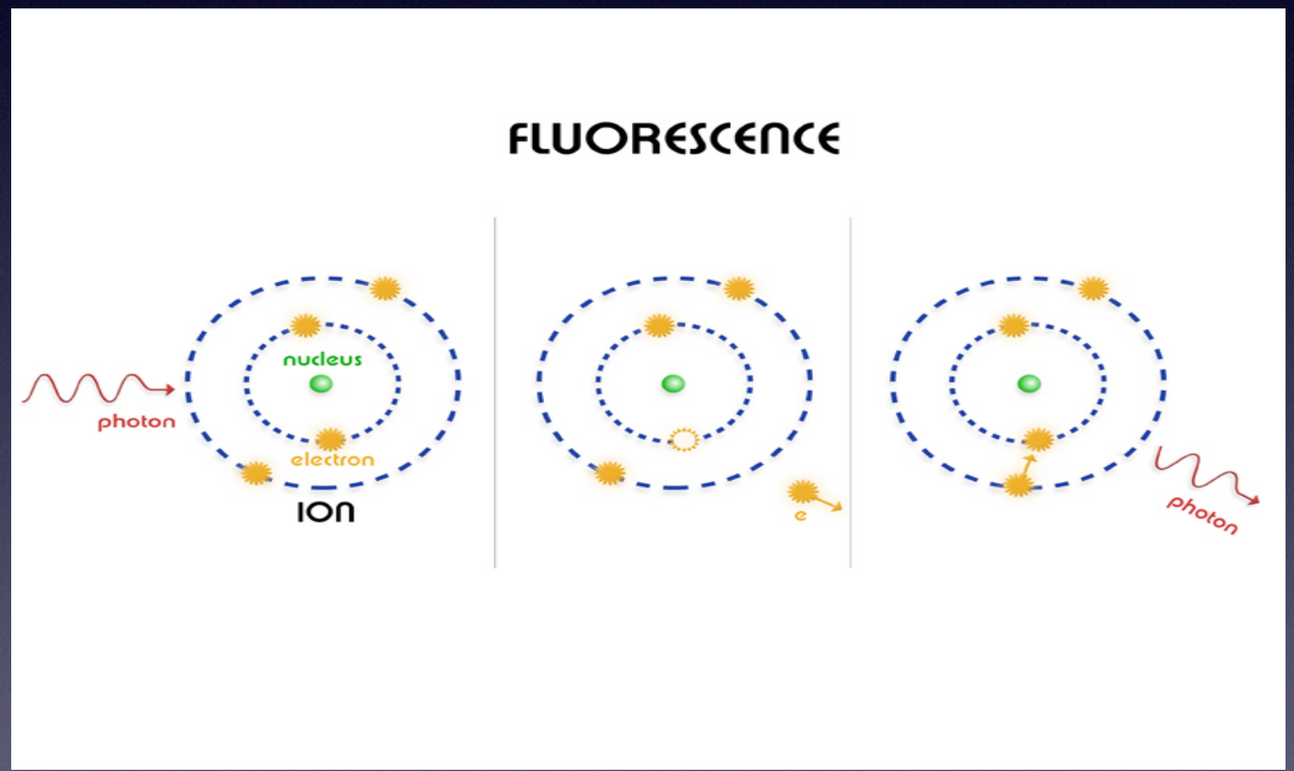

For ionized iron, the outer electrons are less effective at screening the inner K-shell from the nuclear charge and the energy of both the photoelectric threshold and the K line are increased.

BROAD LINE

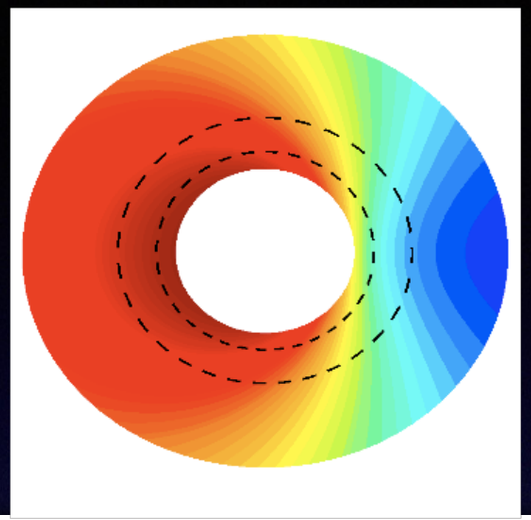

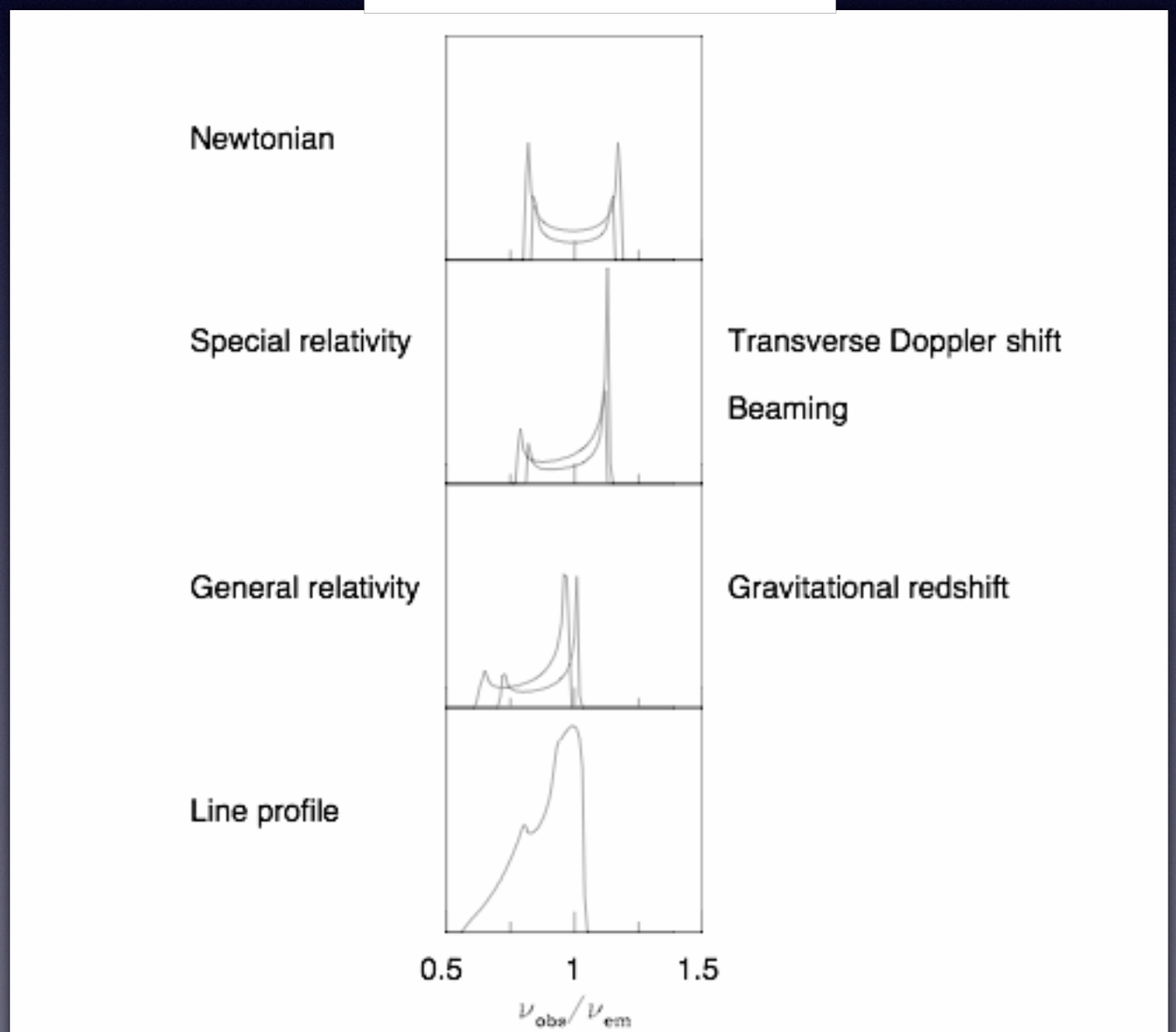

Schwarzschild

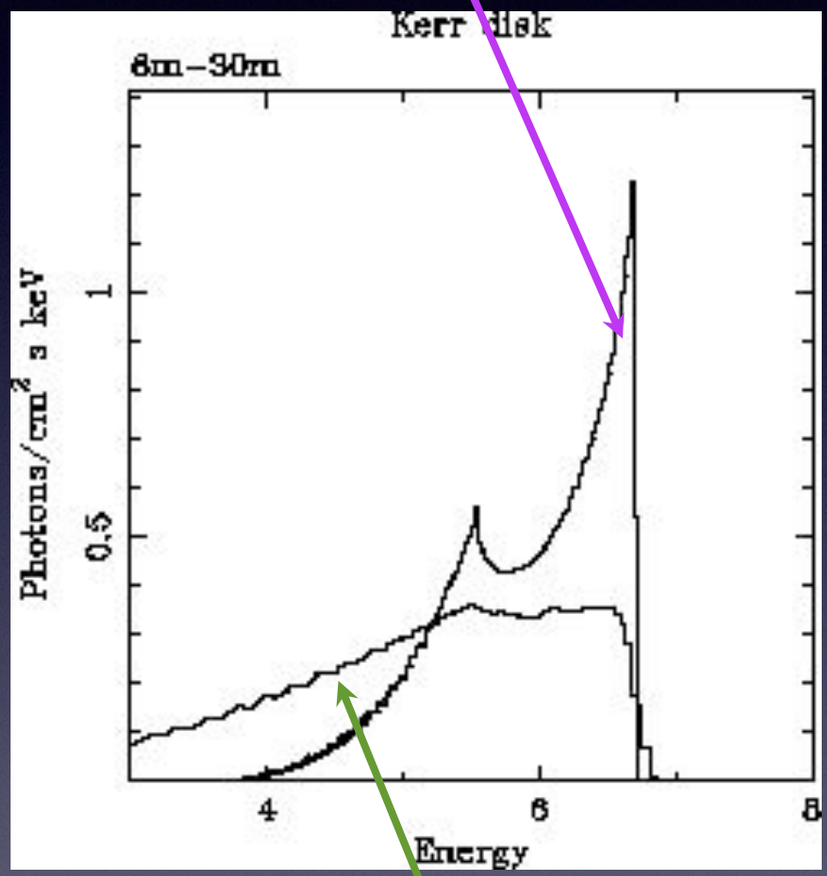

Kerr

IV - Ionized absorption along the line of sight

Photoelectric absorption

Neutral

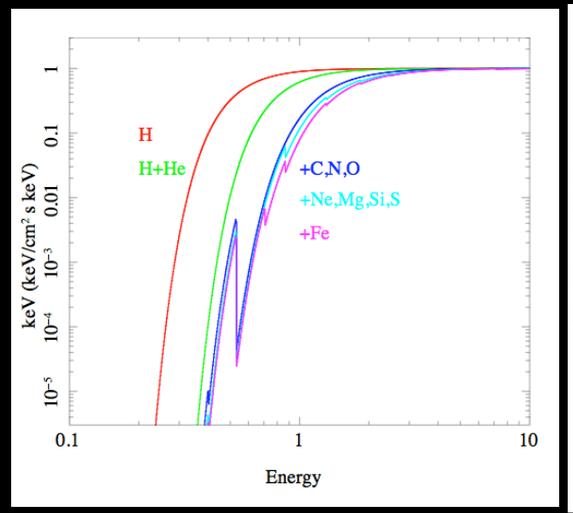

Ionized (Xi=L/nR**2)

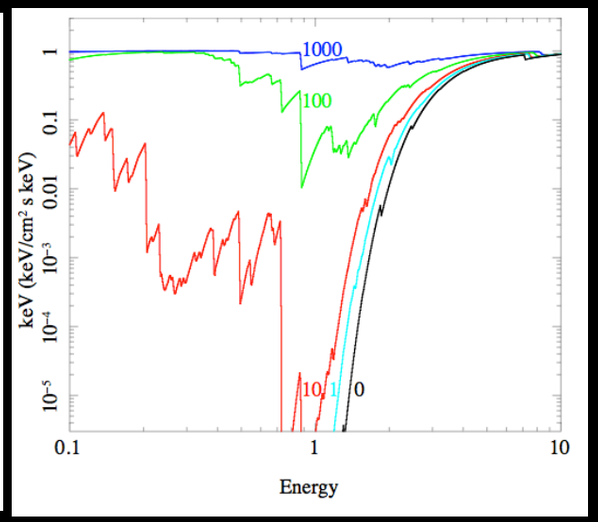

Cappi's lesson

Absorption: Interpretation - Three main wind dynamical models

i) Thermally driven winds from BLR or torus

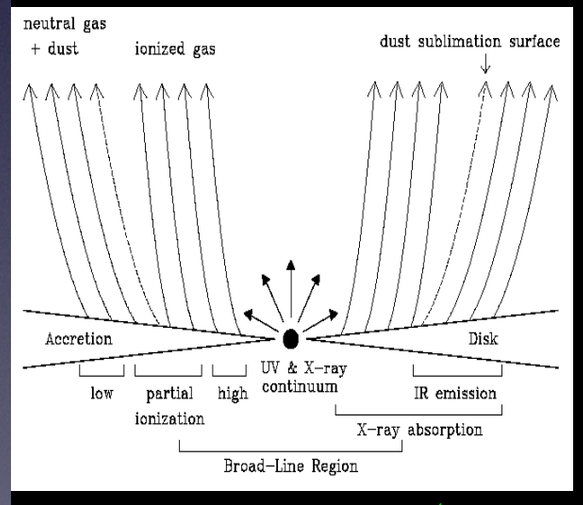

Balsara & Krolik, 93; Woods et al. '96

i) ⇒ Large R, low v

ii) and iii) ⇒ Low R and large v

ii) Radiative-driven wind from accretion disk

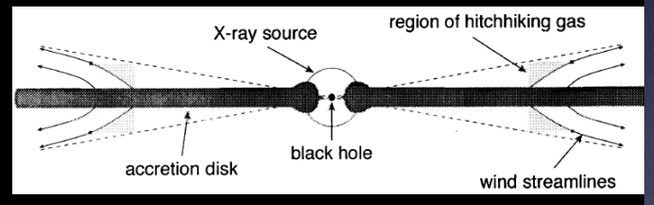

Murray et al. '95, Proga et al. '00

iii) Magnetically driven winds from accretion disk

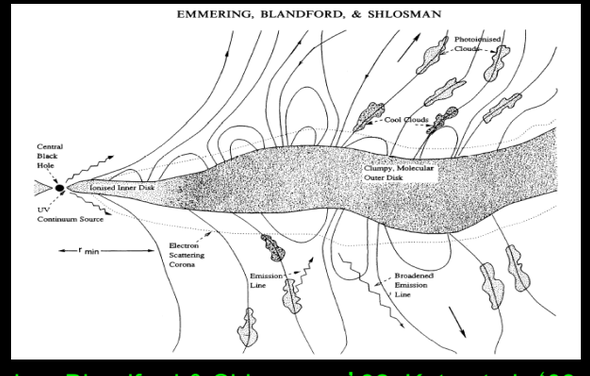

Emmering, Blandford & Shlosman, ' 92; Kato et al. '03

ADAF (Advection-Dominated Accretion Flow)

Energy Equation

$$q^+ = q^- + q^{adv}$$

Thin Accretion Disk

(Shakura & Sunyaev 1973; Novikov & Thorne 1973;...)

Most of the viscous heat energy is radiated

$$q^- \approx q^+ \gg q^{adv}$$

$$L_{rad} : \ 0.1 \dot{M} c^2$$

Advection-Dominated Accretion Flow (ADAF)

(Ichimaru 1977; Narayan & Yi 1994, 1995; Abramowicz et al. 1995)

Most of the heat energy is retained in the gas

$$q^- \ll q^+ \approx q^{adv}$$

$$L_{rad} \ll 0.1 \dot{M} c^2$$

$$L_{adv} : \ 0.1 \dot{M} c^2$$

q^+ is the energy generated by viscosity per unit volume
q^- is the radiative cooling per unit volume
q_{adv} represents the advective transport of energy

ADAF

In this solution the accreting gas has a very low density and is unable to cool efficiently. The viscous energy is stored in the gas as thermal energy instead of being radiated and is advected onto the BH. Ions and electrons are thermally decoupled.

- Very Hot: Ti~ 10^{12}K (R_S/R), Te~ 10^{9-11}K (since ADAF loses very little heat).

- Geometrically thick: H~R (most of the viscosity generated energy is stored in the gas as internal energy rather than being radiated, the gas puffes up

- Optically thin (because of low density)

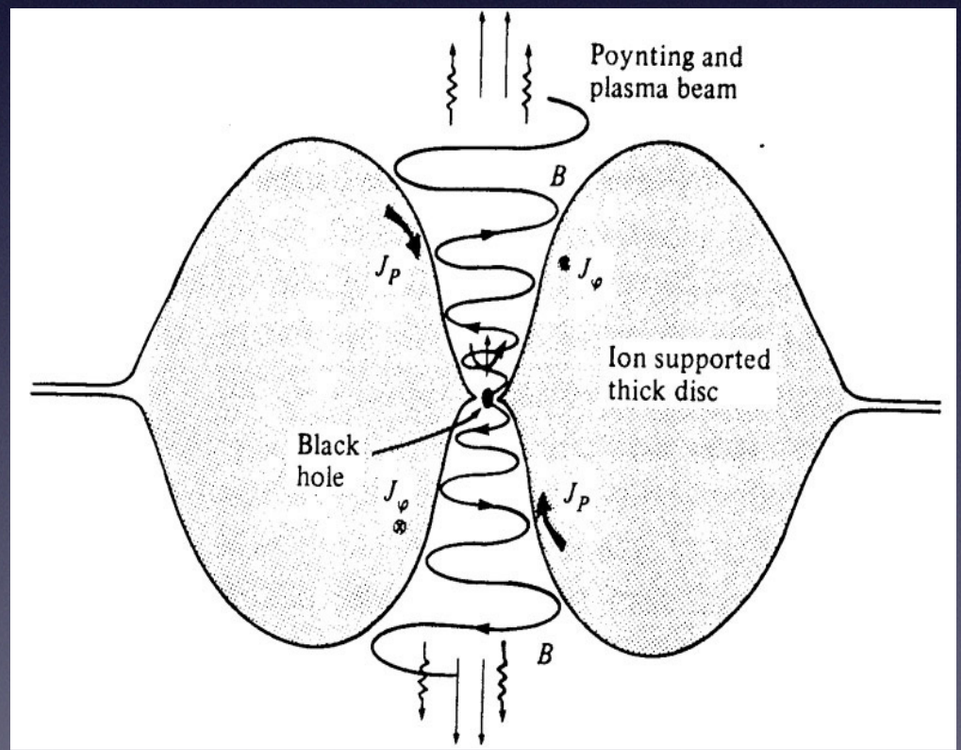

ADAF

The ADAF solution exists only for $\frac{\dot{M}}{\dot{M}_E} \leq 0.05 - 0.1$

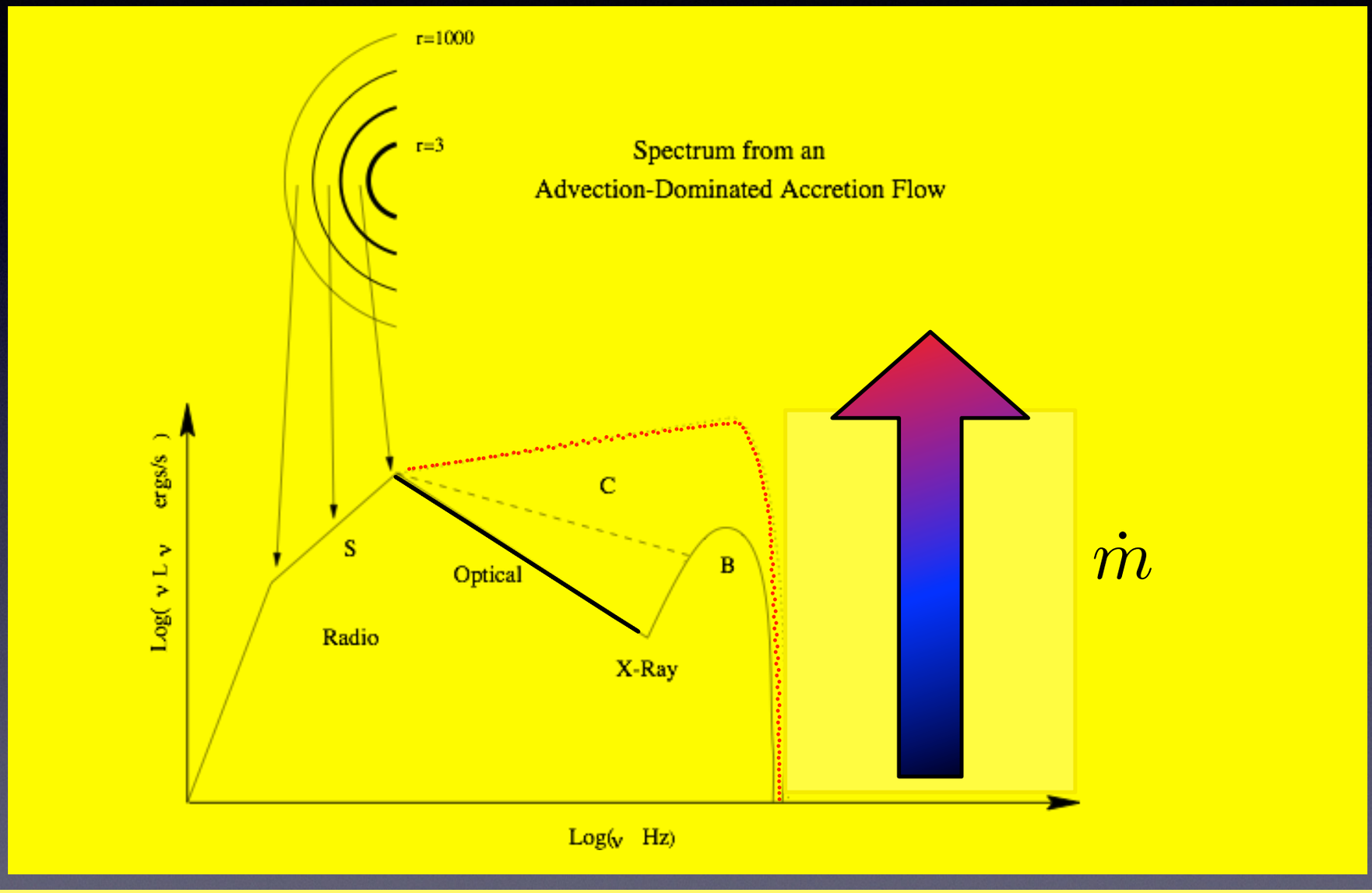

Schematic spectrum of an ADAF around a black hole. S, C, and B refer to electron emission by synchrotron radiation, inverse Compton scattering, and bremsstrahlung, respectively. The solid line corresponds to a low accretion, the dashed line to an intermediate accretion , and the dotted line to the highest (possible) accretion.

ADAF

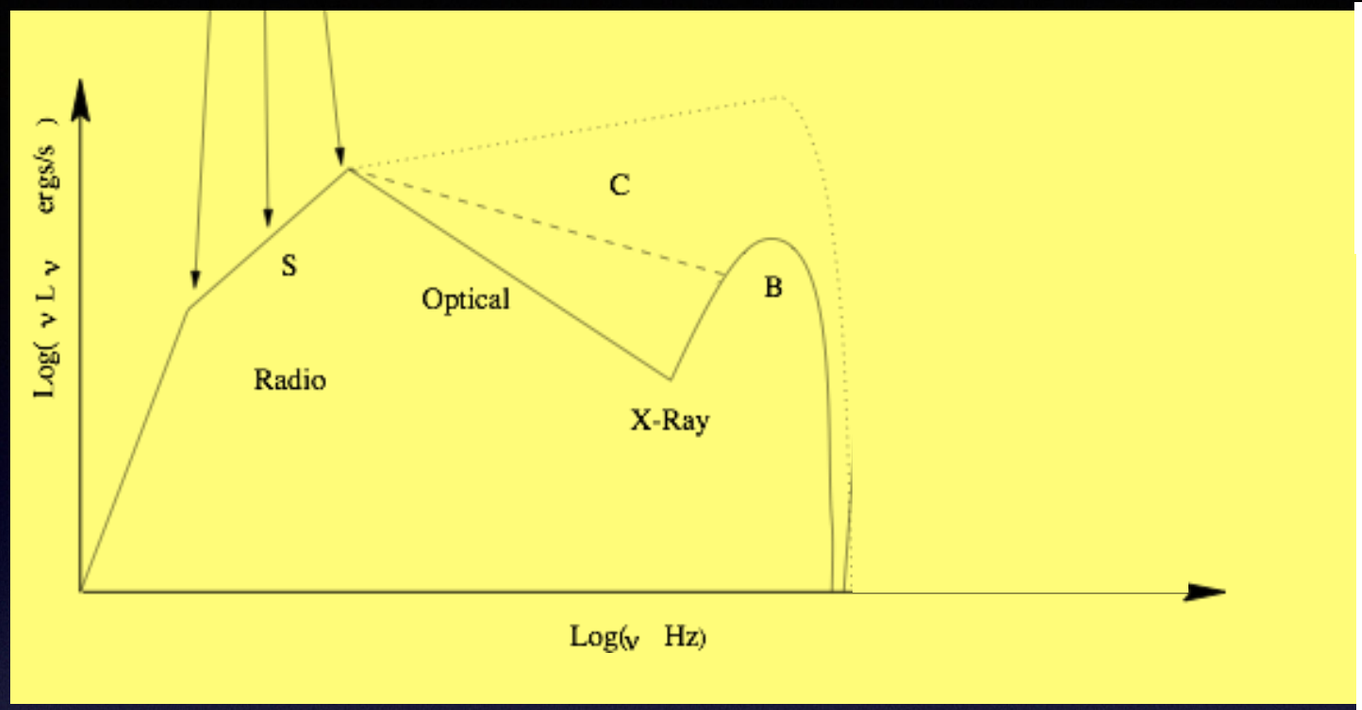

SSD - THIN DISK

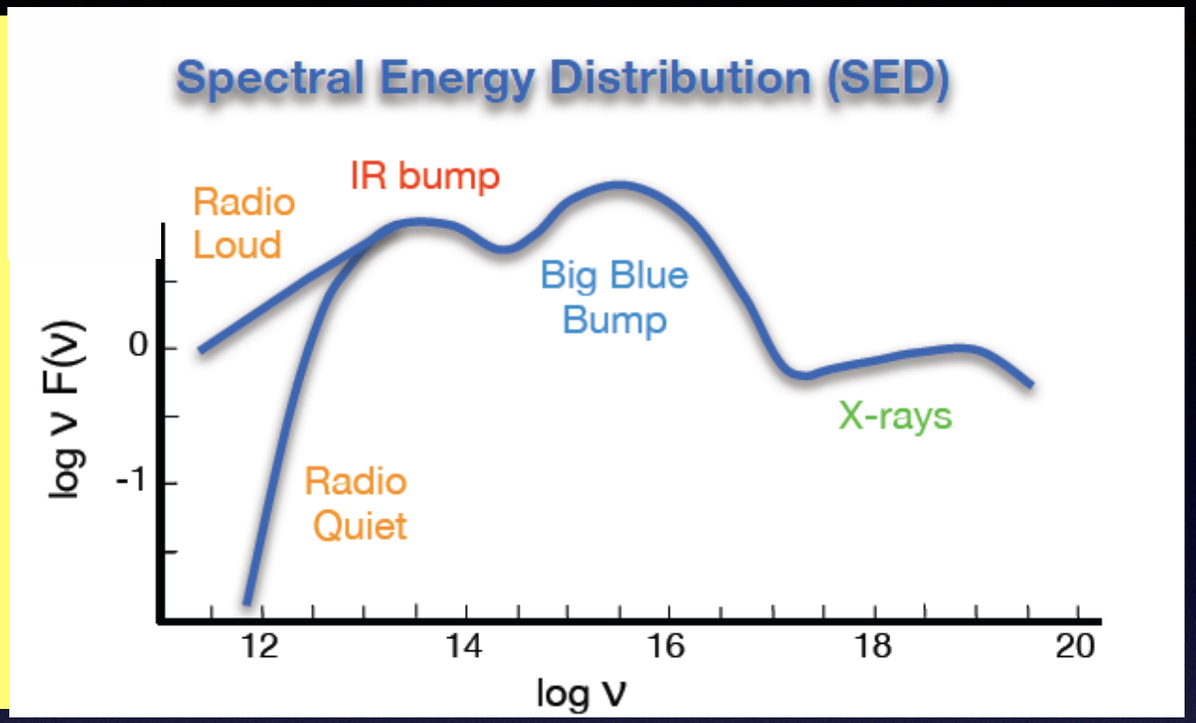

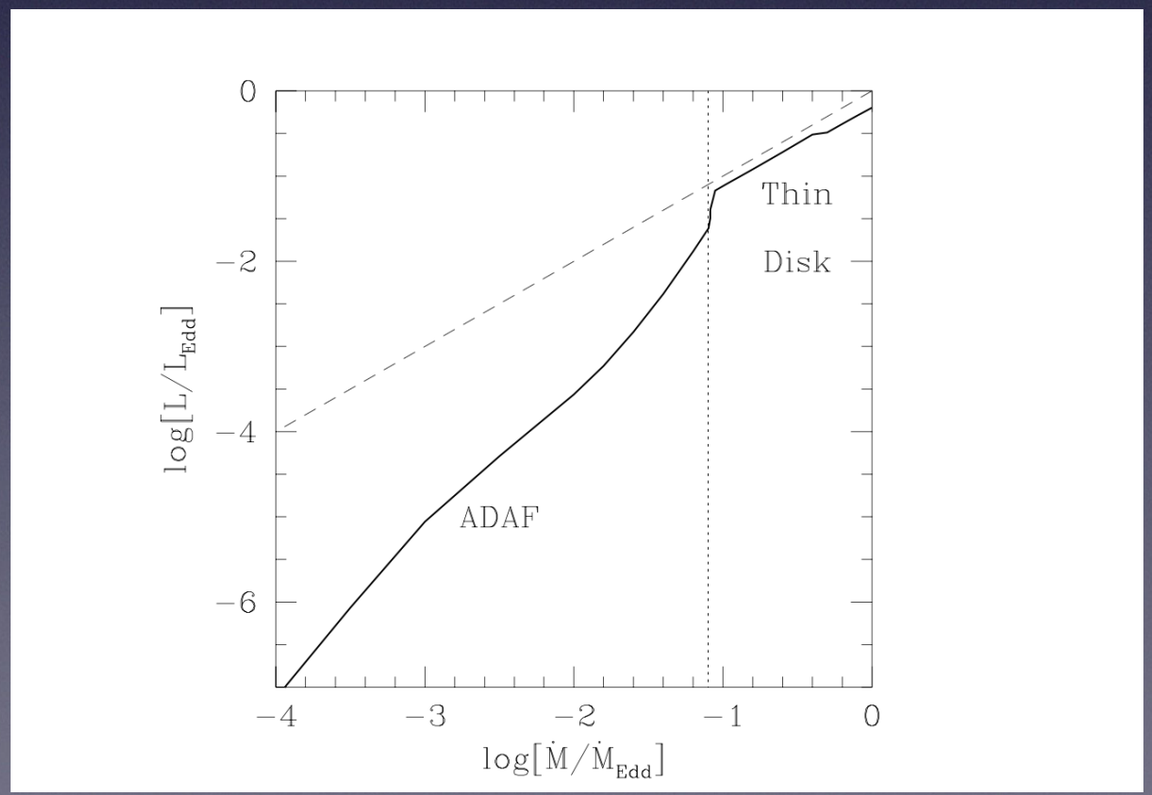

FRI

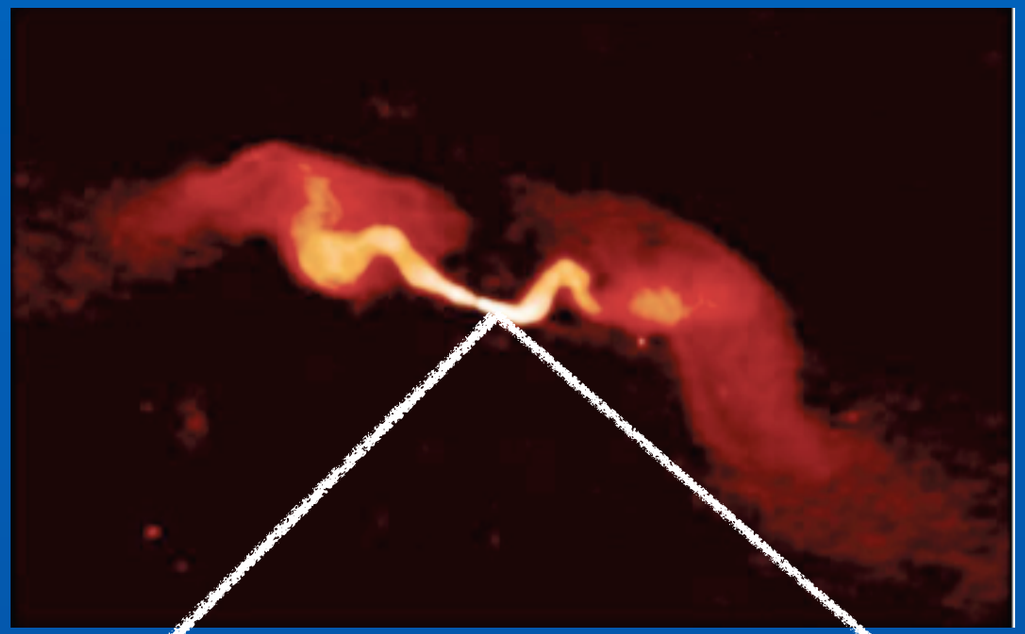

FRII

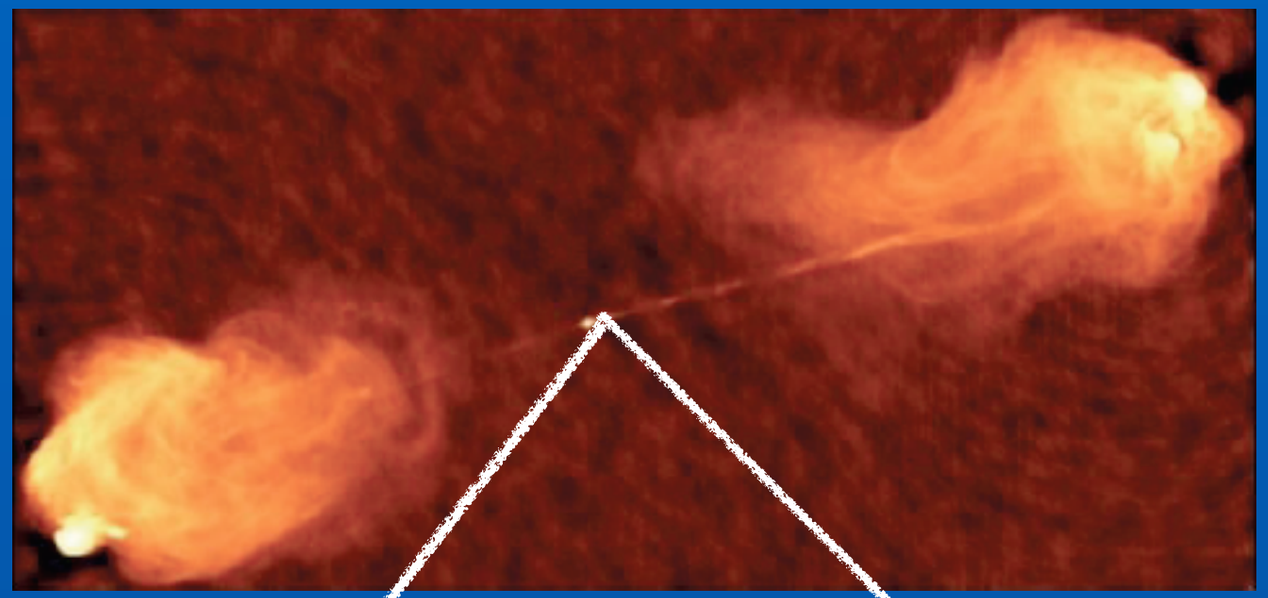

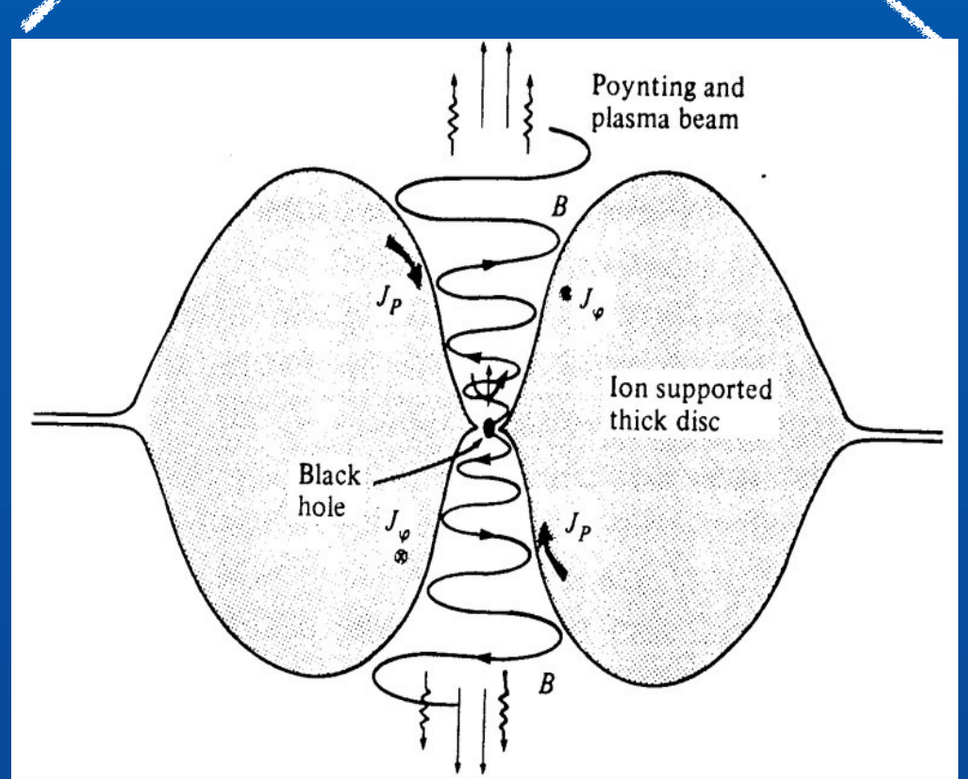

ADAF

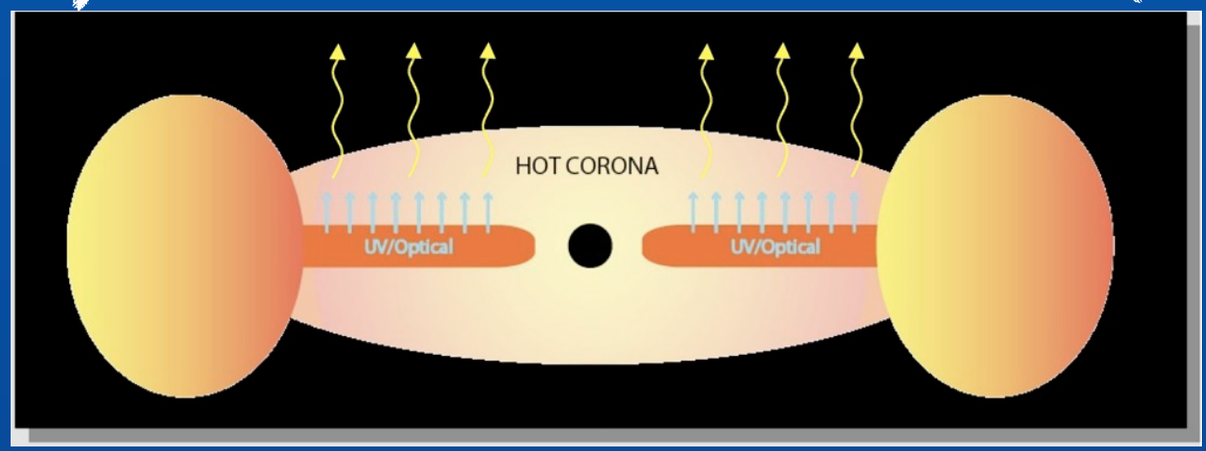

SSD

Jets, Lobes

NON-THERMAL PROCESSES

Synchrotron Radiation

Synchrotron radiation is due to the movement of an electron charge in a magnetic field. As a particle gyrates around a magnetic field, it will emit radiation at a frequency proportional to the strength of the magnetic field and its velocity.

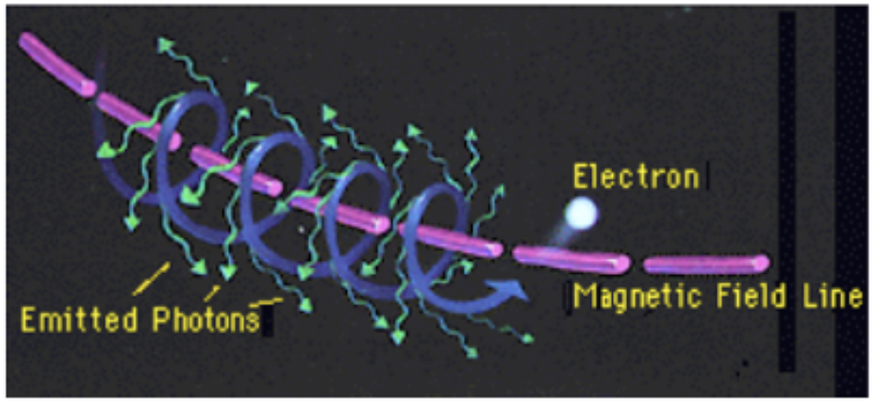

Synchrotron radiation is highly polarized and is seen at all wavelengths. At relativistic speeds, the radiation can also be beamed. It is very common in radio spectrum, but can be seen in x-rays. It is usually fit as a power law. For full details, see the review by Ginzburg & Syrovatskii (1969)

A single electron

The frequency of synchrotron radiation is:

$$\omega_B = \frac{qB}{\gamma mc}$$

The total power emitted by each electron is:

$$\frac{dE}{dt} = \frac{4}{3}\sigma_T c\beta^2\gamma^2 U_B$$

Where the following definitions have been used:

$$U_B = B^2/8\pi \qquad \beta = (1 - \frac{1}{\gamma^2})^{1/2}$$

$$\sigma_T = \frac{8\pi r_o^2}{3} \qquad \gamma = (1 - \frac{v^2}{c^2})^{-1/2}$$

The emission is concentrated into an angle along the direction of motion of order $1/\gamma$

The synchrotron radiation of a power law distribution of electron energies

Synchrotron

$$N(\gamma_e) = K\gamma_e^{-p}\,, \quad \gamma_{min} < \gamma_e < \gamma_{max}\,, p = 1 + 2\alpha$$

$$\epsilon_{sin}(\nu) \propto K B^{\alpha+1} \nu^{-\alpha}$$ erg cm^{-3} s^{-1} sr^{-1}

Inverse Compton scattering

When the electron is not at rest, but has an energy greater that the typical photon energy, there can be a transfer of energy from the electron to the photon. This process is called Inverse Compton to distinguish it from the direct Compton scattering, in which the electron is at rest, and it is the photon to give part of its energy to the electron.

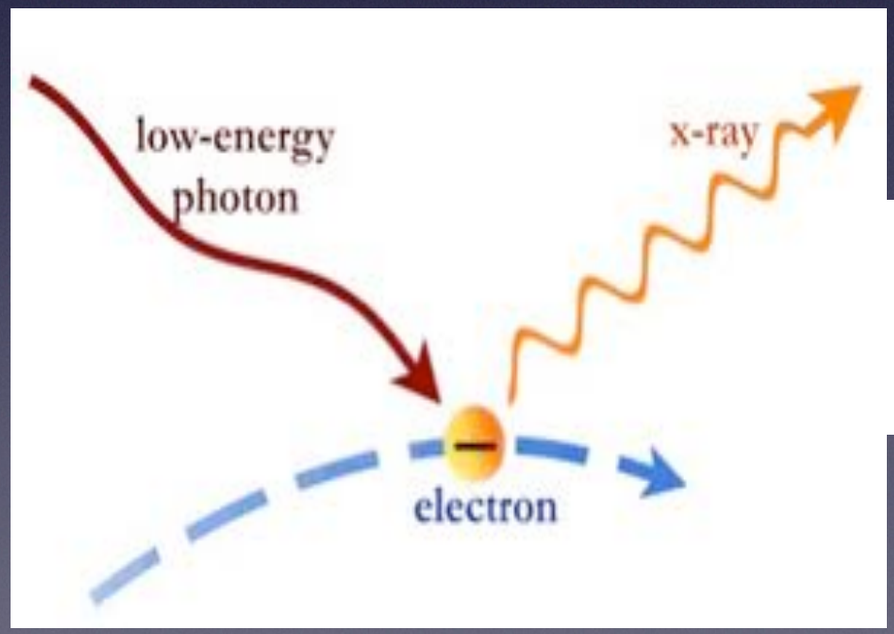

$$< \nu >= \frac{4}{3}\gamma^2 \nu$$

Inverse Compton Radiation

The general result that the frequency of the scattered photons is $\nu \approx \gamma^2 \nu_0$ is of profound importance in high energy astrophysics. We know that there are electrons with Lorentz factors $\gamma \sim 100 - 1000$ in various types of astronomical source and consequently they scatter any low energy photons to very much higher energies. Consider the scattering of radio, infrared and optical photons scattered by electrons with $\gamma = 1000$.

Waveband	*Frequency (Hz)* ν_0	*Scattered Frequency (Hz) and Waveband*
Radio	10^9	$10^{15} =$ UV
Far-infrared	3×10^{12}	$3 \times 10^{18} =$ X-rays
Optical	4×10^{14}	$4 \times 10^{21} \equiv 1.6$MeV $= \gamma$-rays

Thus, inverse Compton scattering is a means of creating very high energy photons indeed. It also becomes an inevitable drain of energy for high energy electrons whenever they pass through a region in which there is a large energy density of photons.

Inverse Compton

For a power law distribution of electrons:

$$N(\gamma_e) = K\gamma_e^{-p}, \quad \gamma_{min} < \gamma_e < \gamma_{max}, p = 1 + 2\alpha$$

Inverse Compton

$$\epsilon_c(\nu_c) \propto K\nu_c^{-\alpha} \int \frac{Ur(\nu)\nu^{\alpha}}{\nu} d\nu$$

erg cm^{-3} s^{-1} sr^{-1}

U_r is the radiation energy density

$$U_r = \int n(\epsilon)\epsilon d\epsilon$$

- Synchrotron photons in the jet
- Environment photons from Accretion Flow, BLR, NLR, Torus
- Cosmic Microwave Background (CMB) photons

6. Journey along the jet

pc-scale jet

kpc-scale jet

lobes

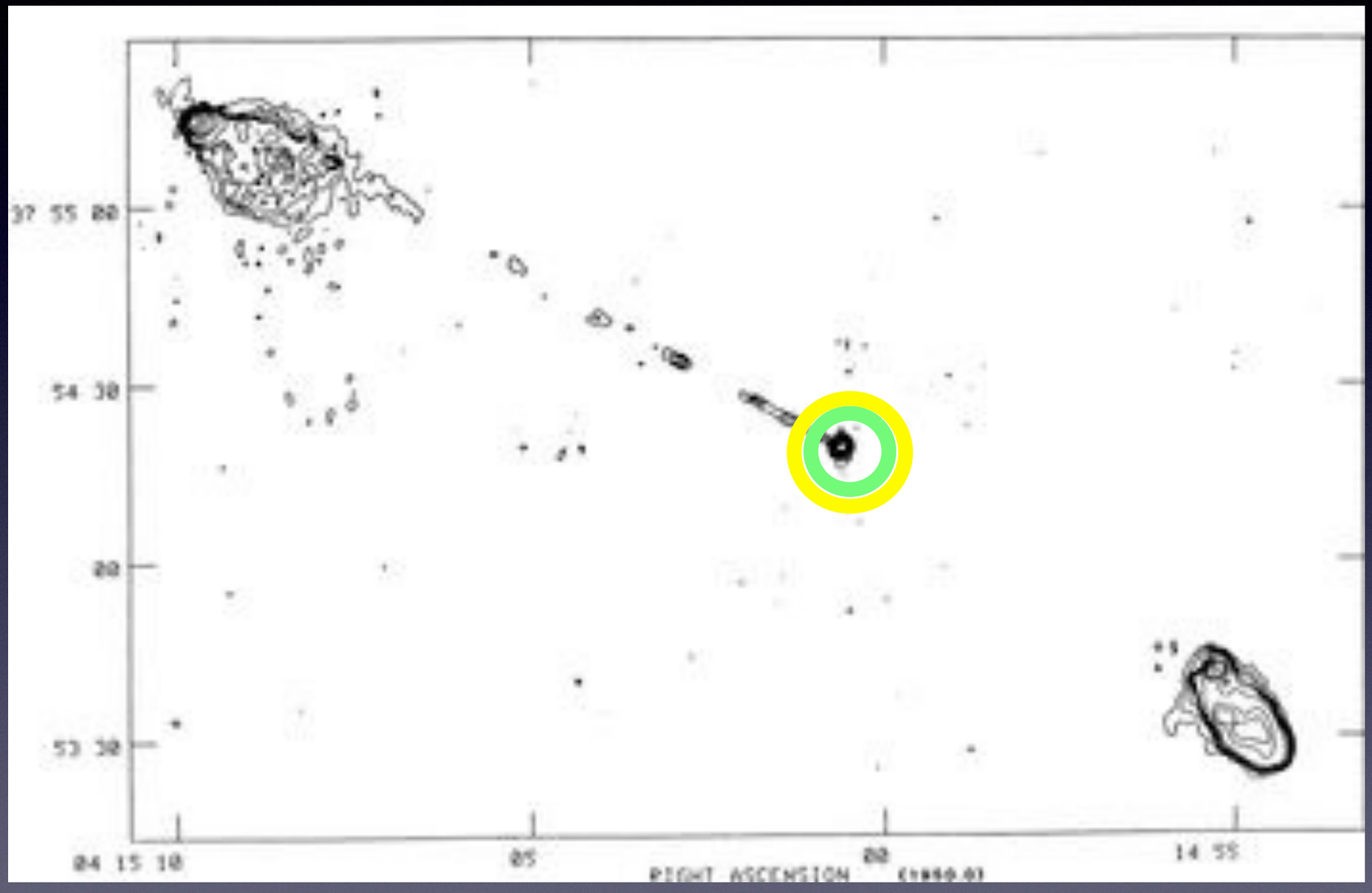
37 55 00
54 30
00
53 30
04 15 10
05
00
14 55
RIGHT ASCENSION

Radio Loud AGNs
JET at sub-pc scale (core)

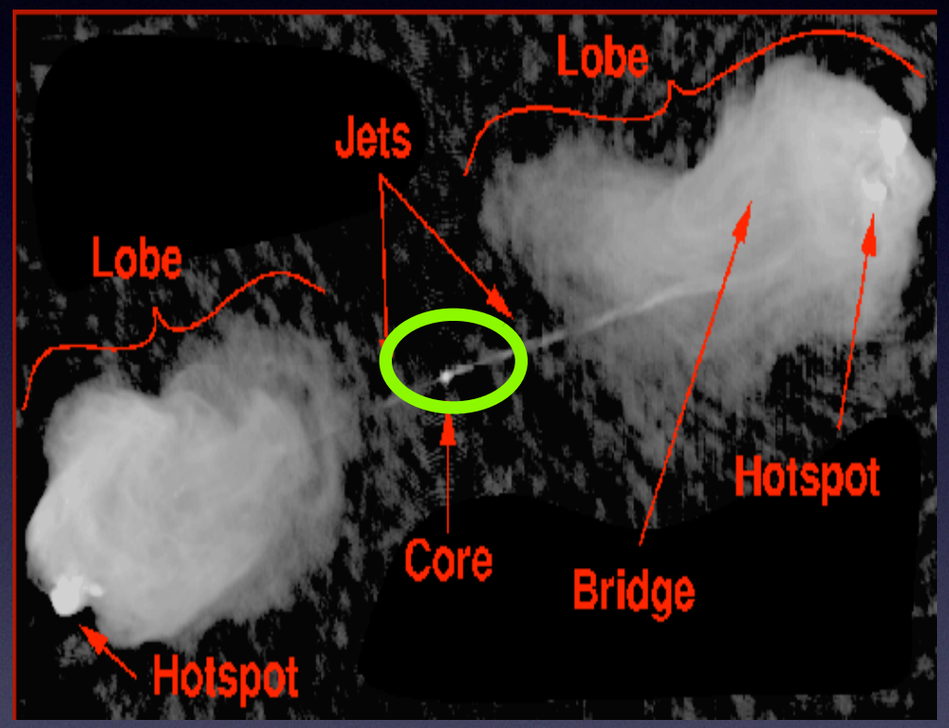

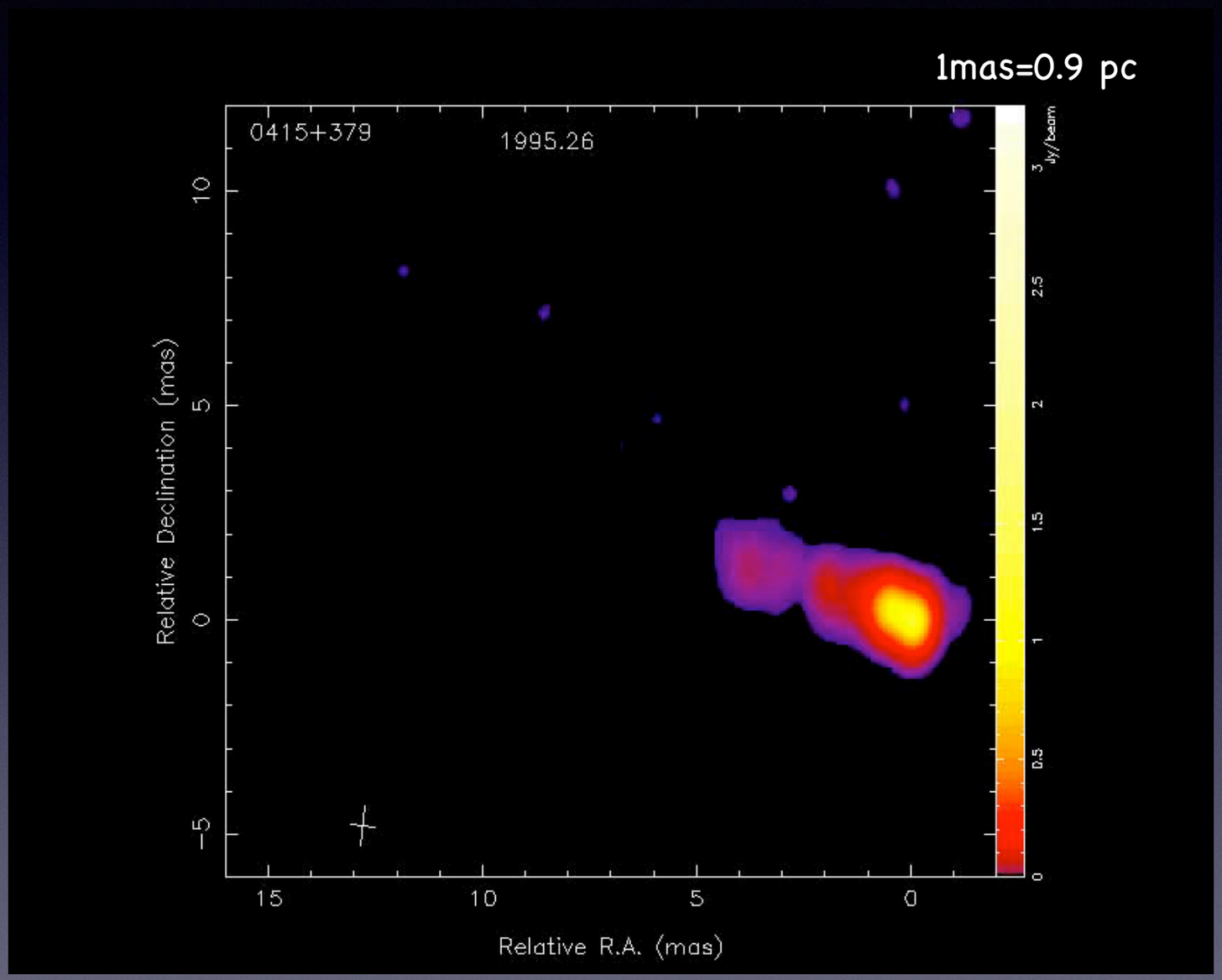

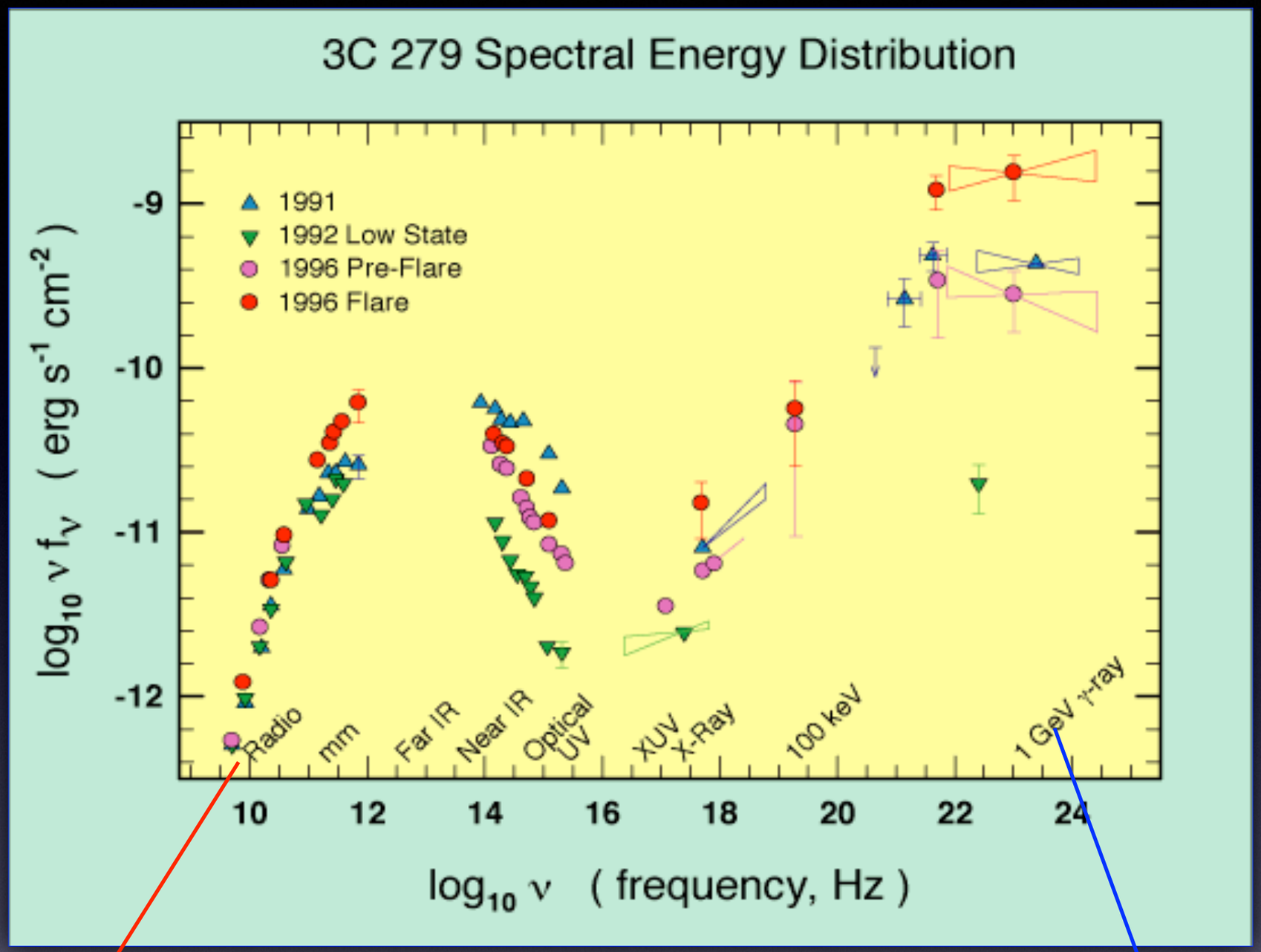

Synchrotron

Inverse Compton

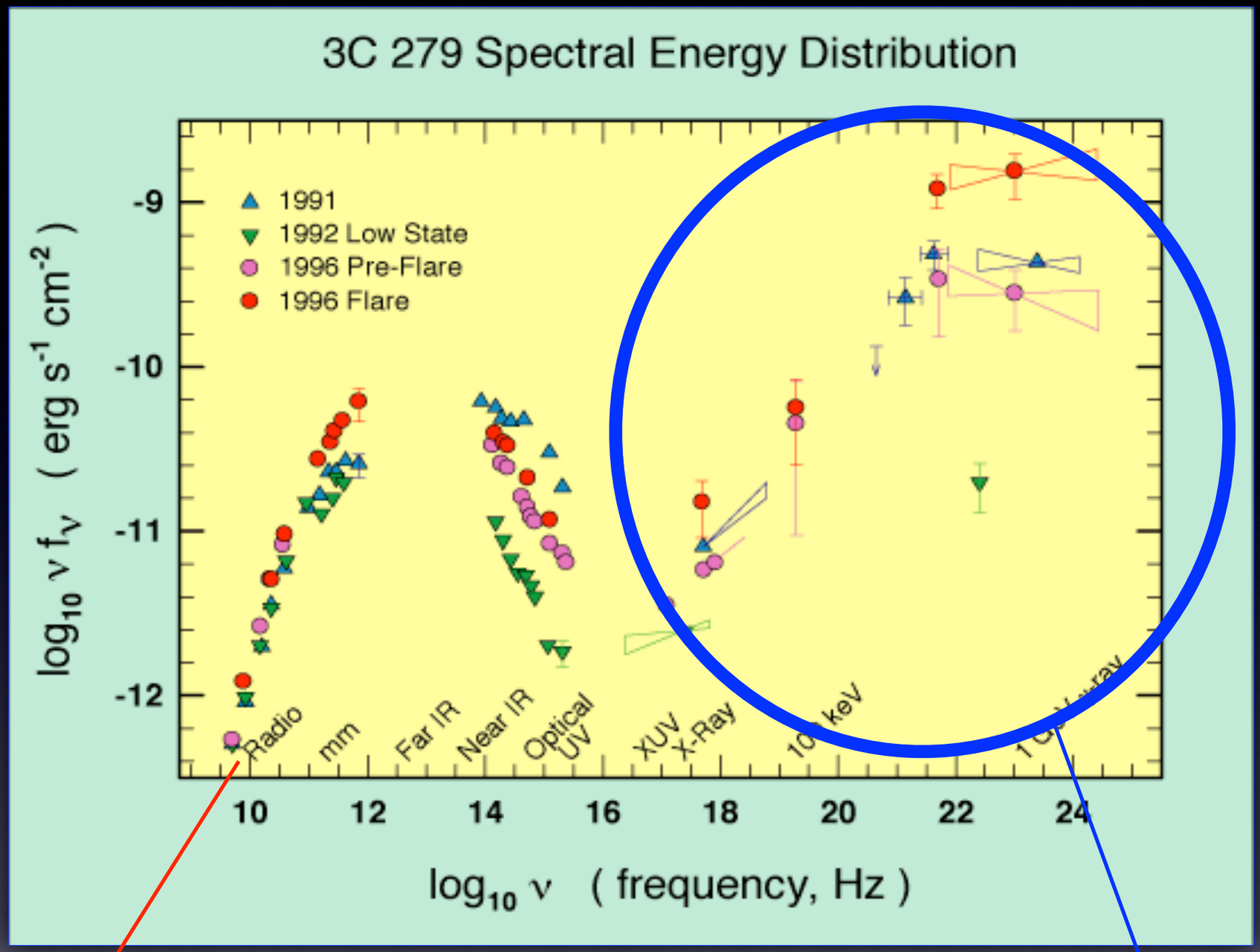

Synchrotron

Inverse Compton

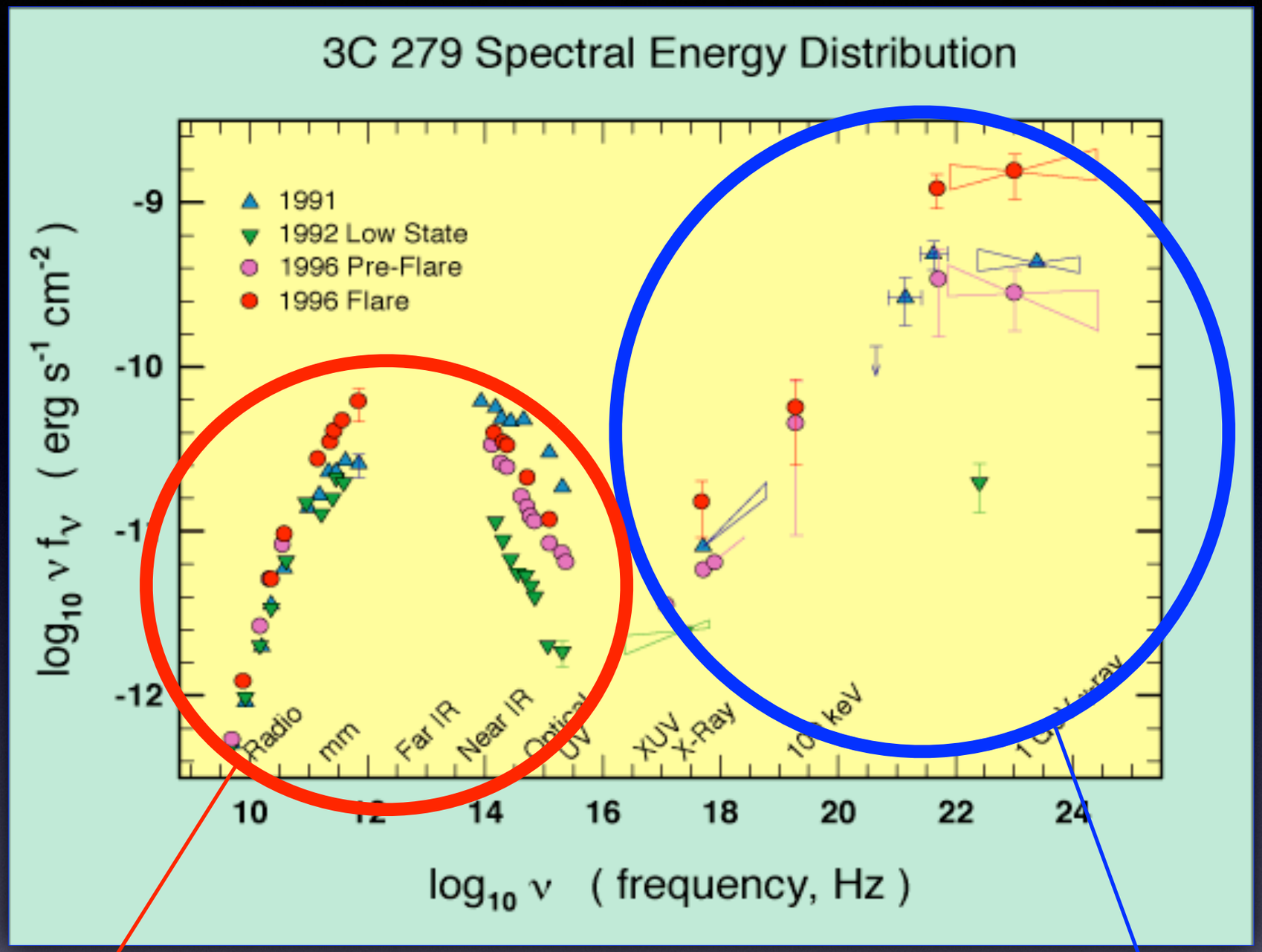

Synchrotron

Inverse Compton

Synchrotron Self–Compton

Consider a population of relativistic electrons in a magnetized region. They will produce synchrotron radiation, and therefore they will fill the region with photons. These synchrotron photons will have some probability to interact again with the electrons, by the Inverse Compton process. Since the electron "work twice" (first making synchrotron radiation, then scattering it at higher energies) this particular kind of process is called synchrotron self-Compton, or SSC for short.

External Compton

The population of relativistic electrons in a magnetized region can also interact with photons externa to the jet produced in the accretion disk, in the broad/narrow line regions in the torus. This particular kind of process is called External Compton, or EC for short.

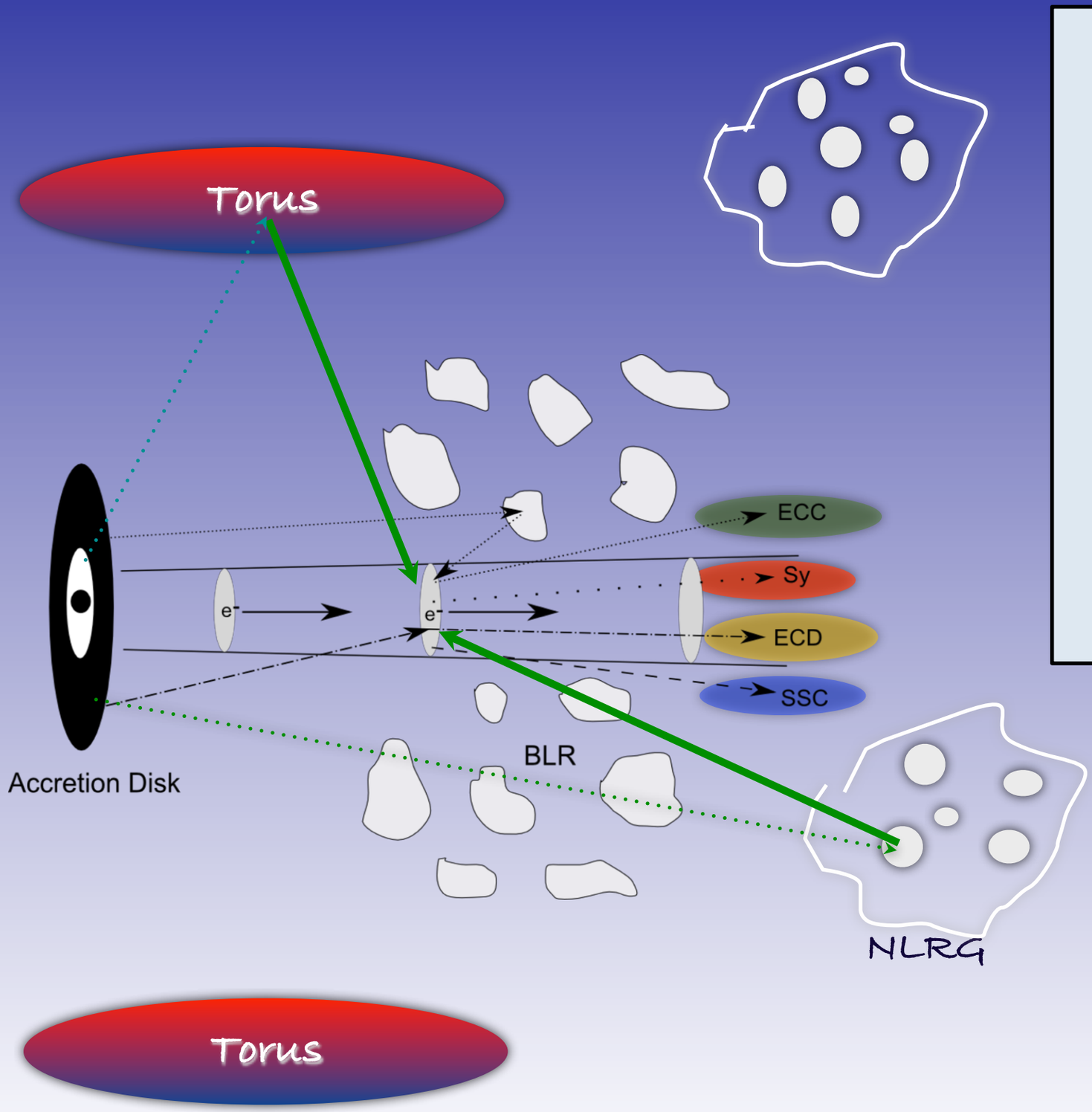
Torus
ECC
Sy
ECD
SSC
e-
e-
BLR
Accretion Disk
NLRG
Torus

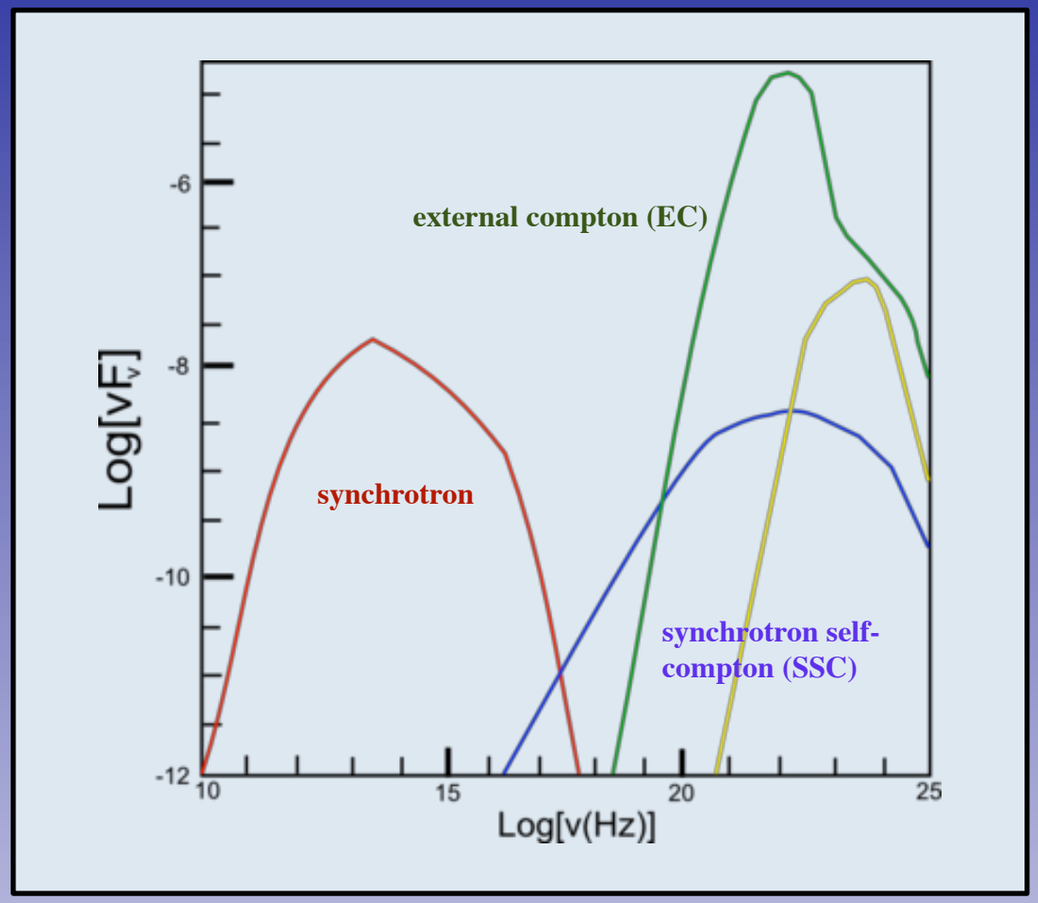
external compton (EC)
synchrotron
synchrotron self-compton (SSC)
Log[νF_ν]
-6
-8
-10
-12
10
15
20
25
Log[ν(Hz)]

Competition between jet and disk

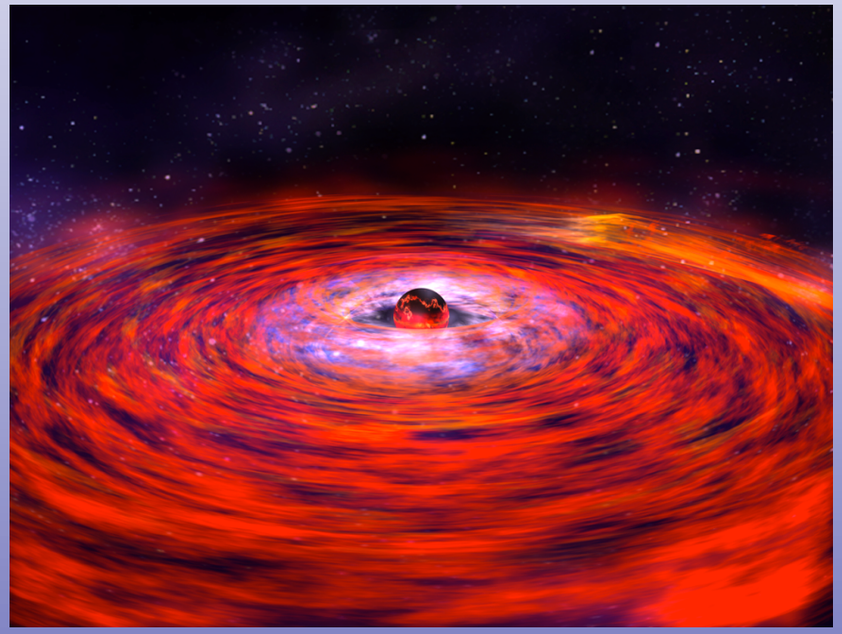

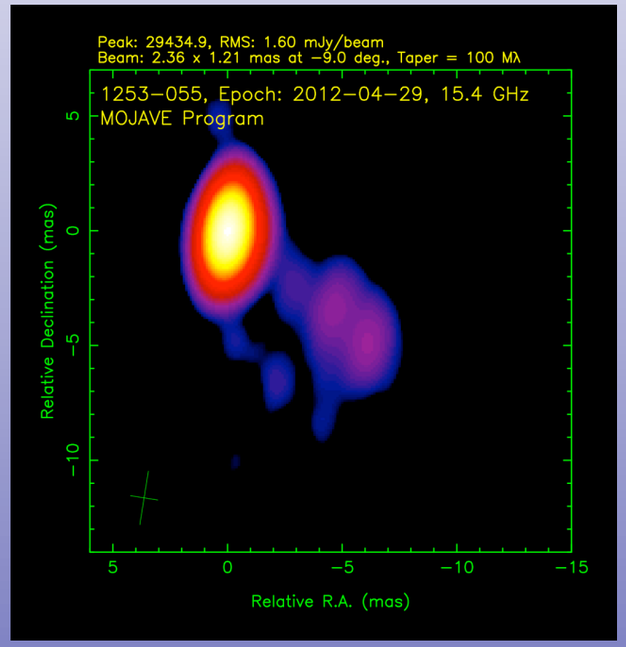

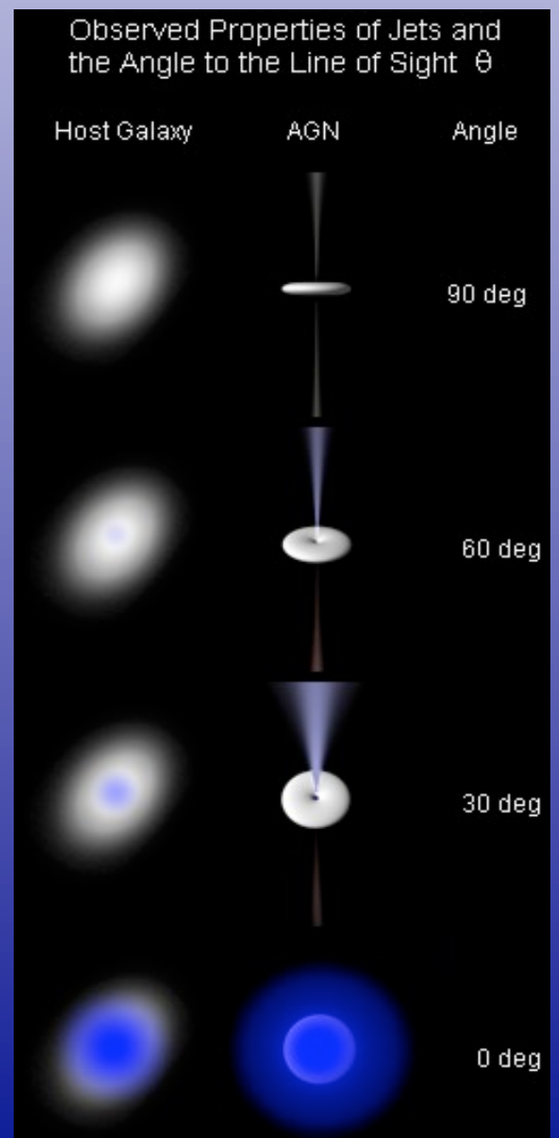

X-ray Spectra:Accretion Disk and pc-scale Jet emission are in competion:

Angle of sight = 0° ==> Jet radiation dominates

Angle of sight = 90° ==> Accretion disk dominates
(+absorption from torus, if present)

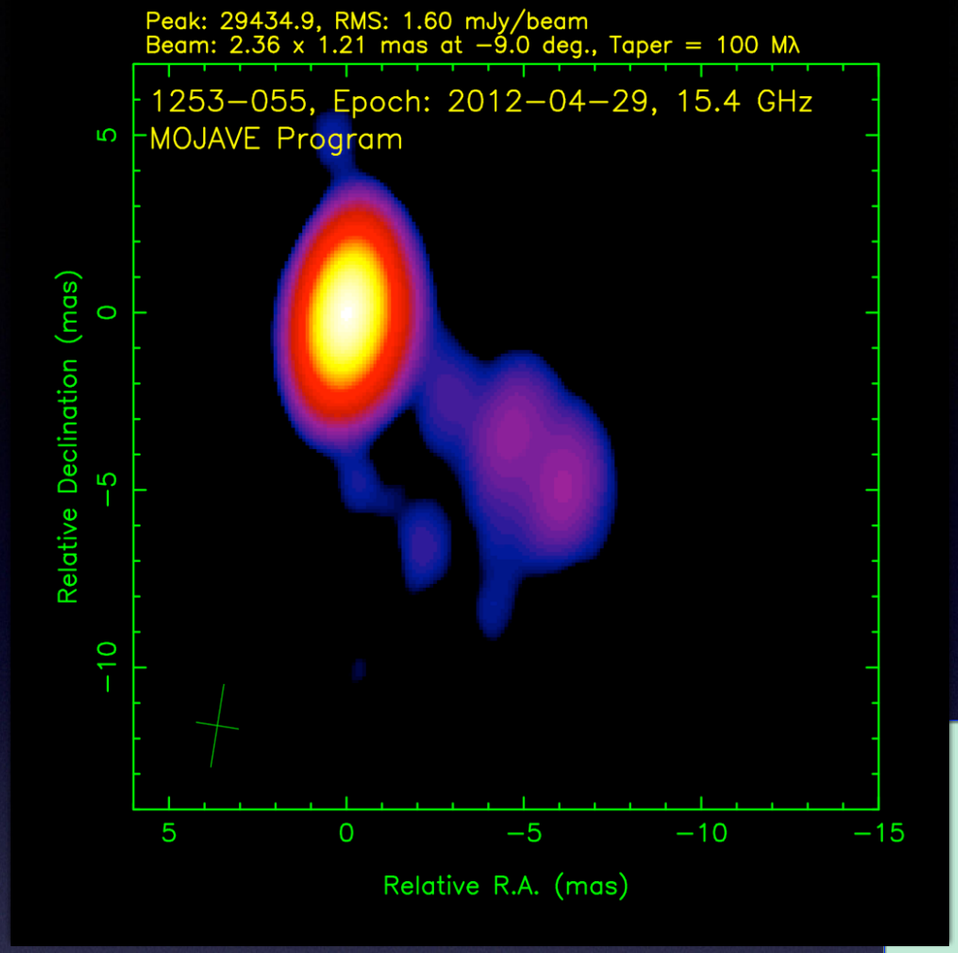

If in FRIs and FRIIs the jet is pointing the observer, only the jet emission is observable => double peaked SED

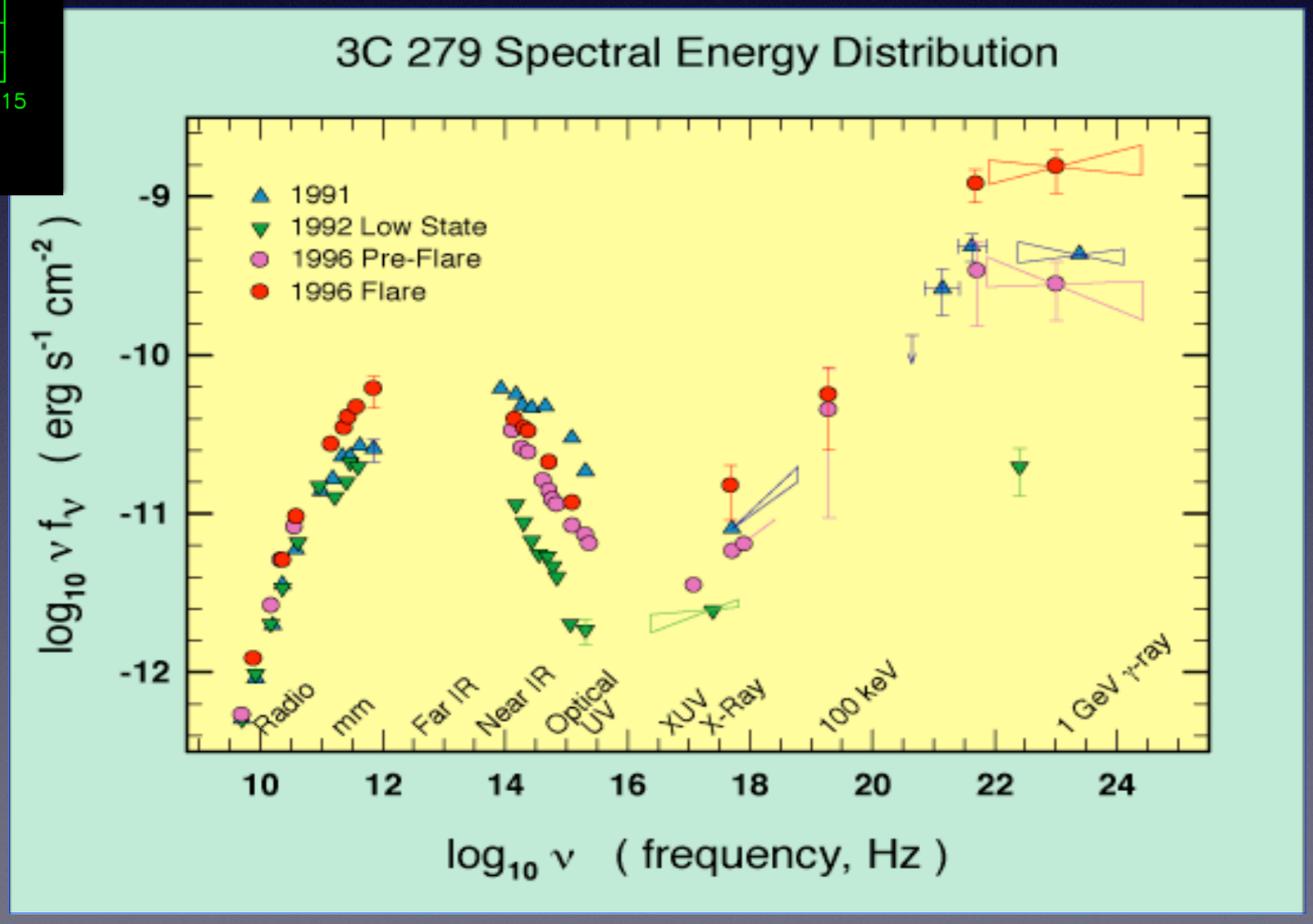

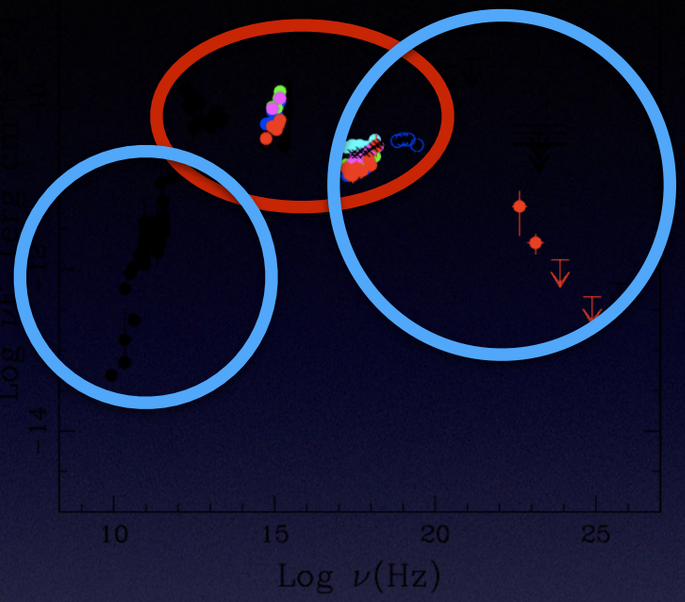

In FRIs and FRIIs the jet inclination is around 10-30 degrees, **non-thermal** (jet) and **thermal** (accretion) emission are in competition. In the SED and in the X-ray spectra can be seen accretion disk features

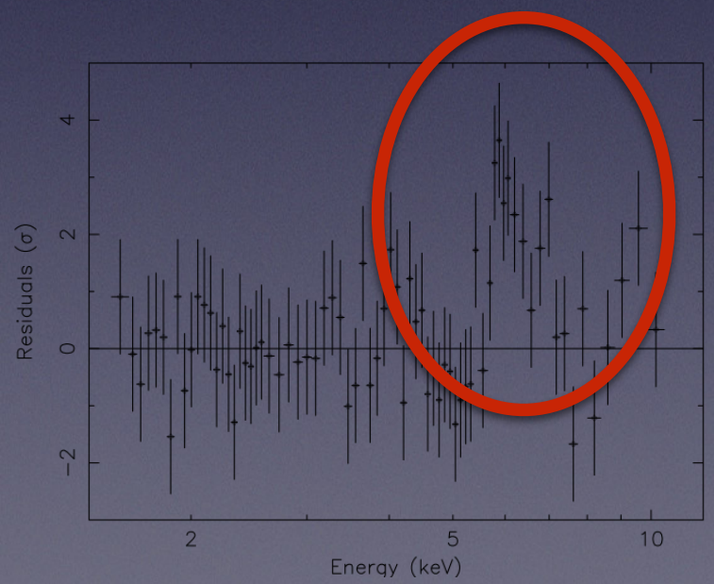

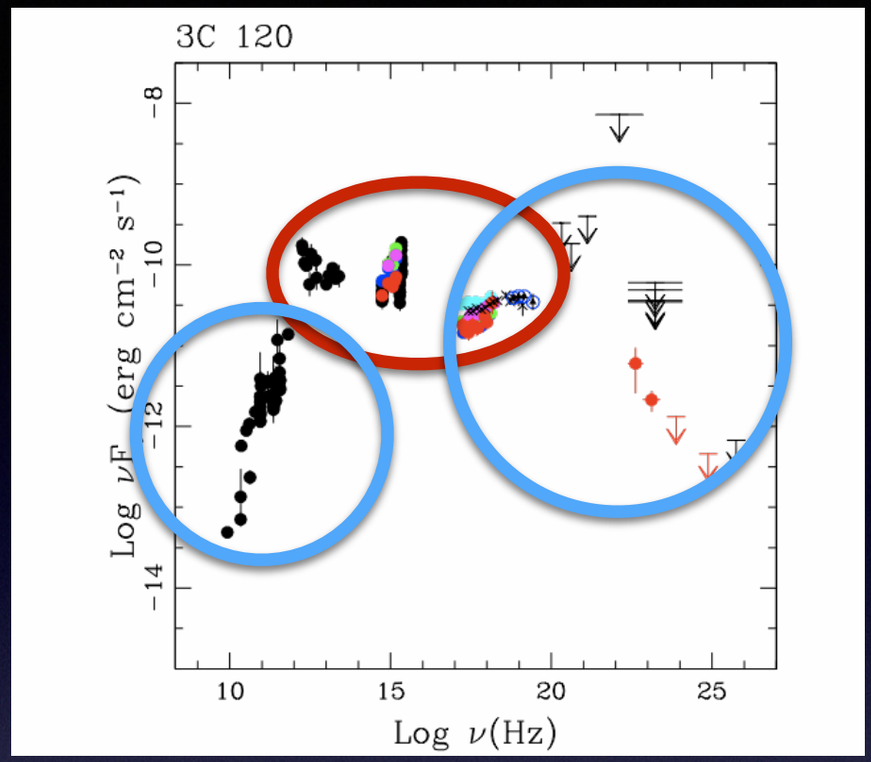

In FRIs and FRIIs the jet inclination is around 10-30 degrees, **non-thermal** (jet) and **thermal** (accretion) emission are in competition. In the SED and in the X-ray spectra can be seen accretion disk features

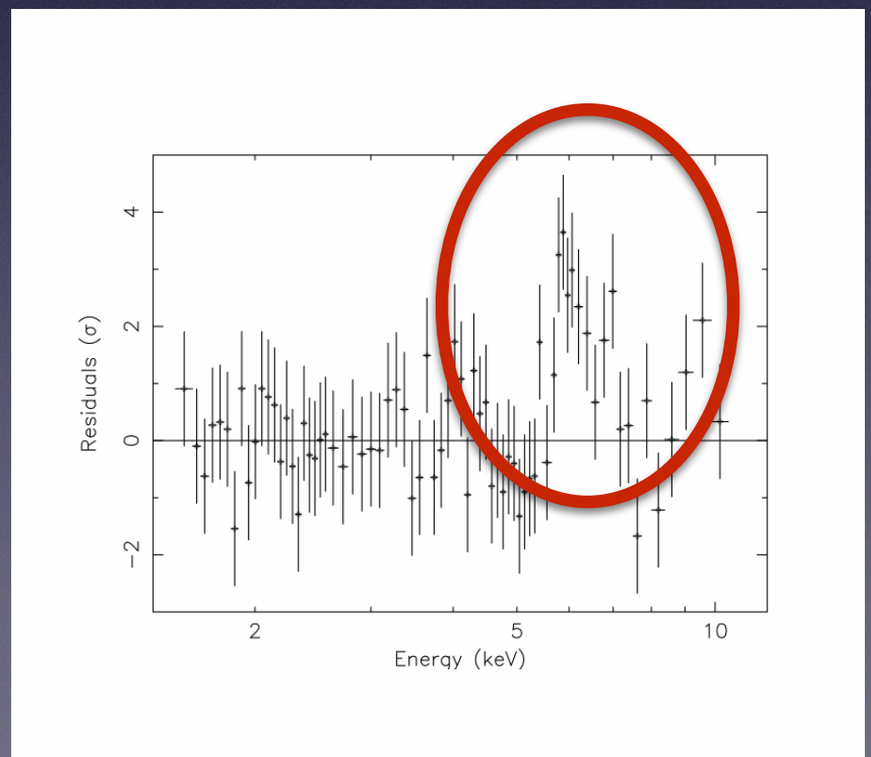

kpc-scale Jet

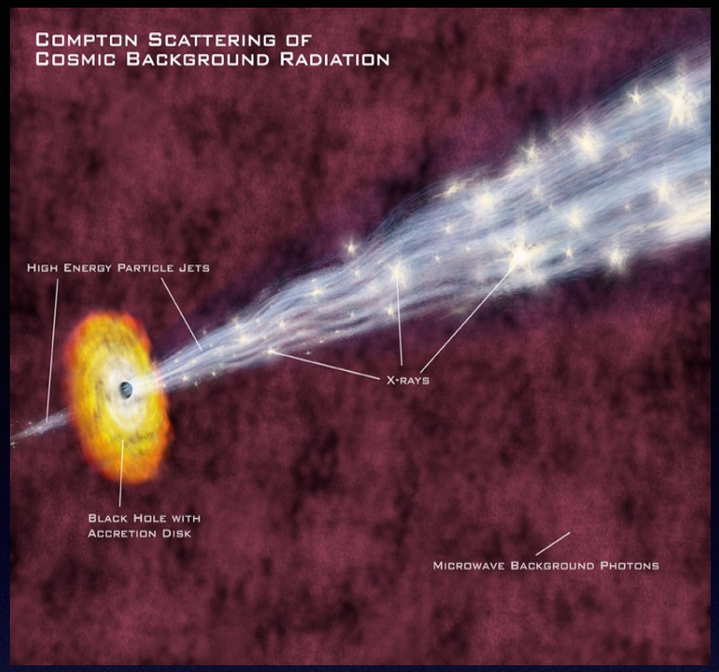

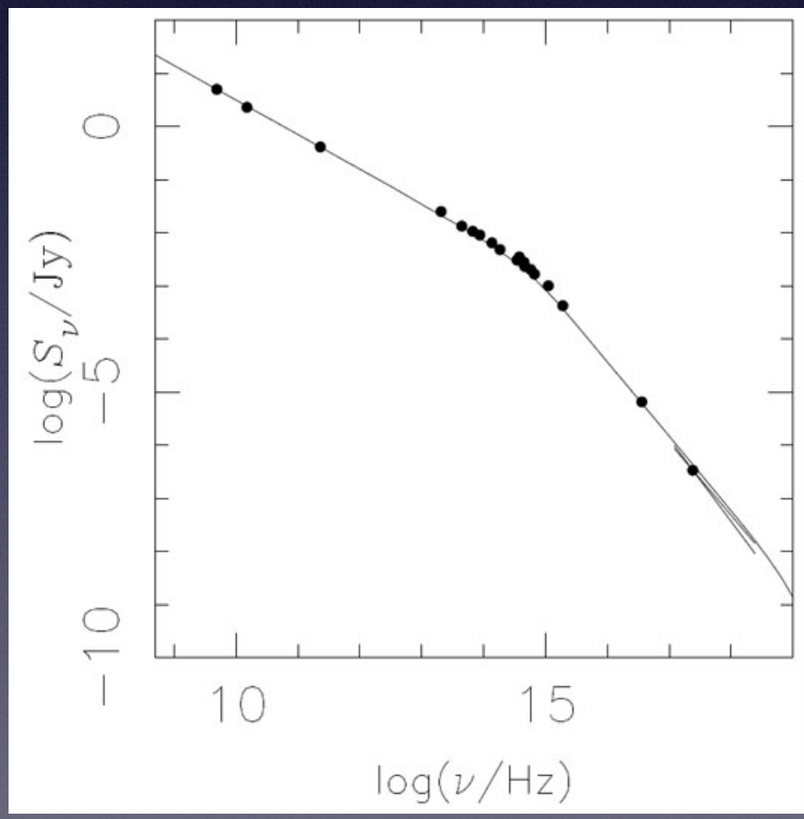

FRI-M87

For low-luminosity (FRI) radio sources, there is strong support for the synchrotron process as the dominant emission mechanism for the X-rays, optical, and radio emissions

Synchrotron process

FRII sources require multi-zone synchrotron models, or synchrotron and IC models (seed photons: CMB).
The most popular model postulates very fast jets with high bulk Lorentz factors Γ (recently rejected in at least 3 sources).

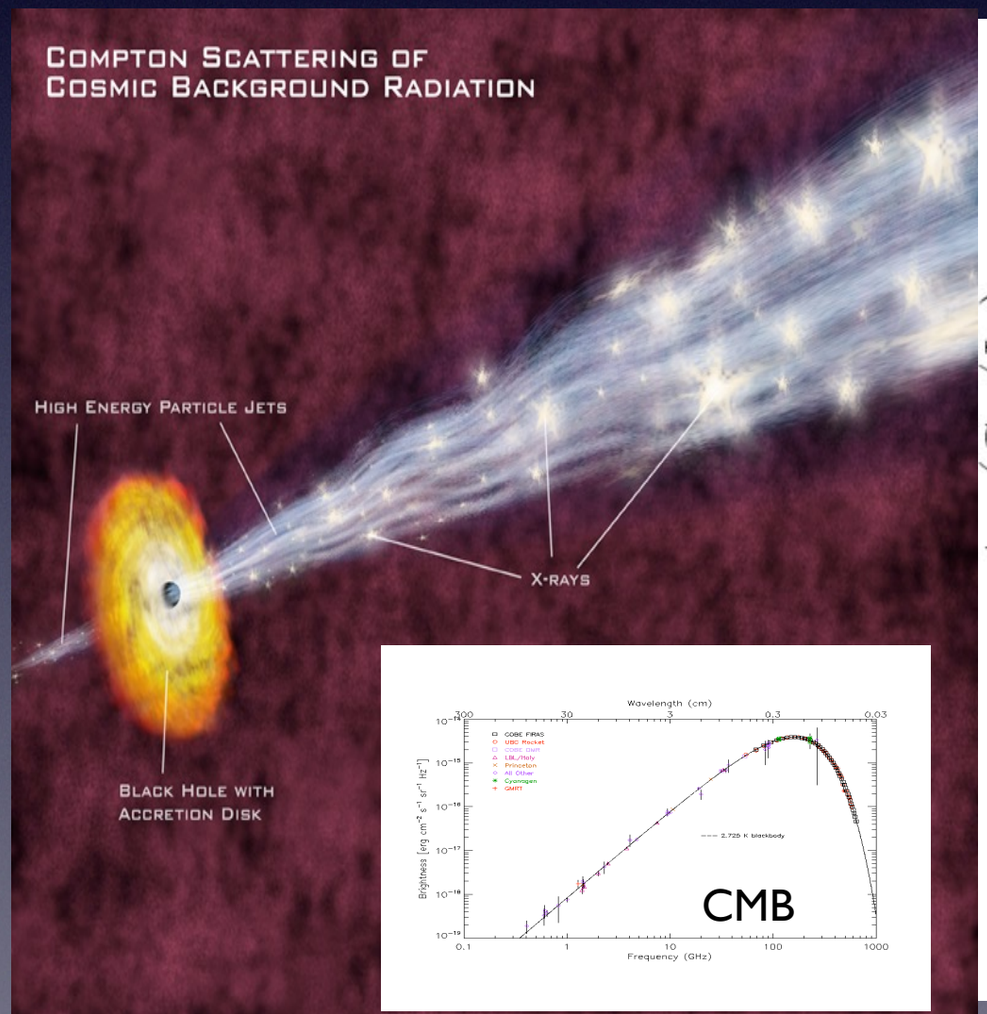

FRII-PKS0637-75

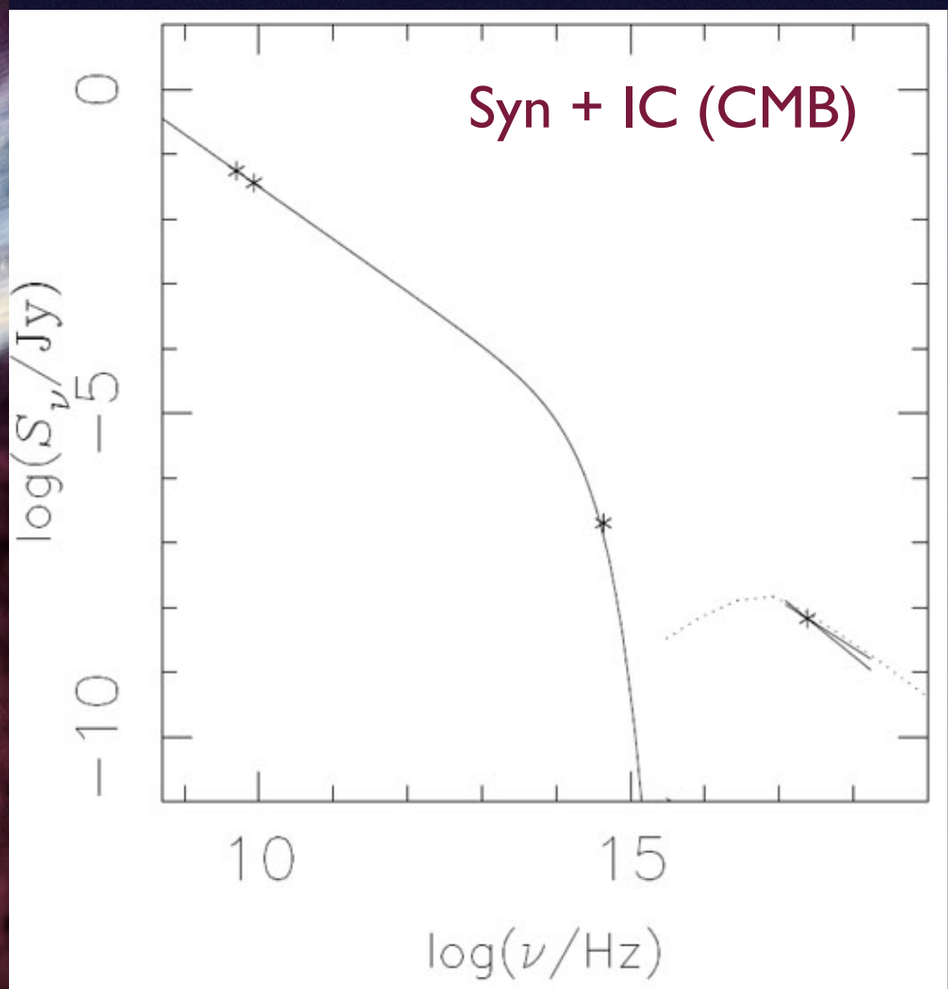

Lobes

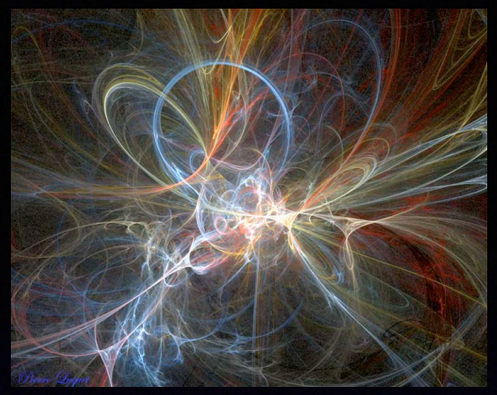

relativistic electrons

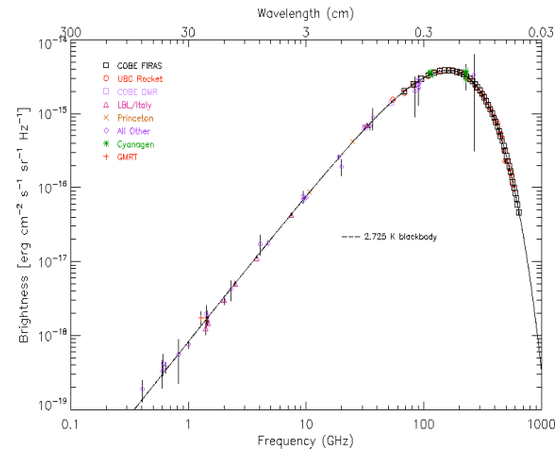

CMB

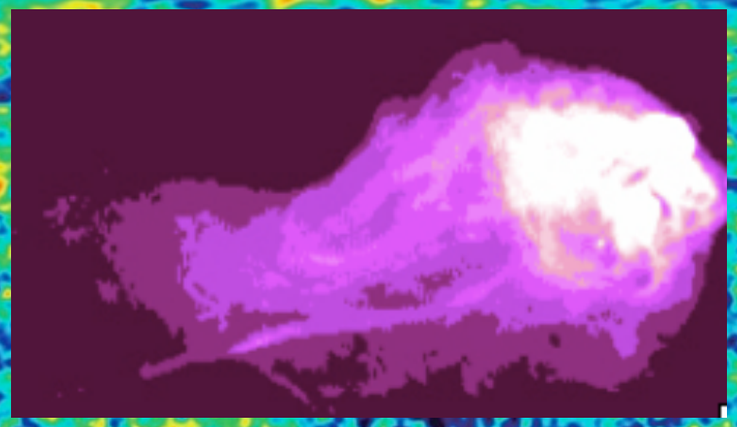

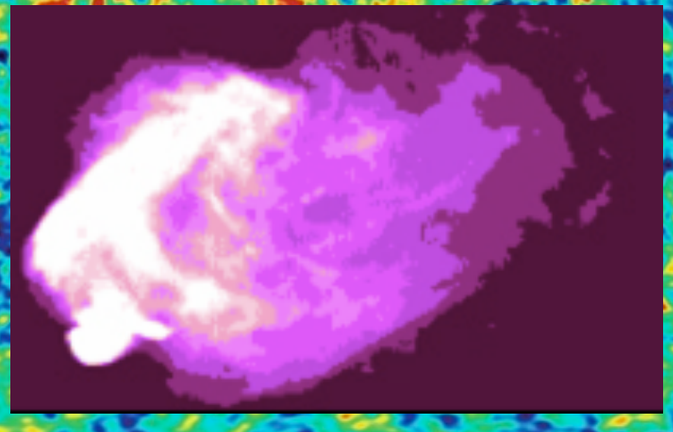

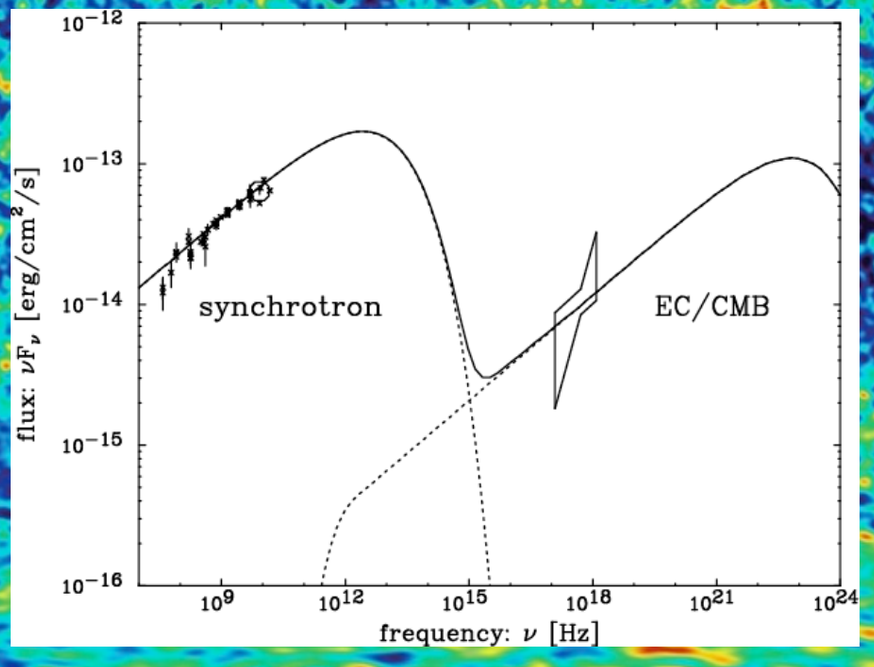

Lobes

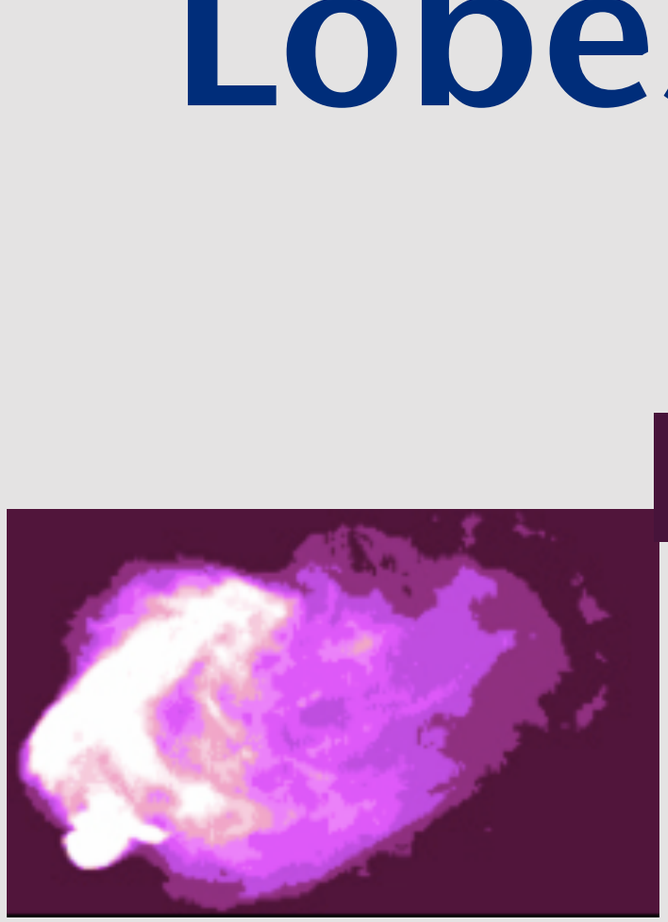

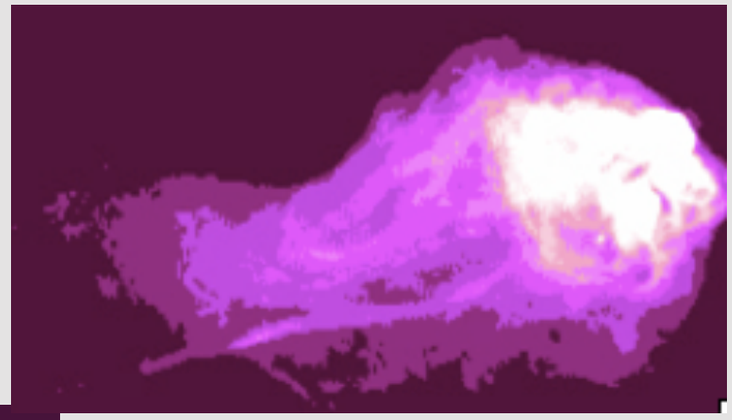

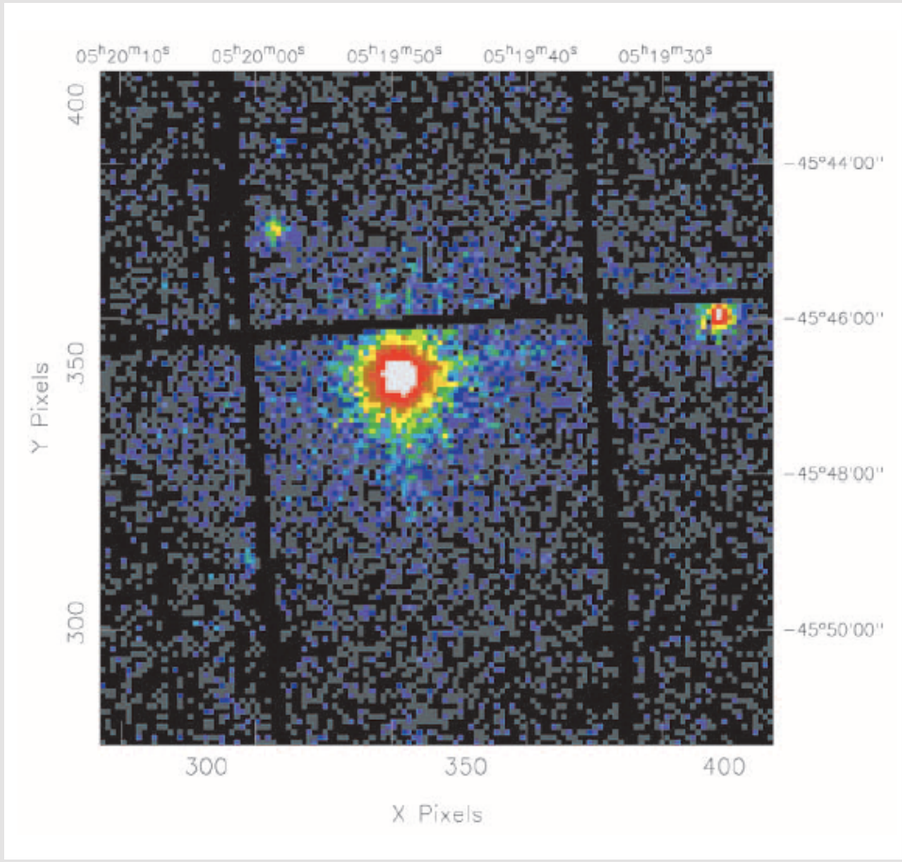
05h20m10s
05h20m00s
05h19m50s
05h19m40s
05h19m30s
400
350
300
Y Pixels
−45°44'00"
−45°46'00"
−45°48'00"
−45°50'00"
300
350
400
X Pixels

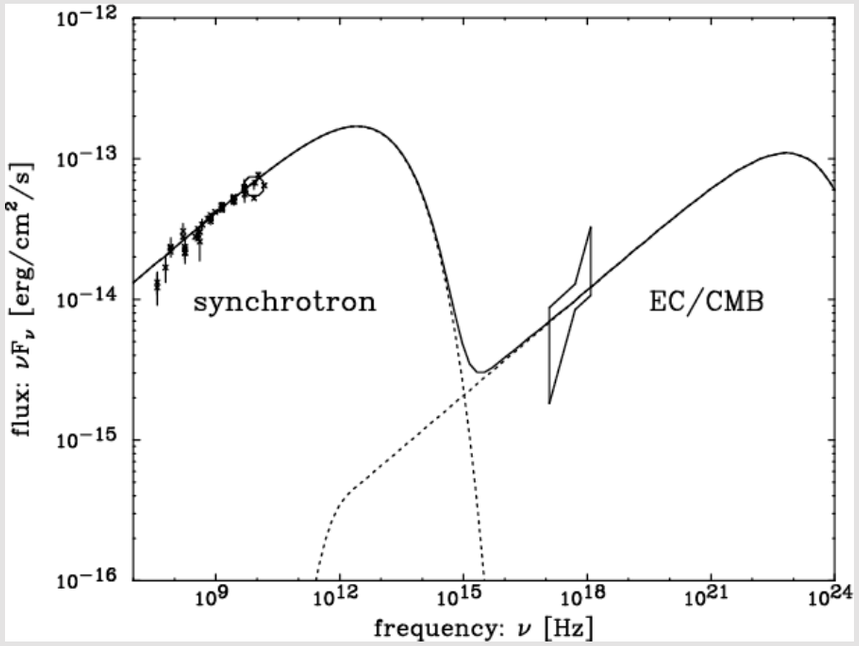
synchrotron
EC/CMB
flux: νF_ν [erg/cm²/s]
frequency: ν [Hz]
10^-12
10^-13
10^-14
10^-15
10^-16
10^9
10^12
10^15
10^18
10^21
10^24

Hot Spots

Terminal hotspots, like knots, are thought to be localized volumes of high emissivity which are produced by strong shocks or a system of shocks. Hot spot spectra are generally consistent with SSC predictions but a significant number appeared to have a larger X-ray intensity than predicted. This excess could be attributed to a field strength well below equipartition, IC emission from the decelerating jet 'seeing' Doppler boosted hotspot emission or an additional synchrotron component, ecc

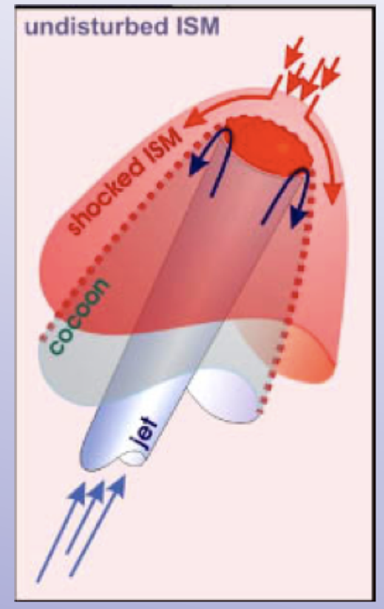

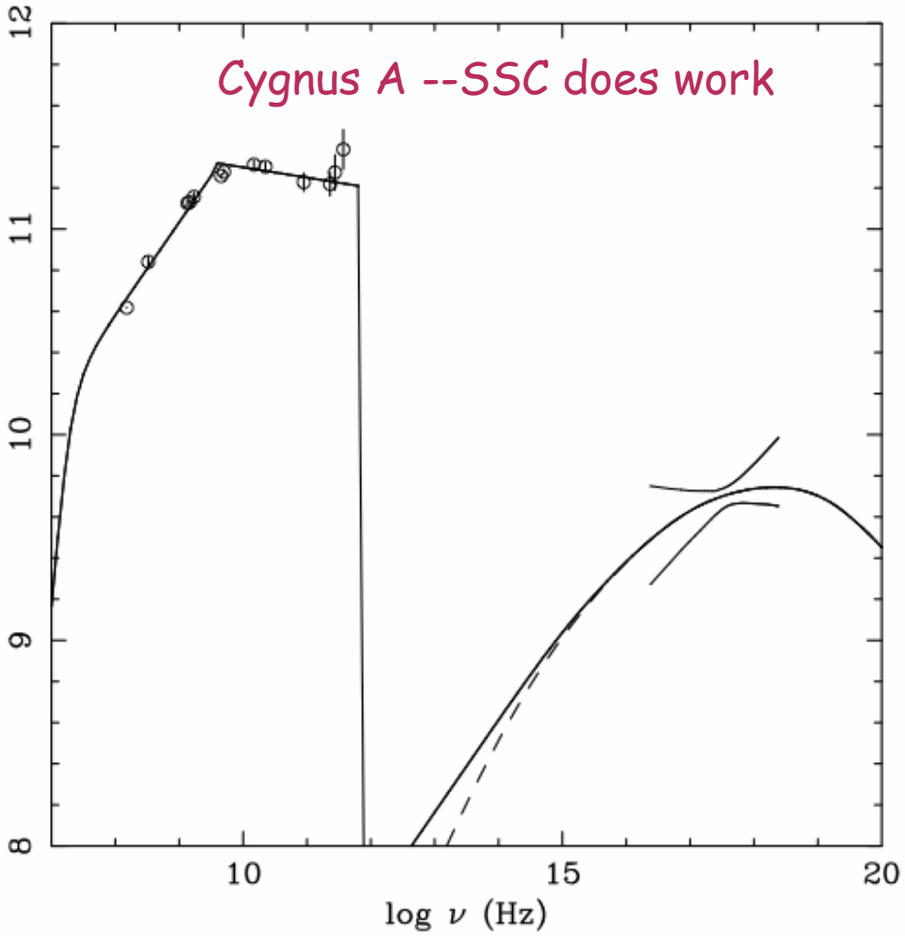

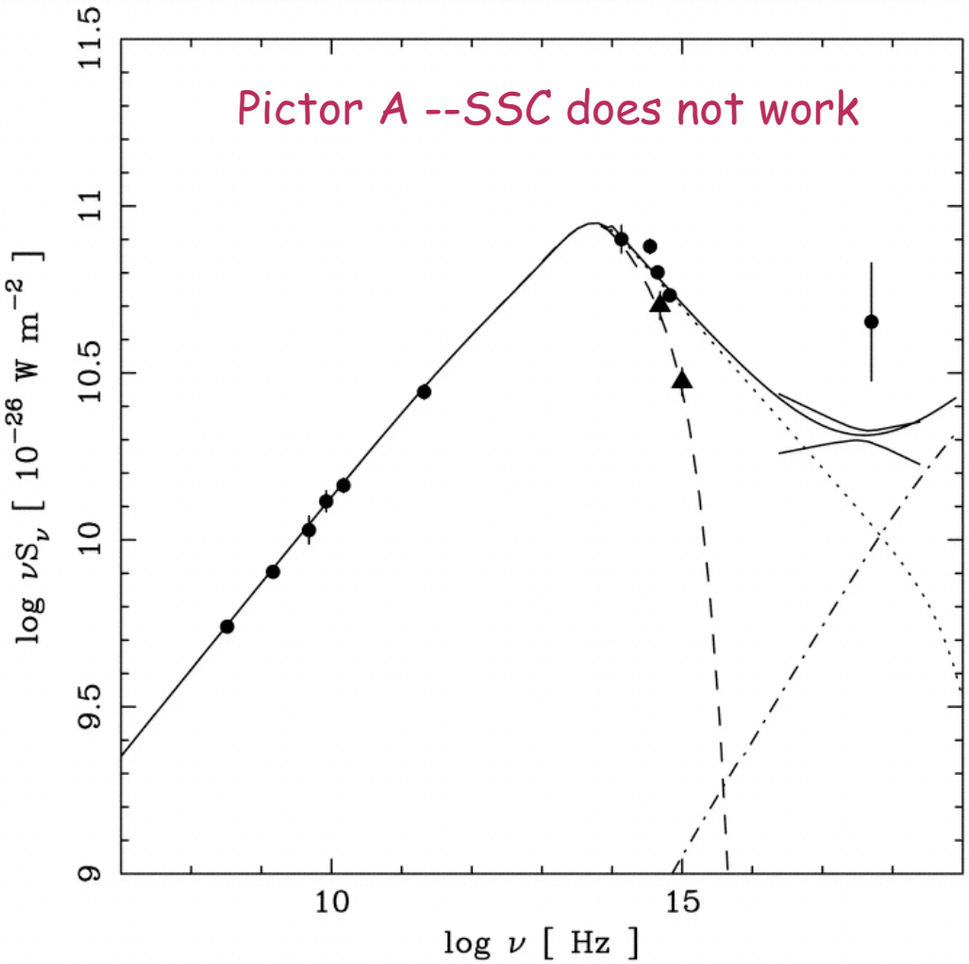

Questions?

Bibliografia:

- Urry & Padovani, 1995, PASPJ, 107, 803;
- Buttiglione et al. 2010, A&A 509, 6
- Narayan et al. 1998:*Theory of Black Hole Accretion Disks,* Cambridge University Press, 1998, p. 148-182 (http://arxiv.org/pdf/astro-ph/9803141v1.pdff)
- Blandford, Netzer and Woltjer, "Active Galactic Nuclei"*, Saas-Fee Advanced Course 20. Lecture Notes 1990. Swiss Society for Astrophysics and Astronomy - Springer-Verlag*
- *Dispense C. Fanti e R. Fanti : Una finestra sull'Universo "Invisibile"*
- *Frank, King and Reine, Accretion Power in Astrophysics.*
- *M. Longair: High Energy Astrophysics*